

ADVANCED SEISMIC BASE ISOLATION METHODS FOR MODULAR REACTORS

E. Blandford, E. Keldrauk, M. Laufer, M. Mieler, J. Wei,
B. Stojadinovic, and P.F. Peterson

Departments of Civil and Environmental Engineering and Nuclear Engineering
University of California
Berkeley, California

September 30, 2009

UCBTH-09-004

FINAL REPORT

Abstract

Advanced technologies for structural design and construction have the potential for major impact not only on nuclear power plant construction time and cost, but also on the design process and on the safety, security and reliability of next generation of nuclear power plants. In future Generation IV (Gen IV) reactors, structural and seismic design should be much more closely integrated with the design of nuclear and industrial safety systems, physical security systems, and international safeguards systems. Overall reliability will be increased, through the use of replaceable and modular equipment, and through design to facilitate on-line monitoring, in-service inspection, maintenance, replacement, and decommissioning. Economics will also receive high design priority, through integrated engineering efforts to optimize building arrangements to minimize building heights and footprints. Finally, the licensing approach will be transformed by becoming increasingly performance based and technology neutral, using best-estimate simulation methods with uncertainty and margin quantification.

In this context, two structural engineering technologies, *seismic base isolation and modular steel-plate/concrete composite structural walls*, are investigated. These technologies have major potential to (1) enable standardized reactor designs to be deployed across a wider range of sites, (2) reduce the impact of uncertainties related to site-specific seismic conditions, and (3) alleviate reactor equipment qualification requirements. For Gen IV reactors the potential for deliberate crashes of large aircraft must also be considered in design. This report concludes that base-isolated structures should be decoupled from the reactor external event exclusion system. As an example, a scoping analysis is performed for a rectangular, decoupled external event shell designed as a grillage. This report also reviews modular construction technology, particularly steel-plate/concrete construction using factory prefabricated structural modules, for application to external event shell and base isolated structures.

CONTENTS

| | |
|---|-----------|
| 1.0 Introduction | 4 |
| <i>References</i> | 7 |
| 2.0 Base Isolation, External Event, and Modular Construction Design Options | 8 |
| 2.1 <i>Seismic Base Isolation</i> | 8 |
| 2.1.1 Dynamics of a Seismically Isolated Structure | 9 |
| 2.1.2 Types of Horizontal and Vertical Seismic Isolation Devices..... | 12 |
| 2.1.3 Supplemental Damping and the Isolation Gap | 14 |
| 2.1.3. Seismic Isolation Design Basis..... | 14 |
| 2.1.4 Benefits and Challenges of Seismic Isolation | 16 |
| 2.2 <i>External Event Shielding</i> | 17 |
| 2.3.1 Coupled above-grade event shell and citadel | 18 |
| 2.3.2 Decoupled above-grade event shell and citadel | 20 |
| 2.3.3 Berms, below grade, and underground construction..... | 23 |
| 2.3 <i>Steel-Plate/Concrete Modular Construction</i> | 24 |
| 2.4 <i>References</i> | 29 |
| 3.0 Simulation Verification and Validation Issues | 31 |
| 3.1 <i>Historical Experience with Seismic Base Isolation</i> | 31 |
| 3.2 <i>Current Analysis Methods and Tools for Reactor Seismic Design</i> | 34 |
| 3.3 <i>Verification and Validation Requirements and Approach</i> | 35 |
| 3.4 <i>References</i> | 36 |
| 4.0 Loading Characterization | 38 |
| 4.1 <i>Earthquake</i> | 38 |
| 4.2 <i>Aircraft crash loading</i> | 40 |
| 4.3 <i>Blast loading</i> | 44 |
| 4.4 <i>Internal and other loads</i> | 47 |
| 4.5 <i>References</i> | 48 |
| 5.0 Integration With Reactor Systems | 50 |
| 5.1 <i>Technology-Neutral Framework (TNF) for Reactor Licensing</i> | 50 |
| 5.1.1 Event Identification and Reliability Functions | 51 |
| 5.1.2 Physical Arrangement and Reactor Safety | 52 |
| 5.1.3 Physical Arrangement and Physical Security Functions | 54 |
| 5.1.4 Major SSCs Requiring Design Integration..... | 55 |
| 5.2 <i>Reactor System Seismic Design Criteria</i> | 55 |
| 5.2.1 SSC Seismic Classification..... | 56 |
| 5.2.2 Implications for Plant Construction | 57 |
| 5.2.2 Modularization | 58 |
| 5.3 <i>References</i> | 59 |
| 6.0 Parametric Analysis | 60 |
| 6.1 <i>Base-isolated NPP Model for Seismic Analysis: Assumptions and Parameters</i> | 60 |
| 6.3 <i>Earthquake Response of the Base Isolated NPP Model</i> | 62 |
| 6.4 <i>Response of Base-Isolated NPP Model to Aircraft Impact</i> | 67 |
| 6.5 <i>Decoupled Event Shell Response to Aircraft Crash</i> | 69 |
| 6.5 <i>References</i> | 76 |
| 7.0 Findings and Conclusions | 77 |

| | |
|--|------------|
| 8.0 Nomenclature..... | 80 |
| Appendix A: Ground motion..... | 81 |
| Appendix B: Earthquake Ground Motion..... | 83 |
| Appendix C: Earthquake Response Results..... | 113 |
| Appendix D: Impact Response Time Histories..... | 115 |

1.0 INTRODUCTION

Structural engineering is commonly pursued at the tail end of the development of new reactor designs, after the major nuclear and mechanical systems have already been designed. As illustrated in Fig. 1, consideration of major structure functional requirements, such as aircraft crash resistance, late in the design process can result in expensive modifications. For Generation IV reactor options, nuclear, mechanical and structural engineering should be integrated in design from the start to optimize the design, increase its safety and security, and improve its economy.



Fig. 1. External event shell steel grillage surrounds the Lucas Heights reactor in Australia.

A recent review of advanced construction technologies for nuclear power plants (Schlaseman, 2004) identified twelve new structural systems and construction and fabrication methods that have a high potential to improve the economy and reduce time required to build new nuclear power plants. The common theme among these technologies is modularization, prefabrication and preassembly. However, the report failed to identify *seismic base isolation*, a technology already deployed to protect conventional building structures and infrastructure facilities from earthquakes, as the paradigm-changing structural design concept that enables modular construction.

Seismic base isolation has the potential to provide significant benefits by simplifying nuclear power plant design requirements. Base-isolation devices limit the amount of seismic energy transferred from the ground to the structures and filter out the high-frequency components of horizontal ground motion: this makes it possible to design standard, site-independent, nuclear power plant structures, systems and components above the base isolation layer. Such designs will be inherently modular. Furthermore, control of the magnitude and frequency content of the seismic input energy enables design and implementation of new reactor concepts. It also helps toward standardization since the same equipment and components can be re-used in multiple sites. For example, seismic base isolation is considered essential for the deployment of pool-type Sodium

Fast Reactors (SFRs) and Advanced High Temperature Reactors (ATHRs), where the reduced horizontal accelerations enable the use of thin-walled reactor vessels. Chapter 2 presents the fundamental principles of seismic base isolation and reviews current base isolator technology.

The U.S. Advanced Liquid Metal Reactor (ALMR) program developed the first fully engineered seismic base isolation system using (at the time, the 1980's) novel laminated rubber and steel sheet isolators. A summary of the analytical studies on the base isolation of the prototype PRISM and SAFR designs as well as experimental studies to assess the lateral deformation capacity and vertical stiffness of layered rubber isolators is presented in by Tajirian et al. (1990). The 1994 ALMR design (ALMR, 1994) used 66 seismic isolators to support a total base-isolated structure weight of 20,900 t (46,000 kips), which included the reactor primary system, steam generators, and associated building structures. The ALMR power conversion system, which consists of a steam turbine power plant fed by two independent reactor modules, was not base isolated. The isolators' stiffness was selected to provide a fundamental vibration period of 1.33 seconds, thus filtering out seismic input energy associated with shorter vibration periods (higher frequencies). While the PRISM plant has not been built, seismic base isolation has been used in power reactors constructed at the Koeberg site in South Africa.

The most important new structural design criterion for new U.S. nuclear power plants, since the original development of the ALMR design, is a new U.S. Nuclear Regulatory Commission (USNRC) requirement that all new plant designs seeking design certification include analysis for crash of a commercial aircraft into the reactor building. Popular discussion of reactor structures commonly refers to a "containment" that is capable of protecting internal equipment from severe external events and containing radioactive materials that might be released in a core-damage accident. In modern reactor structures these two functions are separated.

In this report, we refer to the *external event shell* as the external walls of a reactor building, which accommodates and transfers loads from external missiles such as aircraft, and prevents penetration of objects or fuel into the building. Most commonly, due to their substantial height (typical LWRs and SFRs are 75 to 80 m tall, while AHTRs are 35 to 40 m tall), the reactor building is constructed partially below grade. However, the reactor building can also be constructed fully below grade, with berms, or deep underground at the expense of increased excavation and retaining wall costs, and complications for equipment and personnel access. The Humboldt Bay nuclear plant, a 65-MWe boiling water reactor built in 1963 in California, used below grade construction where a caisson was sunk and plugged and the plant built inside it. But underground construction has not been used subsequently for large nuclear plants. Inside the external event shell, there is a *citadel* that provides the containment or confinement function for retaining radioactive material that might be released from a reactor core during an accident.

If an airplane crashes into a seismically base isolated structure, the crash will impart momentum to the base isolated structure as a whole, with peak linear and angular accelerations being strongly dependent upon the isolated building mass and on the

aircraft mass, speed, and location and direction of impact. In general, for lighter modular reactors the imparted acceleration may be excessive, even if the mass of the power conversion system is added to the base isolated mass. Alternatively, if the external event shell is coupled to the ground, or if the structure is located below grade, limited or no loads will be transmitted into the base isolated structure. Aircraft crash into a reactor building will also generate large localized forces, induce local inelastic response and damage, and produce debris that may act as interior missiles. New methods for steel-plate/concrete modular construction, now being used in the Westinghouse AP-1000 reactor, have substantially improved local inelastic response of the external event shell (called a shield building by Westinghouse) and reduced the chances for penetration and generation of interior missiles, compared to conventional reinforced concrete construction. Nevertheless, sufficient space should be provided between the external event shell and the citadel so that localized inelastic response of the shell or differential movement between the shell and the citadel does not result in damage to the citadel. Chapter 2 discusses the different configuration and construction options for the external event shielding and the citadel.

In order to use simulation results for base-isolated nuclear structures in a USNRC Design Certification application, a significant amount of effort can be expected to demonstrate that the results accurately represent the anticipated physical system. Chapter 3 reviews some of the general verification and validation challenges for the modeling and simulation of base-isolated structures. The discussion includes observations and insights based on limited historical experiences, currently accepted simulation methods, and the representation of the non-linear behavior of base-isolators under large deformations. An approach for the validation of models for isolated structures is presented with anticipated experimental needs.

Reactor-building structural loads arise from several sources. Chapter 4 reviews the loads that are created by earthquakes, aircraft crashes, blasts, and internal loads generated by reactor equipment under normal and accident conditions.

Chapter 5 discusses the role of integrating key reactor safety systems with both seismic base isolation and event shell design options. The design certification process for Gen IV reactor types is currently in the speculative phase with the regulator's focus being primarily on ALWR build proposals. However, it is reasonable to expect that technology-neutral framework will emerge for Gen IV reactors that will be performance-based and risk-informed with some additional conservatism due to potential issues commonly associated with first-of-a-kind technology. The design certification process provides the reactor vendor with the basis for design optimization while ensuring required operational performance. An additional focus of Chapter 4 is to investigate the role of transforming this process into a technology-neutral one where new structural design options can be compared and further evaluated. The role of reactor design criteria with regard to safety and security is also discussed.

Chapter 6 presents simplified parametric analysis for modular reactor structural performance to earthquake and airplane impact excitations. The approach is consistent with ASCE 43-05 principles (ASCE, 2005), which are under study but have not as yet

been endorsed by the NRC. Four performance issues are addressed. First, building lateral and vertical displacements as well as rotations due to accidental torsion and off-center impact are investigated to evaluate the ability of the isolation system to sustain them. Second, potential for non-linear response of the structure above the isolation systems level are investigated. Third, the interface with and impact on reactor safety functions (reactivity control, decay heat removal, containment) and on balance-of-plant (BOP) interface design is evaluated for different safety system and BOP design options. This evaluation provides data allowing a quantitative comparison of the considered base isolation design options.

There is very strong feedback between the design approaches taken to achieve seismic base isolation, to accommodate new requirements for aircraft crash resistance, to accelerate construction using steel-plate/concrete structural modules, to achieve physical security and access control, to control reactivity and decay heat removal, and the design of the balance of plant systems including power conversion. These choices impact design, regulatory review and permitting, as well as construction materials quantities, and construction time, and ultimately affect construction cost. Chapter 7 reviews these issues, to provide a basis for making informed choices between these design options early in the development of Gen IV modular reactors.

References

- ALMR Reactor Facility Seismic Analysis, Bechtel National, Inc., October 1994.
- American Society of Civil Engineers, “Seismic Design Criteria for Structures, Systems and Components in Nuclear Facilities”, ASCE Standard No. 43-05, p. 103, 2005.
- Schlaseman, C. “Application of Advanced Construction Technologies to Nuclear Power Plants”, Technical Report MPR-2610, Revision 2, p. 132, US DoE, September 24, 2009.
- Tajirian, F.F., J.M. Kelley and I.D. Aiken, “Seismic Isolation for Advanced Nuclear Power Stations”, *Earthquake Spectra*, Vol. 6, No. 2, pp. 371—401, 1990.

2.0 BASE ISOLATION, EXTERNAL EVENT, AND MODULAR CONSTRUCTION DESIGN OPTIONS

Multiple technical options exist for implementing seismic base isolation, external event shielding, and modular construction. This chapter reviews these options and discusses tradeoffs.

2.1 Seismic Base Isolation

Structural engineers typically employ one of two strategies to protect buildings from the damaging effects of earthquakes. In the first strategy, engineers design the lateral force resisting system to be very stiff, producing a structure with a short natural period (or high natural frequency), small drifts and large accelerations in design earthquake shaking. Such framing systems will protect drift-sensitive components (such as masonry walls) but could damage acceleration-sensitive components (including mechanical equipment, computers, and electrical systems). Historically, engineers of nuclear structures have used this design strategy to make sure that horizontal deformations in nuclear power plants are very small. Reinforced concrete nuclear power plant structures have been designed using stiff structural systems such as reinforced concrete shear walls or steel braced frames that remain essentially elastic in design earthquake shaking but are detailed per ACI 349 (ACI 2006) to respond in a ductile manner in the event of shaking more intense than the design basis. Nuclear plant structures also commonly use very thick concrete structures to provide radiation shielding. These approaches differ from conventional building design wherein substantial inelastic response and damage is anticipated in design basis shaking.

In the second strategy, engineers design the lateral force resisting system to be flexible, producing a structure with a long natural period (or small natural frequency). Moment frames of structural steel and reinforced concrete are typical flexible seismic framing systems. As a result, earthquake-induced horizontal accelerations and forces are (relatively) small, but transient drifts are large, requiring structural elements and details that allow for large deformation capacity and significant resilience, and residual drifts might be significant. This design approach is common for steam turbine buildings, particularly for pressurized water reactor (PWR) plants. The turbine-generator may be spring mounted to isolate it vertically and horizontally. Gen IV plants may use compact closed gas cycles, which would likely be mounted on the same base-isolated foundation as the reactor. Vertical isolation may still be required for turbine-generator equipment.

Seismic isolation is a structural design approach that aims to control the response of a structure to horizontal ground motion through the installation of a horizontally flexible and vertically stiff layer of *structural isolation hardware* between the superstructure and its substructure. The dynamics of the structure is thus changed such that the fundamental vibration period of the isolated structural system is significantly longer than that of the original, non-isolated structure, leading to a significant reduction in the accelerations and forces transmitted to the isolated structure and significant displacements in the deformable, structural base isolation, layer. The structural base isolation devices are designed to sustain such large deformations without damage and to return the structure to its original positions, thus leaving no residual deformation. The structure above the

isolation layer is designed to sustain the (reduced, and well-known) horizontal forces transmitted through the isolation layer, usually such that it responds in its elastic response range and remains undamaged. Vertical forces are transferred un-attenuated, but in general it is easier to design structures and equipment to sustain vertical forces, and where necessary, individual equipment items can be isolated for vertical forces using spring-damper systems. The design of the isolator system must include sufficient space for access to inspect and replace individual isolators. The components of a horizontally seismically isolated structure are shown in Figure 2.

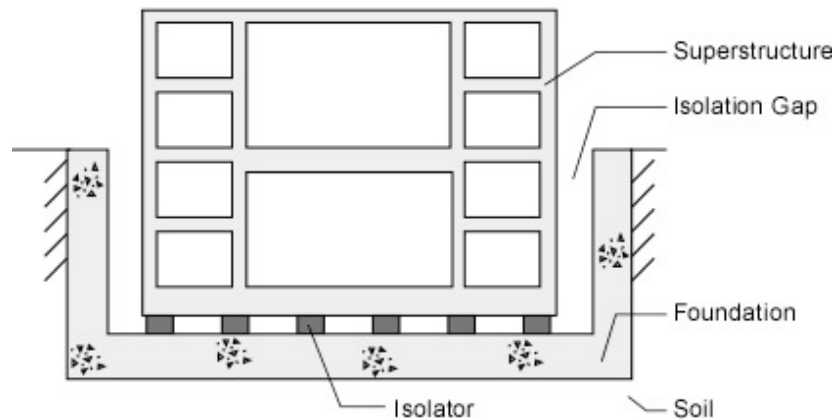


Fig. 2. Components of a base isolated structure shown in elevation.

Application of base isolation spread to the nuclear power industry with the completed construction of plants in Cruas, France (1983) and Koeberg, South Africa (1984). Both plants utilized neoprene pads and sliders, a system later deemed inappropriate for seismic application in the United States and subsequently rejected in future plans in favor of newer isolation types (Malushte and Whittaker, 2005). To date, there are 6 nuclear power plants utilizing base isolation, all in France or South Africa.

Despite the lack of approved base isolated NPP designs in Japan and the United states, regulations exist in both countries which could eventually make them a reality. High seismicity and the expectation of high-frequency ground motions have led to harsh design guidelines which retard the approval of NPP designs in the US. US Nuclear Regulatory Commission Regulatory Guide 1.165 (NRC, 1997) imposes the strict requirement that the seismic design of NPP's be based on a probabilistic seismic hazard assessment (PSHA) for a 100,000-year return period. Although many contend that base isolation is a cost-effective way to achieve adequate response under such extreme loading events, the relative infancy of the technology and limited in-field data of its response hinder its implementation in new NPP designs.

2.1.1 Dynamics of a Seismically Isolated Structure

The seismic design acceleration and displacement spectra shown in Fig. 3 illustrate the trade-off between horizontal displacements and horizontal accelerations in seismically isolated structures. A seismic design spectrum plots the peak spectral acceleration or spectral displacement versus the fundamental vibration period of a structure under expected earthquake ground motion excitation. Fundamental vibration

periods for an isolated and fixed-base (or non-isolated) structure are shown: clearly, as the fundamental vibration period of the structure increases (the structure becomes more flexible), horizontal accelerations and, therefore, the seismic inertial forces decrease. Simultaneously, horizontal displacements increase as the vibration period increases. These increased displacements of the isolated superstructure, however, are concentrated in the seismic isolation layer because it is much more flexible than the superstructure. These displacements are accommodated by providing enough space around the superstructure, a seismic isolation gap (Fig. 2), for it to freely travel during an earthquake. The deformation (inter-story drifts) and horizontal floor accelerations in the isolated superstructure will be smaller than those in its fixed-base counterpart because the inertial forces acting on the superstructure are much smaller.

The efficacy of any isolation system is dependent on the ability of the isolators to alter the fundamental period of the structure such that it is significantly larger than that of the non-isolated structure, inducing a response that is far past the acceleration-sensitive region of the earthquake spectrum (Chopra, 2007). This means that base isolation is most appropriate for structures with naturally short non-isolated periods, such as nuclear reactor buildings, existing in environments where damaging earthquake motions are expected to have short predominant excitation periods. In such environments, the period shift will greatly reduce superstructure accelerations and drifts. Care must be exercised, however, to consider potential earthquake motions that may include significant longer-period accelerations, as may be the case for softer types of soil conditions. An example is presented in Chapter 6. A typical force-displacement relationship for a seismic isolation device or system is shown in Figure 4. The isolation device is expected to respond to an increase in displacement in a non-linear manner: the yield point (designated as (F_y, u_y)) marks a significant change in the stiffness (inverse of compliance) of the device. Comparatively low post-yield stiffness causes the elongation of the fundamental vibration period of the structure and limits the force transferred through the isolator device to the structure. In the frequency domain, the isolator device acts as a filter for high-frequency components of the horizontal ground motion excitation. Furthermore, the hysteretic energy dissipated by the isolation device during repeated cyclic horizontal motion serves to reduce the lateral displacement of the isolator devices and to further reduce the inertial forces transmitted to the isolated superstructure.

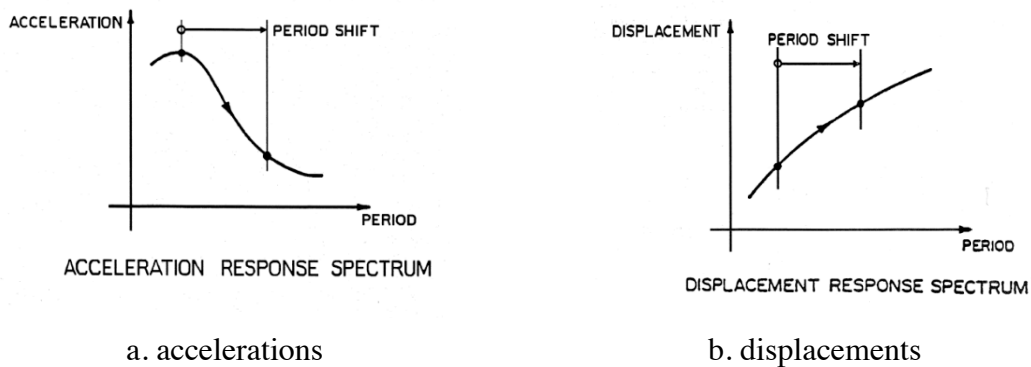


Fig. 3. Impact of period elongation obtained by seismic isolation on accelerations and displacements of a structure.

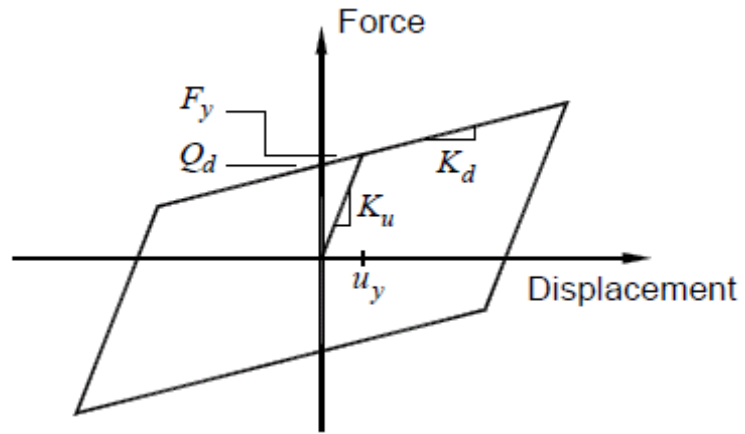


Fig. 4. Typical relationship between displacement and force for a seismic isolation device.

2.1.2. Types of Horizontal and Vertical Seismic Isolation Devices

Horizontal isolation systems are categorized as either elastomeric or sliding systems, with different mechanical properties for each. These systems are briefly summarized in the following paragraphs. Vertical isolation is also possible using spring-damper systems. However, given the large mass of a typical nuclear reactor building, vertical isolation would normally be provided only for individual, sensitive equipment, or for isolated volumes such as a reactor control room, but not for the entire reactor building.

The first type of horizontal seismic isolation device is a laminated elastomeric bearing, shown in Fig. 5. The elastomeric material in the bearings is natural rubber, which has low horizontal shear stiffness but high vertical compressive stiffness. The low horizontal stiffness and large deformation capacity of the elastomeric material is used to provide the horizontal flexibility necessary for structural seismic isolation. The rubber is present in horizontal layers that are bonded to horizontal steel shim plates in a process called vulcanization, which forces the rubber to deform in shear and prevents vertical buckling. The resulting bearing is more stable and its motion is more predictable. The horizontal stiffness of the bearing depends primarily on the shear modulus of the rubber, the bonded area of rubber, the total thickness of rubber and the lateral displacement of the device. The reduced stiffness not only increases the building period, but also filters-out higher order mode participation by capitalizing on the principle of modal orthogonality. Additionally, elastomeric bearings re-center after earthquake shaking due to the forces generated by elasticity of the rubber layers.

There are three main types of elastomeric bearings: low damping bearings, lead rubber bearings, and high damping bearings. Two of the three, low-damping rubber (LDR) and lead-rubber (LR) are suitable for nuclear power plant applications (Huang et al. 2009).

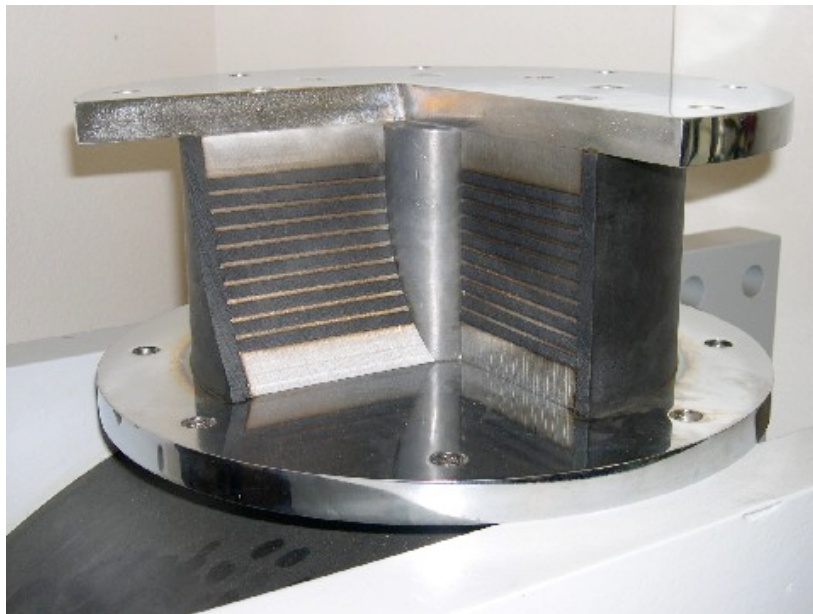


Fig. 5 Cross section of a typical lead-rubber seismic base isolation bearing.

The second type of seismic isolation devices is the sliding bearing. Horizontal flexibility of such isolation systems is provided by sliding, while their vertical stiffness is provided by direct contact of the bearing elements. Control of motion of sliding bearings is achieved by designing the shape of the contact surfaces, by designing the friction coefficients between the contact surfaces, and/or by adding supplemental damping. The friction specifically limits the amount of force transferred to the superstructure. Typical European devices use friction and supplemental damping to dissipate energy. On the other hand, the Friction Pendulum™ family of bearings that dominates the US market, shown in Fig. 6, uses a concave contact surface to control the motion of the bearing and the isolated superstructure. As the isolated structure moves horizontally due to earthquake excitation, the concave surface of the bearing forces it to also move upward, against gravity, and slows it down. The radius of the concave contact surface, as well as the friction coefficients between the sliding surfaces, are designed to give the Friction Pendulum bearings desirable dynamic properties, such as stiffness and hysteretic damping. More important, the concave surface insures re-centering, thus making the Friction Pendulum bearing also suitable for use in nuclear power plant applications.



a. Single concave



b. Triple concave

Fig. 6 Friction Pendulum™ bearings (courtesy of Earthquake Protection Systems, Inc.)

Vertical isolation can be achieved using spring and damper systems. Figure 7 shows a typical example. Because of the stability issues associated with isolating large vertical loads, development of vertical isolation systems for entire structures has lagged in comparison to horizontal systems.



Fig. 7 Helical springs and viscous dashpots (GERB) for vertical isolation.

2.1.3. Supplemental Damping and the Isolation Gap

Isolation systems are often designed with supplemental damping systems in order to reach adequate levels of energy dissipation. Supplemental damping can also be used to reduce high amplitude response, however, design of isolation systems should be accompanied by the caveat that excessive amounts of damping can fundamentally inhibit their efficacy.

Isolation gaps are designed to assure the superstructure responding to design-level ground motions remains isolated from the surrounding structure. However, surrounding structure, or barrier, serves an essential role in reducing the beyond design-basis displacements. The exact response and underlying mechanics of collisions with the barrier should continue to be studied.

2.1.3. Seismic Isolation Design Basis

A base isolated nuclear facility structure has three components: the super-structure, the isolation layer and the foundation embedded into the underlying soil, as illustrated in Fig. 2. The seismic isolation devices are treated as structural components and thus fall inside the domain of structural design code requirements. Thus, for this study the design basis for all three components is consistent with ASCE Standards 4, 7 and 43. Beyond these ASCE standards, NRC requirements must also be considered, as discussed in the USNRC Standard Review Plan (NUREG 0800, Sect 2.5) and Regulatory Guide 1.122 Rev.1.

ASCE 43-05 defines a Design Basis Earthquake (DBE) using Probabilistic Seismic Hazard Assessment (PSHA) to derive a Uniform (or Equal) Hazard Response Spectrum (UHRS) for the site and modify it further using a Design Factor. The Design Factor is calibrated to limit the annual seismic core damage frequency to under 10^{-6} considering the failure probabilities specified in current structural design codes and the design goals proposed in ASCE 43.

The design goal is to *reasonably* achieve both of the following design objectives:

1. Less than 1% probability of unacceptable performance for the Design Basis Earthquake DBE ground motion defined in Section 2.0 of ASCE 43-05.

2. Less than 10% probability of unacceptable performance for a ground motion equal to 150% of the DBE ground motion defined in Section 2.0 of ASCE 43-05.

A probabilistic design method proposed in ASCE 43-05 achieves these two objectives simultaneously by specifying performance goals. The performance goal has a quantitative and a qualitative part. Quantification of the performance goal is probability-based: a mean annual hazard exceedance frequency H_D (associated with the UHRS) and a Target Probability Goal in terms of annual frequency of exceeding acceptable behavior, P_F , are defined. The (H_D, P_F) pair defines the quantitative probabilistic performance goal, expressed conveniently as a probability ratio $R_P = H_D/P_F$. The qualitative performance goal is defined using the Limit State concept to describe qualitatively the acceptable structural behavior. ASCE 43 defines 4 Limit States, based on structural deformation levels, to describe levels of acceptable structural damage. These damage states range from significant damage with a structure close to collapse (state A) to no significant damage with a structure in operational condition (state D). The qualitative and quantitative portions of the performance goal are combined in the definition of the Target Probability Goal P_F .

ASCE 43 defines 5 Seismic Design Categories (SDC). Categories 3, 4 and 5 are associated with nuclear facility structures, systems and components (SSC) through ANSI/ANS 2.26. Table 1 lists the Target Probability Goals for each of these categories.

Table 1. Target annual probability goals for ASCE 43 Seismic Design Categories 3, 4, and 5 (from ASCE 2006)

| | SDC3 | SDC4 | SDC5 |
|-----------------|---------------------|---------------------|---------------------|
| P_F | 10×10^{-5} | 4×10^{-5} | 1×10^{-5} |
| H_D | 40×10^{-5} | 40×10^{-5} | 10×10^{-5} |
| $R_P = H_D/P_F$ | 4 | 10 | 10 |

The target performance objective for nuclear power plant structures is SDC-5D. This performance objective is associated with an annual probability of unacceptable performance of 1×10^{-5} . Acceptable performance in fixed-base nuclear power plant structures is described as “essentially elastic behavior”. This performance description is associated with conventional structural framing such as concrete shear walls and moment frames and the foundations.

In base-isolated nuclear structures, the accelerations and deformations in structures, systems and components are expected to be relatively small, such that the SSC’s are expected to remain elastic for both DBE shaking and beyond design basis shaking. As such, unacceptable performance of an isolated nuclear structure will involve either the failure of isolation bearings or impact of the isolated superstructure against the surrounding building or geotechnical structures. Therefore, unacceptable performance of

seismic isolation devices is defined as: 1) permanent damage to the isolation device, such as tearing or disassembly; 2) exceedance of displacement limits of the device. The acceptance criteria for isolation devices should be set such that there is a high confidence of low probability of failure and that the overall target annual seismic core damage frequency does not exceed the value required by USNRC. The superstructure and the foundation of the isolated structural system are required to comply with the SDC-5D performance objective set in ASCE-43.

2.1.4 Benefits and Challenges of Seismic Isolation

The potential benefits of seismic isolation to the nuclear power industry are numerous. Seismic isolation can simplify the design, facilitate the standardization, and reduce the cost to build new nuclear power plants, as well as improve the seismic performance, enhance the safety margins, and enable a more accurate evaluation of the probability of failure. The notion of seismic base isolation can be expanded to a general concept of structural response modification and control. Thus, seismic isolation devices can be viewed as a part of a portfolio of force limiting, vibration filtering, damping and energy dissipation devices that can be passive or actively controlled. Response modification technologies are being developed for conventional structural systems, but have not yet matured to the level of application in construction achieved by the seismic base isolation technology.

There are challenges for design, implementation and construction of base isolated nuclear power plant structures. The first group of challenges is associated with the site of the power plant. The seismicity of the site may include hazards stemming from near-by faults, expected to cause large unit-directional velocity pulses and permanent ground displacement at the site, as well as hazards from far-away faults capable of developing extremely large ground motions, expected to induce long-duration ground shaking with the majority of the seismic energy in the long-period (low-frequency) range. A base isolated structure may suffer large single-pulse displacements or resonate with the ground motions in the long-period range in these cases, presenting a design challenge.

The soil conditions at the site may present a design and an analysis challenge. Soil-structure interaction (SSI) must be analyzed in design. If the soil column under the foundation is soft, it may adversely alter the frequency content of the incoming ground motion such that the energy is shifted towards the long-period (low-frequency) range. Similar to the long-duration ground motion, this may cause the base-isolated structure to resonate with the motion and develop large displacements in the isolation system. The non-linear response of the isolators (and the underlying soil) requires time-domain non-linear modeling and analysis capabilities. While such software exists, it has not been used to design nuclear power plants in the past. Deployment of such time-domain analysis method would be a departure from the frequency-domain analyses done to date, but may be unavoidable because of the expected non-linear behavior of the seismic isolation devices.

The second group of challenges is associated with the response of the seismic isolation devices to ground motion excitation. In response to the horizontal components of the ground motion, the isolation devices will sustain large displacements, requiring the

superstructure to move. If the superstructure is embedded and/or enclosed by the external event shell, the seismic isolation gap needs to be large enough such that there is a very small chance of the superstructure impacting the surrounding structures. Such impact may damage the isolators and induce high-frequency high-intensity forces in the isolated structure: thus, it should be avoided by conservative design, as well as the potential provision of dampers or bumpers. In response to the vertical component of the ground motion, the two types of isolation devices considered for nuclear power plant applications (lead-rubber bearings and Friction Pendulum bearings) will transmit this excitation to the superstructure without any reduction. Furthermore, overturning moments and, possibly, uplift, may cause additional amplification of the vertical excitation. Additional research is needed to develop a better understanding of the propagation of vertical ground motion through soil and the seismic isolation layer into the structures. For equipment mounted on slabs and for horizontal runs of piping, vertical accelerations may be as severe or more so than horizontal motion.

The third group of challenges is associated with the transfer of the generated power from the isolated part of the nuclear power plant, the citadel, to the balance of the plant. Regardless of the medium used to transfer this generated power (electricity or heated fluid), these conduits as well as many others (utilities, power, instrumentation) will have to traverse the seismic isolation gap and accommodate the differential motion between the two anchor points. Design of such “umbilicals” presents a mechanical engineering challenge. This is particularly the case for high-temperature, high-pressure fluids like steam, where beyond-design-basis displacements of main steam lines may result in a main steam line break (MSLB). Because the break would occur at the base isolation gap, which is outside the reactor containment, valves would be available to isolate the steam generator from the break, but the MSLB would still result in a severe thermal transient for the steam generator and would disable its capacity to act as a long-term heat sink. Conversely, Gen IV modular reactors that use compact, closed gas cycles (supercritical CO₂ or multi-reheat helium Brayton cycles) may mount the reactor and power conversion system in a common base-isolated structure and eliminate the need for high-temperature umbilicals. In addition, due to the very large mass of reactor buildings the design of umbilicals must consider long-term soil settlement that can generate similar differential offsets between the building and surrounding structures.

While serious, the three groups of challenges for use of seismic base isolation in nuclear power plant structures have been encountered and successfully solved to seismically isolated conventional, but critical, building structures such as hospitals and lifeline facilities such as long-span bridges and LNG storage tanks.

2.2 External Event Shielding

Malicious crashing of a commercial aircraft creates loads that greatly exceed those that might be expected from missiles generated by natural events such as tornados. Aircraft crash into a structure can be expected to generate both significant global structural demands that may exceed design basis earthquake or wind loads as well as localized inelastic structural response in the vicinity of the impact point. Additional demands on the NPP structures, systems and components in this beyond design basis

event may come from blast air pressure waves, penetrating aircraft parts and/or structural debris acting as interior missiles, and fire. This section presents a comparative analysis of structural layout concepts for an external event shell of a seismically isolated nuclear power plant. Section 2.3 provides a comparison of the conventional reinforced concrete construction and newly proposed steel-plate/concrete modular construction technologies with respect to local behavior at the impact point. Section 6.4 presents design and impact load response analysis for a sample conventional reinforced concrete external event shell.

In general, three major design variants can be considered for external event isolation of a base-isolated reactor, as illustrated in Fig. 8. First, the entire reactor building structure, including the external event shell, can be base isolated (Fig. 8A). This option may be acceptable for very heavy structures, such as large LWR reactor buildings. Second, base-isolated citadel may be placed inside a separate, decoupled external event shell (Fig. 8B). Various options may exist to use the volume between the external event shell and citadel productively, for example to house non-safety related equipment or redundant safety related equipment, or to act as a duct for intake of external air for emergency decay heat removal. Finally, the entire reactor building may be base isolated and constructed fully below grade, with or without berms (Fig. 8C). These design options involve issues related to construction cost and schedule, access for personnel and equipment for operations and maintenance, umbilical arrangements for transferring the generated power from the plant and transmitting control commands to the plant, and ducting arrangement if external air is used as a heat sink for decay heat removal. Also, for partially or fully below-grade event shells, steady-state and seismic soil and hydrostatic loads may be substantial and must be considered in design, and the pits must have drainage and dewatering system.

The following sections describe each major design option in greater detail.

2.3.1 Coupled above-grade event shell and citadel

Conceptually, the simplest way to implement seismic base isolation is to isolate the entire reactor building, including the external event shell, on a single base isolated foundation, as shown in Fig. 7A. This approach allows conventional reactor building arrangements to be adopted with minimal changes, and is the approach used in the original ALMR design (ALMR 1994). Note, it is assumed that the foundations for conventional reactors will be at least partially excavated to remove the shallow surface soil and reach rock and/or firm soil layers. Thus, the seismic isolation gap required for base isolated designs would have to be provided by the increased size of the excavated opening: this configuration is commonly called the “isolation moat”.

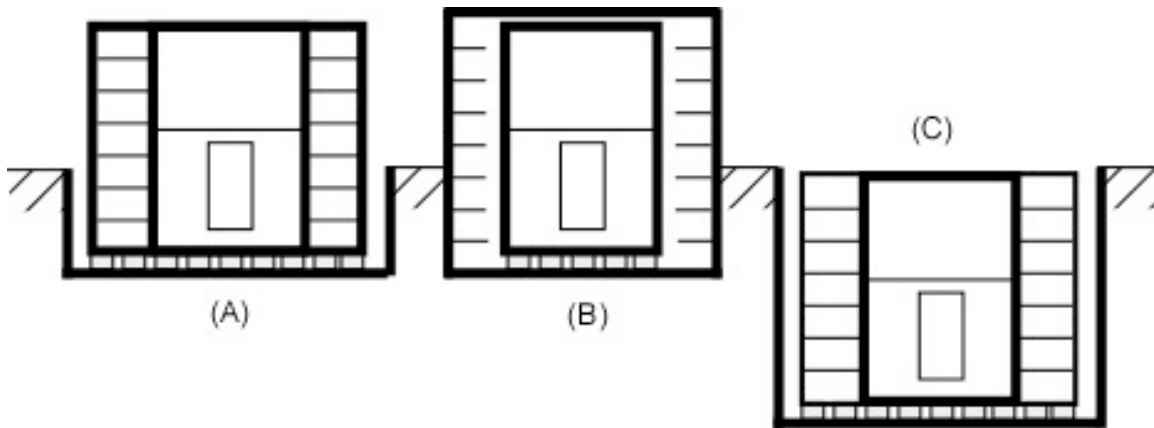


Fig. 8 Three major external event isolation design options for base isolated reactors: (A) above-grade, coupled event shell and citadel, on a single base isolated mat, (B) above-grade, decoupled event shell and citadel, and (C) fully below-grade construction.

The major design issue with a coupled event shell and citadel relates to the accelerations that are imparted into the citadel during an airplane crash. These accelerations are dependent upon the mass of the isolated structure, as well as the mass and speed of the aircraft and its location and direction of impact. Increasing the isolated mass is beneficial. For example, two or more reactor modules might be constructed on a single base-isolated foundation. Likewise, the plant power conversion system might be coupled to the reactor building foundation. This particular option has the additional benefit of eliminating the need for high-temperature intermediate coolant pipes to span a base-isolation gap to the power conversion system and to be designed to sustain substantial deformations during earthquakes (discussed in Chapter 5).

Typical modular reactor designs may have reactor building masses ranging from 20,000 to 60,000 metric tons, with the larger values being possible when the power conversion system is isolated on a single foundation along with its power conversion system, or if two modules are isolated on a common foundation. Modern LWR reactor buildings can be much heavier, as for the EPR and ABWR shown in Table 2. With the trend toward passive safety systems for LWRs, reactor building sizes and masses will likely decrease toward lower values, as for the early design of the ESBWR reactor building given in Table 1.

A reasonable criterion to establish the minimum acceptable reactor building mass is that the acceleration induced by aircraft crash be enveloped by the accelerations originating due to seismic motion, so that the aircraft crash beyond design basis case does not end up affecting equipment seismic qualification requirements. As discussed in Chapter 6, for reactor buildings in the mass range of modular reactors, accelerations induced by aircraft crash are likely to substantially exceed those induced by earthquakes. Furthermore, it can be assumed that the design-basis aircraft crash may evolve over time to include crashes of increasingly heavier aircraft.

Some possibility exists that advanced isolation devices could be designed that would lock-out under aircraft crash conditions, transferring the crash loads to the ground and

limiting acceleration of the base isolated mass. Absent such an approach, however, this report recommends that the external event shell for modular reactors be decoupled to the base isolated mass of the citadel.

Table 2 Approximate total mass of typical LWR reactor buildings (Peterson et al., 2005).

| Reactor | Concrete (m ³) | Steel and Iron (metric tons) | Total Weight (metric tons) |
|----------------------|----------------------------|------------------------------|----------------------------|
| 1970's PWR (1000 MW) | 22,600 | 7,500 | 59,500 |
| ABWR (1350 MW) | 67,500 | 18,500 | 174,000 |
| EPR (1600 MW) | 61,900 | 18,500 | 161,000 |
| ESBWR (1500 MW)† | 29,200 | 8,900 | 76,000 |

† The ESBWR underwent a substantial structural redesign that increased its weight from the value shown here.

2.3.2 Decoupled above-grade event shell and citadel

With a decoupled “box-in-box” external event shell, the shell transfers aircraft impact loads directly to its foundation. The event shell foundation can be coupled to the foundation of the base-isolated citadel, such that the impact load is transferred to the ground, as it would be in a conventional, fixed-base NPP. The reactor citadel, inside the event shell, is base isolated. A gap is provided between the event shell and the citadel. This gap must accommodate the differential motion between the shell and the citadel due to earthquakes (the seismic isolation gap) and that due to the deformation of the event shell or its foundation caused by aircraft crash. Likewise, the gap must be sufficient to accommodate rocking and torsion generated by eccentric loads, particularly for hard rock sites.

Two basic geometries can be considered for external event shells. The curved surface of a cylindrical event shell (Fig. 9A) increases the structural strength of the shell through arching action. This allows impact loads to be transferred to the ground in part as tensile and compressive stresses in the wall, rather than as bending stresses (except locally at the point of impact). The seismic separation gap between the cylindrical shell and the base isolated citadel can be smaller compared to that required for rectangular geometries because radial symmetry makes it easier to accommodate maximum ground motion demands and torsion caused by mass eccentricity, rocking, and vertical interactions. Cylindrical event shells are particularly well suited for reactors that use large, dry containments. In the AP-1000, this gap is used to duct external air flow in through vents located near the top of the shell, down an annulus formed by a baffle plate, and then up over the metal containment vessel to remove decay heat during accidents.

A rectangular external event shell has large, flat walls (Fig. 9B), which may enable simpler construction methods. These walls must act as plates to transfer impact loads to the side walls and roof diaphragms by bending, which then transfer the loads by bending and shear to the base mat. Bending resistance of the exterior event shell wall may be

efficiently increased by integrating beam and columns into the inside surface of the wall, either in a honeycomb or ribbed configuration. In particular, floors inside the event shell can act as beams (Fig 9B) offering the required structural depth. This approach may be attractive because this creates an accessible volume that is available to house equipment, piping, cabling and ventilation ducting and to provide personnel access. However, if the internal citadel is base isolated, a gap must be engineered into the floors, with a grating and an expansion joint system, to allow for large differential motion between the shell and citadel. The grating system must also function as a water-proof and debris-clean barrier. Sumps and pumps are needed at the bottom of the pit to keep it dry, and must be redundant in case of a system failure. Note that the equipment and piping that are supported by the external event shell must be qualified for seismic loading expected in fixed-base structures, while equipment which is mounted on or cantilevered from the base isolated citadel can be qualified based upon the seismic response of the attachment points of the seismically isolated structure.

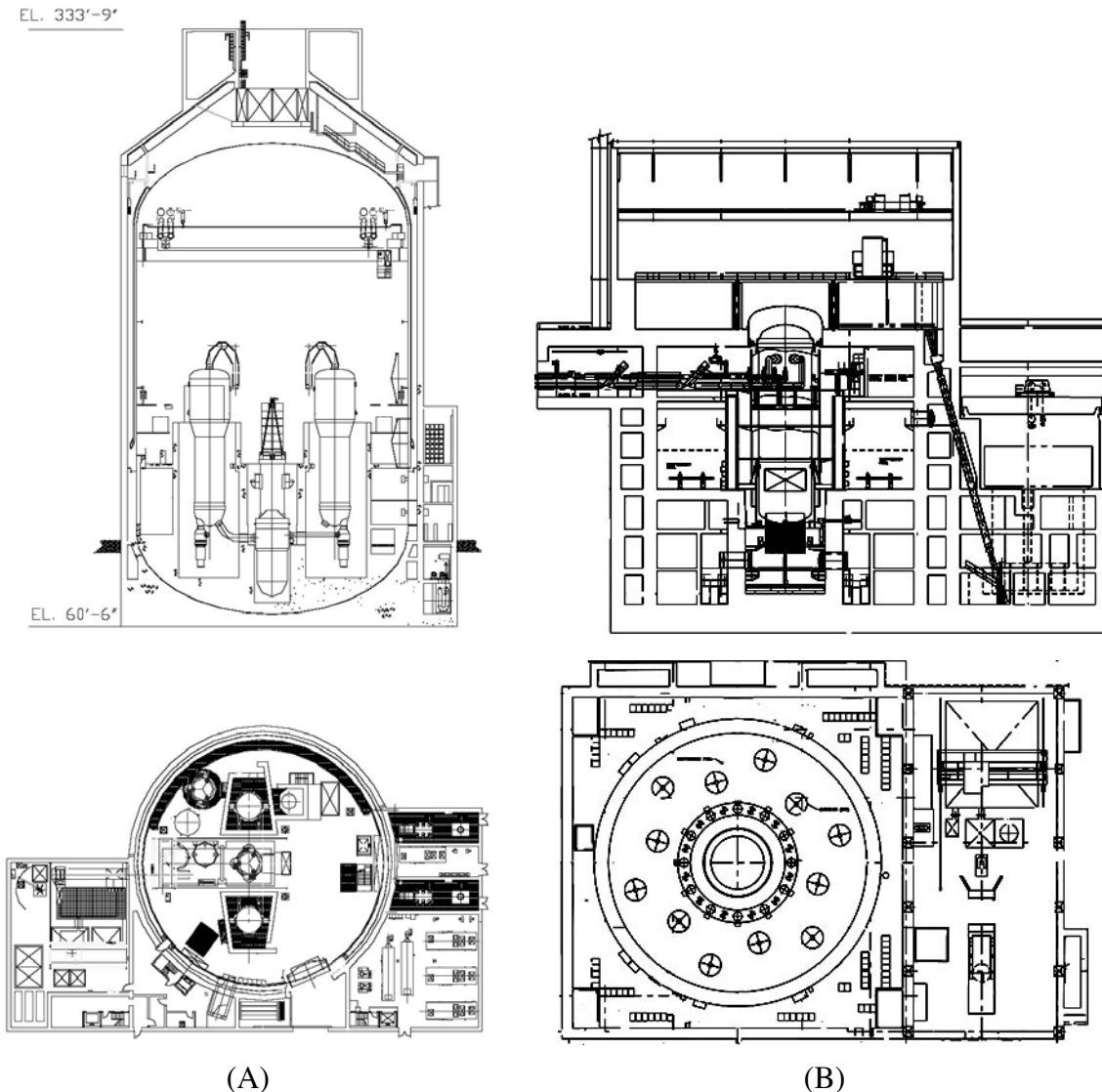


Fig. 9 Examples of (A) a cylindrical external event shell (AP-1000) and (B) a rectangular external event shell (ESBWR).

The principal design challenge in decoupled event shell and citadel configuration are the overhead cranes mounted on rails resting on opposite walls of the structure. Crane rails can be supported on columns framed into the base isolated citadel structure, so that the crane is also isolated from seismic motion, and so that differential motion between the crane and reactor structures is minimized during earthquakes. But it is optimal to design cranes to be capable of picking up loads close to walls: in a decoupled design significant portions of the floor space attached to the fixed-base event shell structure may not be reachable by the crane mounted on the base isolated citadel. This requirement may limit the space for and configuration of the stiffening ribs or honeycomb on interior of the external event shells, if rail-based reactor-service cranes are located in an open volume above the reactor citadel (as is common practice for boiling water reactors, Fig. 9B).

2.3.3 Berms, below grade, and underground construction

Construction of a reactor below-grade requires that the reactor be constructed in a deeply excavated space. Excavation can be performed by either open-cut or top-down methods, with crane access being easiest with top-down methods. An important constraint on below-grade construction is the fact that reactor buildings are commonly very tall structures, with typical LWR, SFR, and MHR buildings being 70 to 80 m in height from the bottom of the base mat to the top of the reactor building. The depth of such excavations requires stabilization of the sides of the excavated opening against both passive and active earth and water pressures and may require dewatering and water-proofing. Furthermore, the substantial depth complicates the construction process and increases its cost and schedule. If needed for plant operation, dewatering systems must be redundant and seismic category SI.

The depth and cost of excavation can be reduced compacting the excavated soil into berms around the periphery of the isolation moat, at the expense of increasing the footprint occupied by the reactor substantially and potentially complicating the capability to locate supporting structures such as turbine buildings. In some reactor designs the reactor floor is at the external grade level, such that the structures above grade support and enclose the reactor high bay space. If the reactor refueling floor is sufficiently hardened, it is possible that the structure enclosing the high bay space above the floor does not need to be engineered to have the strength required to exclude penetration by aircraft. However, this may require complex engineering and security analysis for activities such as refueling where the crane is being used to access equipment below the reactor floor, and to analyze for effects large fires on the refueling floor. If the above grade crane-bay structure is hardened to exclude aircraft, then the building falls into the above-grade category.

For reactors that use external ambient air for passive decay heat removal, as is the case for most SFR designs, the air intake and exhaust vents are normally located substantially above grade to prevent snow drifts or drifting sand from blocking the intake vents, and to reduce accessibility for potential sabotage. If below grade construction or berms are used, the associated chimneys extending above grade must be hardened sufficiently to survive aircraft impact loads.

Underground siting has also been studied for nuclear power plants. The California Energy Commission (CEC, 1978) considered two major options, (1) mined-cavern siting, and (2) berm containment and cut-and-cover construction. In mined cavern siting, large caverns, some 30-m wide, 60-m high, and a few hundred meters in length, would be excavated from solid rock. The nuclear reactor is then constructed in the cavern, after all rock motion has ceased. In the second option, a large pit approximately 120-m in diameter and 45 m deep is excavated, and the nuclear power plant built in the pit. The excavated material is then mounded over the entire plant. The CEC study identified several potential benefits from underground siting, including more effective containment of radionuclides following a severe core damage accident, improved earthquake resistance, easier decommissioning, improved resistance to sabotage, and urban siting (CEC, 1978).

The CEC study concluded that construction of both mined-cavern and berm contained plants would be technologically feasible. Construction costs for n-th of a kind plants were expected to be 14% higher for berm-contained plants, and 25% higher for mined-cavern plants, compared to a surface-sited plant. Likewise, construction time for n-th of a kind plants was expected to be 22 months longer for berm-contained plants, and 19 months longer for mined-cavern plants. While the study found potential benefits, it concluded that underground siting should not be mandated, due to uncertainty over costs and construction time, the existence of “what appear to be moderately effective and less expensive technical alternatives,” and the opportunity to implement remote siting. Today, because reactor structures can be engineered to accommodate the effects of severe external events, the additional cost and schedule delays associated with underground siting are likely still not warranted.

2.3 Steel-Plate/Concrete Modular Construction

Conventional, fixed-base, nuclear power plant structures are constructed using the reinforced concrete structural shear wall elements to form the primary gravity and lateral load structural systems. In addition to their load-carrying ability, such walls offer good radiation protection, provide a satisfactory pressure barrier, and offer good fire resistance. The isolated superstructure and the foundations of seismically isolated nuclear power plants may also be constructed using this conventional technology.

The structural reinforced concrete shear walls are erected using the cast-in-place construction method. The forms for such walls are erected first. The reinforcement is placed into the forms, usually using pre-assembled reinforcement cages. Finally, the concrete is poured into the forms, vibrated into place, and left to cure to a strength that allows for removal of forms. While there is ample experience with such construction method in the industry, three obstacles still remain. One is the design of the forms to sustain the weight of the flowing concrete: this limits the height of the pouring lifts, thus constraining the speed of construction. Second is the time needed for concrete to cure to the level where forms can be removed to advance construction. Use of slip-forming for cylindrical walls can accelerate construction. And third is the need to completely remove the forms such that, over time, wood debris left behind does not cause unwanted corrosion. Liner corrosion problems have been observed at existing U.S. nuclear plants due to wood debris left during construction.

The solution for these construction problems is to use so called “stay-in-place” forms. Such forms are, by themselves, structural elements that are capable of sustaining the load of flowing concrete and additional formwork above the pour level. In addition, they can be composited with the poured concrete to become part of the larger structural element. Stay-in-place forms can, furthermore, be pre-fabricated and pre-assembled into large modules, enabling significant speedup in construction.

Stay-in-place forms have been made using a variety of materials. It is not uncommon to use thin reinforced concrete plate elements, or plates made of fiber-reinforced mortars or polymer composites to form structural walls and leave them in place. However, the most common material used for stay-in-place forms is steel plate. As shown in Figure 10(A), steel plates forms can be pre-fabricated as modules of significant size, lifted and

assembled into place, and welded at the contacting seams before additional reinforcement is placed into them (if needed). The concrete pour is then the same as in conventionally-formed walls. Supplementary steel reinforcement may be required in thicker stay-in-place form walls and on the top side of stay-in-place form slabs where no steel plate exists; however, the amount of rebar is greatly reduced. The steel plates are advantageous in that they do not provide unidirectional resistance like rebar. Thus, material savings of concrete, forms, and steel bars/plates were estimated to be 6%, 97%, and 19%, respectively (Takeuchi, 1995). Accordingly, a shift towards prefabrication and on-site skilled steel workers (i.e. welders) is anticipated.

The principal advantage of steel stay-in-place forms is that the form steel can be composited with the interior concrete to form a composite steel-concrete structural element (sometimes called sandwich walls). Steel-concrete composite construction is regulated by structural design code documents: ASCE 7-05 for design of composite structural systems, and ANSI/AISC 360-05 and ANSI/AISC 341-05 for design of composite structural elements for non-seismic and seismic applications, respectively. In particular, a number of research studies support the code design provisions for composite steel plate shear walls, where structural concrete is encased by steel plates and the bond between steel and concrete is maintained to ensure composite load carrying action. The additional confinement of concrete and inhibition of concrete spalling by the surface plates enable higher ultimate strengths and increased ductility of the composite members, particularly under cyclic loading conditions (Munakata, 2009). Figure 10(B) shows the tie bars and steel studs used to maintain spacing of plates during concrete pouring as well as achieve the composite action between steel and concrete. In addition, steel members known as ribs or stiffeners are continuously connected to the steel plates such that they can sustain the hydrostatic pressure of flowing concrete and maintain their form.

An additional advantage of stay-in-place steel forms is the ability to pre-fabricate large and complex modules. Using ship-building techniques, modules comprising a variety of structural openings, corners and attachments can be pre-fabricated in a controlled factory environment and shipped to the construction site. The only limit is the shipping and lift-and-place capability. Figure 11 shows a recent installation of a large (over 700 ton) steel module assembled from factory-prefabricated modules at an AP-1000 NPP construction site in Sanmen, China. Such modules can be pre inspected at the construction yard and match-assembled to ensure easy installation and welding on site (a technique long-used in long-span bridge construction).

Earlier experience with steel-plate composite structure construction exists from application by General Electric to boiling water reactor containments. The GE Mark III fleet (STRIDE Program) has a drywell vent structure designed and built as a composite steel-plate/concrete structure. The Mark III drywell vent structure is about 46 m (150 ft) diameter and about 18 m (60 ft) high with conventional concrete construction above it, above the suppression pool. The Mark III reactor pressure vessel pedestal and shield wall use the same technology but smaller diameters. These Mark III's have operated successfully for over 20 years at sites including River Bend, Perry, and Grand Gulf (Solorzano, 2009).

The GE Mark III pedestal and shield wall fabrication used modules assembled in a fabrication shop area. A special on-site shed was used for fabrication because the modules were so large, circumferentially and vertically. Workers fitted the modules up, placed alignment devices and match-marked for re-assembly at the site. The people who were responsible for assembling the modules on site were present to witness this fit-up operation.

Steel-plate/concrete construction has been identified as a very promising technology for construction of new nuclear power plants (Schlaseman, 2004). However, while earlier experience exists with BWRs, this technology still entails significant challenges.

The first group of challenges concerns the design and modeling of steel-plate/concrete walls. The experimental data available for such walls has been obtained by testing scaled-down specimens, with overall thickness between 100mm and 300mm and steel plate thickness between 2mm and 6mm. The prototype wall thicknesses are larger than 1,000mm while the plate thicknesses remain between 6mm and 12mm. Recognizing that full-scale test may not be possible using the existing structural laboratories, more tests on correctly scaled specimens are needed to establish the benchmarks for calibrating computer models for thick steel-plate/concrete walls. That said, the existing computer models for composite steel concrete structures need to be validated for situations where structural shapes are used to tie the two plates together, to carry the bi-axial shears, and where studs are provided to prevent the thin liner plates from debonding during pouring or unexpected internal out-gassing pressures. For limitation of buckling the studs also play a useful role because only a small amount of support is needed to prevent buckling from occurring.

The second group of challenges concerns construction of steel/plate composite walls. While construction of the wall itself is made much easier, implementation of the wall-to-floor connections is challenging. The GE Mark III pedestal, for example, required large embedded plates in the base mat foundation, with alignment bars and backup blocks for welding. Furthermore, design and implementation of structural connections between steel-plate/concrete and conventional reinforced concrete elements has not been extensively studied, although again the top of the GE Mark III containment composite structure is designed to provide a transition to conventional reinforced concrete construction. Since the concrete curing process emits a large amount of water vapor which cannot permeate the steel layer covering the concrete, vents are needed in stay-in-place form structures. As walls get thicker, elaborate venting/cooling system become an important design issue to remove large amounts of water that remain deep within concrete members as a byproduct of curing. If not removed from the structure, small water deposits have the potential to initiate and propagate cracks under high temperatures, such as in response to fires. Finally, implementation and anchoring of piping and equipment attachments to the steel skin of steel-plate/concrete walls remains an important design issue.

The third group of challenges concerns inspection and service of steel/plate composite walls over the life of the nuclear power plant. It is universally recognized that the composite walls offer superior resistance to extreme loading conditions, such as

aircraft impact and earthquake loading. Under impact, the steel skin increases the resistance of the wall to local perforation, scabbing and penetration (shear cone punching) compared to conventional reinforced concrete walls. Under earthquake loading, properly designed steel-plate/concrete walls (with details to delay elephant-foot buckling and formation of buckled compression diagonals) should be significantly more ductile than the correspondingly reinforced conventional reinforced concrete walls. However, long-term degradation of steel-plate/concrete walls is not fully understood, although experience exists with steel liners commonly used on the internal surfaces of reactor containments, such as the GE Mark III containment. The exposed steel plates may need to be protected against corrosion. Inspection methods to establish the conditions of inaccessible portions of the walls have not been evaluated, particularly concerning the state of bond between steel plates and concrete. Behavior of such walls under elevated temperatures during accidents and fires has not been studied at the size and scale used in nuclear power plants.

Finally, the forth group of challenges concerns decommissioning of nuclear power plants after the end of their service life. Methods for effective deconstruction of the steel-plate/concrete walls have not been investigated. In particular, it is not clear how to deal with portions of such walls that may be irradiated or otherwise contaminated during the regular service life of a nuclear power plant.

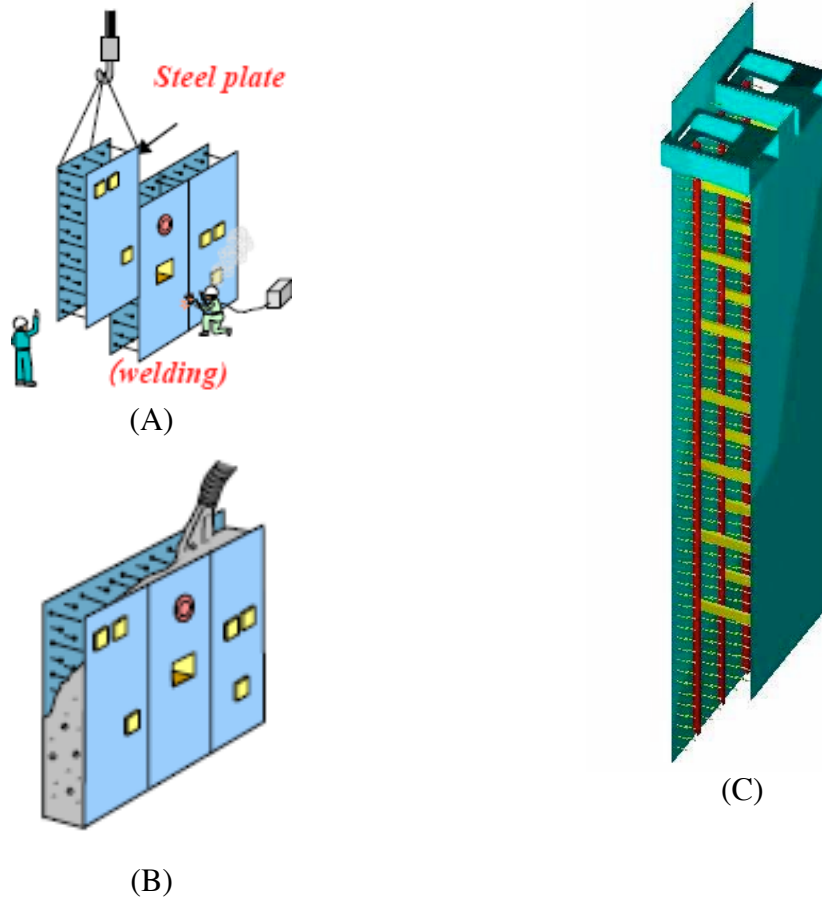


Fig. 10 Schematic illustration of steel plate concrete construction method (A, B) and a typical Westinghouse AP-1000 “CA01” structural sub-module (C) (credit Westinghouse).



Fig. 11 An example of steel-plate concrete construction, a ~20-m high AP-1000 auxiliary building is assembled from factory-prefabricated modules and is set in place by a heavy lift crane in Sanmen, China (Credit Westinghouse).

2.4 References

- ALMR Reactor Facility Seismic Analysis, Bechtel National, Inc., October 1994.
- California Energy Commission, “Underground Siting of Nuclear Power Reactors: An Option For California,” Staff Report, Nuclear Assessments Office, June, 1978.
- Chopra, Anil K. Dynamics of Structures. New Jersey: Pearson Prentice Hall, 2007.
- Huang, Y.-N., Whittaker, A. S., Kennedy, R. P. and Mayes, R. L., "Assessment of base-isolated nuclear structures for design- and beyond-design basis earthquake shaking." *MCEER-09-0008*, Multidisciplinary Center for Earthquake Engineering Research, State University of New York, Buffalo, NY, August 2009
- Malushte, Sanjeev R., and Andrew S. Whittaker. “Survey of Past Base Isolation Applications in Nuclear Power Plants and Challenges to Industry/Regulatory Acceptance.” 18th International Conference on Structural Mechanics in Reactor Technology (SMiRT 18, 2005). K-10-7.
- Munakata, Yoshinari, Takashi Maki, Yoshiyuki Sato, Keiji Sekine, Takamasa Nishioka, Nobuyuki Niwa, and Osamu Kontani. “Study on Radiation Shielding Performance of Reinforced Concrete Wall: Loading Test on Concrete Walls and Modeling of Concrete Cracks.” 20th International Conference on Structural Mechanics in Reactor Technology (SMiRT 20 - 1866, 2009).

- Peterson, P.F., Haihua Zhao, and Robert Petroski, "Metal And Concrete Inputs For Several Nuclear Power Plants," Report UCBTH-05-001, UC Berkeley, February 4, 2005.
- Schlaseman, C. "Application of Advanced Construction Technologies to Nuclear Power Plants," Technical Report, MPR-2610, Revision 2, P. 132, US Department of Energy, Sept. 24, 2009.
- Solorzano, E., Personal communication, October 20, 2009.
- Takeuchi, M., H. Akiyama, M. Narikawa, K. Hara, H. Tsubota, and I. Matsuo. "Study on a concrete filled steel structure for nuclear power plants: (Part 1) Outline of the structure and the mock-up test." 13th International Conference on Structural Mechanics in Reactor Technology (SMiRT 13 – H02 – 1, 1995).
- US Nuclear Regulatory Commission (NRC) Regulatory Guide 1.165 (1997), "Identification and Characterization of Seismic Sources and Determination of Safe Shutdown Earthquake Ground Motion"

3.0 SIMULATION VERIFICATION AND VALIDATION ISSUES

To use simulation results in USNRC Design Certification of a base-isolated nuclear reactor, both the structural engineers and the regulators will have to have a sufficient level of confidence that the results provide an accurate representation of the physical system. The process of establishing this confidence is commonly referred to as *verification and validation* (V&V). This process, which can often be very intensive, includes establishing both that one has correctly solved the desired system of equations (verification) and that the chosen model sufficiently represents physical reality for the intended purposes (validation).

This chapter reviews some general challenges for the modeling and simulation of base-isolated structures based on limited historical experiences, currently accepted simulation methods, and the unique validation requirements to represent the non-linear behavior of base isolators. Similar V&V issues exist for the modeling of structural response to large aircraft crashes, particularly the inevitable localized inelastic response of the structure. However, because this report specifically recommends that base isolated structure be decoupled from the external event shells, specific V&V issues for aircraft crash modeling are not discussed here.

3.1 Historical Experience with Seismic Base Isolation

The response of base-isolated structures to historical earthquakes will be an important source of information for the validation of computational models used for future designs. Currently this data set remains quite limited due to the small number of existing isolated structures and the relatively long earthquake return period (i.e. few large earthquakes). As more isolated structures are completed and instrumented, additional data should become available over time that will be invaluable in the assessment of computational modeling tools.

The best source of historical data for base-isolated structures in the US is the magnitude 6.8 Northridge earthquake that struck the Los Angeles area on January 17, 1994. Three base-isolated, steel-frame structures experienced strong ground motion recordings above 0.20 g. Table 3 summarizes the data for these three structures. While the USC Teaching Hospital appears to have behaved well, it is apparent from these results that not all isolation systems behaved as expected since the two other structures experienced roof accelerations larger than the peak ground acceleration. This amplification was not expected for these isolated structures, and may have been caused in part by retrofits that compromised the isolation gap. Although the peak accelerations exceeded the PGA, it is worth noting that these accelerations are likely less than what the non-isolated peak accelerations would have been assuming the superstructure had a small non-isolated period and was located at a site with adequately-strong soil composition. These concepts will be developed further in Section 6.3.

| Name | Epicenter Distance (km) | Isolation System | Peak Horizontal Ground Acceleration (g) | Peak Horizontal Roof Acceleration (g) |
|---|-------------------------|------------------------------|---|---------------------------------------|
| University of Southern California Teaching Hospital | 36 | Lead-Rubber Bearings | 0.37 | 0.21 |
| L.A. Fire Command and Control Center | 38 | High Damping Rubber Bearings | 0.22 | 0.32 |
| Santa Monica Private Residences | 21 | GERB Spring-Damper | 0.44 | 0.63 |

Table 3. Summary of response for base-isolated structures with strong ground motion from the Northridge Earthquake (Clark et al 1996).

The Teaching Hospital at the University of Southern California experienced large ground accelerations in the Northridge earthquake and demonstrated the effective reduction of accelerations within the isolated structure. The structure is an eight-story steel frame supported by 68 lead-rubber isolator and 81 elastomeric isolators (Clark et al 1996). The periods for the first mode of the structure are 1.32 in the east-west direction and 1.38 in the north-south direction, compared to 0.92 and 0.76, respectively, if the structure had a fixed base (Nagarajaiah and Xiaohon 2000). Significantly, the peak roof acceleration was observed to be 43% less than the peak ground acceleration.

The analysis of the USC hospital response to the Northridge quake is supported by the characterization of the bearings through cyclic loading tests performed by Dynamic Isolation Systems. Nagarajaiah and Xiaohon (2000) used this data to develop bearing properties for a smooth bilinear hysteretic model and a simplified equivalent linear displacement model. Their analysis using the computer code 3D-BASIS showed that the nonlinear hysteretic model more closely matched the observed response spectra than the equivalent linear-isolation system. Qualitative observation of the results shows that the linear models tend to under-predict the structural accelerations. However, these discrepancies are not quantified in the analysis by Nagarajaian and Xiaonon.

The experience from the USC Teaching Hospital demonstrates the potential effectiveness of base-isolation and the ability to characterize the bearings and model the system response, as well as the difficulty in selecting appropriate models to describe the system accurately. For the simulation of base-isolated nuclear facilities, it will be more difficult establish a case for the models used in the analysis since the goal of such efforts are predictive and real data from an isolated reactor in a strong earthquake will probably not be available for some time.

The ability to pre-predict the response of the USC hospital (i.e. accurately predict the response before evaluating the observed response) could be one important validation metric for analytic methods used in isolated reactors. Since nuclear structures are generally stiffer than the USC hospital, their dynamic response would more closely

approximate the ideal isolated rigid structure (Chopra 2007). The use of this historical case would therefore be useful for validation since the USC hospital structural response may be more difficult to characterize than nuclear structures and will help to establish confidence in the modeler and the model approximations used for the response of lead-rubber bearing isolators.

The Los Angeles County Fire Command and Control Facility (FCCF) is a two-story steel frame structure completed in 1990 with 32 high-damping rubber isolators supporting a structure of 1930 metric tons (4230 kips). The isolation system is designed for a peak displacement of 24.4 cm (9.6 in) and has the unusual feature of chains installed at the center of each bearing that are set to engage at displacements of 31.8 cm (12.5 in) (Clark et al. 1996).

The response of the FCCF included several high frequency spikes in the east-west direction that resulted in amplification ratios much greater than 1.0. The behavior in the north-south direction resembled the expected behavior with amplification ratios on the order of 0.5. The divergent east-west response is believed to be the result of a compromised isolation gap where sacrificial elements were re-enforced after being damaged in the 1991 Sierra Madre earthquake. The contact between the isolated structure and the re-enforced elements would lead to pounding consistent with the observed high frequency spikes.

The experience with the FCCF shows that special care needs to be taken for any maintenance and repair work that may impact the isolation gap for a base-isolated nuclear structure. Any changes to structures or components that span or may be impacted by the isolation gap will require special attention and any significant modifications could require additional simulation and analysis. This experience also re-emphasizes the importance of reducing uncertainties associated with knowledge of the as-built state of the structure through the careful application of design control.

The other isolated structures to experience strong ground motion were two identical steel frame residences in Santa Monica supported by GERB helical springs and viscous dashpots. These structures experienced significant amplification in both the horizontal and vertical directions. The high frequency acceleration spikes observed are most likely the result of a compromised isolation gap from architectural and construction details, but interpretation is difficult due to poor quality of the data (Clark et al 1996). The strict quality assurance required for nuclear facilities suggests that nuclear structures would not have similar design and construction issues as the Santa Monica residences. The experience primarily reiterates the lessons from the FCCF structure to minimize the uncertainties between the modeled system and the as-built system.

Currently, there is only a small sample of responses from base-isolated buildings to earthquakes and only one case, the USC Hospital in the 1994 Northridge earthquake, that can be used to simulate the response to a large ground motion with effective base isolation. It will be important for structural engineers for base-isolated reactor designs to stay informed as more experience is gained with these systems. As more base-isolated structures are constructed in seismically active regions, one should anticipate additional

valuable experience and data to emerge that should be essential to the validation case for computational models.

3.2 Current Analysis Methods and Tools for Reactor Seismic Design

Analysis methods for base-isolated nuclear structures will most likely be based on those methods currently in use for advanced light water reactors. For these cases, the documentation provided in the design control documents for the Westinghouse AP-1000, General Electric ESBWR, and Areva EPR demonstrates current modeling practices used for reactor design certification. The analysis for each of these reactors is similar in the use of simplified stick models for reactor systems combined with more detailed finite element models using standard commercial software tools. Among these three designs, the AP-1000 is the only one that has received design certification.

The details of the AP-1000 seismic design are covered in detail in the Rev. 17 of that reactor's Design Control Document (Westinghouse, 2008). Detailed seismic analysis was done for Category I structures including the containment building (steel containment vessel and containment internal structures), the external event shell, and the auxiliary building. These structures are situated on a common base mat and are collectively referred to as the nuclear island.

The analysis of the AP1000 nuclear island is based on the coupling of lumped-mass stick models for important reactor systems and components (e.g. reactor coolant loop, pressurizer, core makeup tank, and polar crane) to finite element shell models of concrete structures. Detailed (3D) finite element models were used for the reactor systems to determine the modal properties (frequencies and effective masses) for the lumped-mass stick models.

ANSYS was used for all of the lumped-mass stick and finite element shell models and SASSI was used for non-rock sites to model the soil-structure interaction. Additional verification and validation material was not provided in the Design Control Document to support the use of these analysis tools in the seismic modeling of the AP1000. The verification and validation case for the software used for this analysis falls almost entirely to the software vendor. The burden on the modelers is to establish competence using the computation tools and justify the analysis methods based on current civil engineering practices. Mesh refinement studies, a common and relatively simple verification test, are not discussed in the analysis, though two meshes were used for the ANSYS models: a fine mesh (element size ~10 ft) for static analysis and dynamic analysis for a hard rock site and a coarse mesh (element size ~20 ft) for studying the soil-structure interaction.

Following a long sequence of USNRC Requests for Additional Information and Westinghouse responses, the USNRC staff determined that the completed analysis was acceptable under the guidelines of the USNRC Standard Review Plan Section 3.7 (USNRC 2004). It is also important to note that the seismic analysis for the AP1000 includes non-linear analysis in limited cases for the interaction of foundation mat uplifting and shear wall stiffness reduction. Current USNRC guidance is that nonlinear analysis may be acceptable in certain special cases and must be reviewed on a case-by-case basis. Subsequently, additional licensing issues have arisen for the AP-1000 due to

design changes to implement steel-plate/concrete construction for the external event shell (e.g., shield building).

3.3 Verification and Validation Requirements and Approach

For the simulation of seismically base-isolated nuclear structures, a significant amount of work will be required to accurately characterize the system in order to have sufficient confidence in the analytic results. The majority of these efforts will be required to characterize the response of the base isolators for both static and dynamic conditions. It should also be noted that the analytic complexity required for the structure above the isolators will likely decrease since accelerations will be less than the rigid-base case, so the overall analysis effort for the structure may be reduced. Additional validation efforts will be needed to establish that the interactions between the isolators, structure, and reactor systems are sufficient to estimate the maximum accelerations on sensitive components.

The design of base isolation systems is focused largely on the analysis of horizontal response, where reduced accelerations transmitted through to the structure. In the application of base isolation for nuclear systems, it will also be important to characterize the response of the system in terms of vertical motion, rotation (overturning), and in-plane torsion since these modes may have a greater impact on components in the reactor. This would be relevant for components that are particularly sensitive to vertical accelerations or, in the case of fast reactors, rotational modes could lead to reactivity control issues (USNRC 1994). Slabs are particularly sensitive to vertical accelerations.

For the modeling and simulation of base-isolated structures, a greater burden will fall upon the design engineers to establish the validation case for a specific design. This case should consist of collaboration with the isolator vendor to characterize both the static and dynamic response of the specific components for the design. These tests should be designed to determine the characteristic behavior of the isolators both in the expected operational regime and close to the isolator limits. Tests should also include detailed study of the vertical stiffness and damping of the bearings. Potential failure modes, both horizontal and vertical, should be studied to understand the true limits of isolator behavior.

One challenge for modeling isolated structures is that it can be difficult to determine whether the models used for the base-isolators will produce conservative results for the dynamic response of the superstructure. These complications often arise due to the inherent non-linear response of the isolators themselves and how this is accounted for in simplified linear models of isolator response. Equivalent-linear methods have the significant weakness that they cannot characterize the isolation system based on its physical parameters and therefore often requires iteration and tuning. In comparison to nonlinear time history responses developed by Ryan and Chopra (2005), the equivalent-linear procedures can under-estimate the isolator deformation by 20% to 50%.

The potential need for non-linear models for the base-isolated structure will likely introduce some additional verification difficulties for simulation efforts and dynamic properties of materials in that regime. In current practice, code verification is done

primarily by the software vendor and supported by proper quality assurance and oversight to make sure that the modeled systems are represented as intended. The verification of non-linear systems will require an additional degree of user sophistication in order to assure proper convergence to the correct solution.

In some cases, it has also been shown that the standard equivalent-linear analysis approaches to handle energy dissipation in seismic isolators can lead to non-physical results. These arise due to artificial damping in the first mode response that can lead to estimates of roof displacements 10% to 25% below those of an ideal rigid structure model (Ryan and Polanco 2008). In modeling the response of a base-isolated reactor, it will be important to appropriately characterize the isolator behavior under realistic conditions to ensure that estimated accelerations in the reactor systems are not unrealistically reduced.

In addition to testing and determining the bearing behavior, additional qualification and experiments will be required for the joints used on piping systems that span the isolation gap. Historical experience from the 1994 Northridge Earthquake shows how sensitive isolated structures can be to failures of the isolation gap. The crucial aspect for simulation validation for the flexible piping systems will be to have a high degree of confidence that the system modeled is as close as possible to the expected as-built design and the tight clearances where component impacts could occur are avoided.

Modeling efforts to accurately characterize base-isolated nuclear structures will require a set of shake table tests for simplified representations of the reactor systems being modeled. These tests should be performed on isolators that will give similar responses to those observed in the true system. The study of system response for different earthquake time histories will allow for the modeling and validation of three dimensional behavior for the base-isolated structure including vertical motion, torsion, and rocking. IEEE-344 requirements for testing components should be followed.

As mentioned previously in this chapter, additional data for validation will come from the seismic instrumentation of current and future base-isolated structures. With a sufficient amount of data in this category and further work to develop standard analysis procedures to different base isolation systems, it is possible that more validation work could be handled by the software vendors, who will likely seek these simulation capabilities for both nuclear and non-nuclear structures. Until these analyses become more standardized, however, the verification and validation of base-isolation simulations will require a significant amount of analysis and experimentation specific to the modeled system.

Laminated rubber isolators and friction-pendulum isolators will have different non-linear response characteristics. The significance of these differences, and the implications for code validation, has not been studied.

3.4 References

Chopra, Anil K. Dynamics of Structures. New Jersey: Pearson Prentice Hall, 2007.

Clark, Peter W., Masahiko Higashino, and James M. Kelly. "Performance of Seismically Isolated Structures in the January 17, 1994 Northridge Earthquake." *Proceedings of*

the Sixth U.S.-Japan Workshop on the Improvement of Building Structural Design and Construction Practices in the United States and Japan. Victoria, B.C., Canada: Applied Technology Council and Japan Structural Consultants Association. ATC-15-5. 1996.

Nagarajaoaj, Satish and Sun Xiahong. "Response of Base-Isolated USC Hospital Building in Northridge Earthquake." *Journal of Structural Engineering*, Vol. 126, No. 10. October, 2000.

Ryan, Keri L. and Anil K Chopra. "Estimating the Seismic Response of Base-Isolated Buildings Including Torsion, Rocking and Axial-Load Effects." *U.C. Berkeley Earthquake Engineering Research Center*, Report No. EERC 2005-01. June, 2005.

Ryan, Keri L. and Jose Polanco. "Problems with Rayleigh Damping in Base-Isolated Buildings." *Journal of Structural Engineering*, Vol. 134, No. 11. November, 2008.

U.S. Nuclear Regulatory Commission. *NUREG-1368: Preapplication Safety Evaluation Report for the Power Reactor Innovative Small Module (PRISM) Liquid-Metal Reactor.* January, 2004.

U.S. Nuclear Regulatory Commission. *NUREG-1793: Final Safety Evaluation Report Related to the Certification of the AP1000 Standard Design.* September, 2004.

Westinghouse. *AP1000 Design Control Document Rev. 17.* Submitted to U.S. Nuclear Regulatory Commission September 22, 2008.

4.0 LOADING CHARACTERIZATION

Reactor-building structural loads arise from several sources. This chapter reviews the loads that can be created by earthquakes, aircraft crashes, blasts, and internal loads generated by reactor equipment under normal and accident conditions. For the purpose of this scoping study, load levels are determined from code requirements, availability of applicable databases, and revision of past research in loading characterization. Together they assure that current sources of structural risk are adequately modeled for the purposes of this scoping study. The results of this chapter provide the inputs for the software models utilized for the parametric analysis in Chapter 6.

4.1 Earthquake

The response of base-isolated reactor structures to earthquake excitation is modeled using either a linear-elastic (Chopra, 2007) or bilinear analysis of the isolation system supporting either a linear-elastic or a rigid reactor building while subjected to a suite of applicable ground motions. Although a linear-elastic analysis does not account for inelasticity in the structure or isolation system, the model is rather accurate for base-isolated structures because the isolation system will reduce the superstructure accelerations and deformations into the elastic range, as long as total displacements (including rotation) do not exceed the gap width between the isolated structure and surrounding structures resulting in impact. The analysis includes higher mode contributions as well as structural and isolation damping to increase the model accuracy. Bilinear isolator models are compared with the linear-elastic cases and serve to demonstrate possible unconservative inaccuracies of using elastic models for isolator analysis. Additionally, the linear-elastic superstructure models are compared with the rigid superstructure models to ascertain the level of superstructure response amplification.

As opposed to the design for a typical residential or commercial structure, a nuclear reactor must be qualified for a higher hazard level due to the performance objective for safety-critical facilities to remain functional under rare (i.e. very strong) seismic events. The American Society of Civil Engineers Standard ASCE 43-05 (ASCE, 2005) specifies that the design of nuclear power plants (Seismic Design Category 5) shall consider ground motions with an annual frequency of exceedence of 1×10^{-4} . Note that this hazard level exceeds that used for this project.

A typical procedure for selection of applicable ground motions includes site-specific hazard analyses (Kramer, 1996) that are either deterministic or probabilistic in nature. Both methods require the consideration of all earthquake sources capable of producing significant response in the form of a predetermined ground motion parameter at the site. The deterministic seismic hazard analysis (DSHA) focuses on the specific source and earthquake capable of producing the worst response whereas the probabilistic seismic hazard analysis (PSHA) requires inclusion of all significant sources and ruptures, each characterized by a probability of exceeding the chosen response parameter. After considering all possible sources of uncertainty, the data is integrated to form a seismic hazard curve representing the probability of different hazard levels being exceeded. A

Poisson model can be used to find the probability of exceedence of a set hazard over a finite period of time.

Once the hazard is set, determination of the structural response at different building periods is found by sending the motions through a single degree-of-freedom model to form a uniform hazard spectrum. The hazard at a site can be deaggregated in order to determine the controlling event magnitude and site-source distance for the hazard. Existing earthquake records from similar source types measured at locations with similar soil conditions to that being analyzed are selected and scaled such that the median record response matches the target spectrum over the period range of interest (Bray, 2008). Time scaling of earthquake groundmotion data is highly discouraged due to the induced change in frequency content. The use of existing ground motion databases in congruence with the above procedure allows designer to form a suite of ground motions for a particular location. A PSHA-based methodology for choosing and scaling ground motions, as well as for developing hazard and fragility curves specifically for nuclear applications is presented in Huang (2008). Suites of ground motions with an annual frequency of exceedence of 1×10^{-4} (the nuclear criterion) can be compiled using such a framework.

For simplicity, rather than using the ASCE 43-05 requirements, this project utilizes existing suites of ground motions with a probability of exceedence of 2% in 50 years (having an annual probability of exceedence of 4×10^{-4}), the highest hazard for which ground motion suites are readily available. A 2% in 50 years hazard level is significantly higher than what is considered in typical design of residential and commercial structures, and provides a useful basis to study the impacts of base isolation. The hazard level refers to the likelihood of an event from any source causing a ground motion parameter (e.g. PGA, PGV, PGD, etc.) to be exceeded at a specific site over some period of time. Since these ground motion parameters often increase with increasing earthquake magnitude, a reduction in the hazard probability usually means that larger magnitude earthquakes must be considered. Therefore, the choice of a lower hazard level for this project results in a lower seismic response than what would be expected for the design under the ASCE 43-05 hazard level set at 1×10^{-4} . A special-purpose selection of ground motions to match the ASCE 43-05 hazard level would significantly complicate this study without yielding additional insight: thus, readily available ground motion suites were used in this study.

A project initiated under the joint venture of the Structural Engineers Association of California, the Applied Technology Council, and the California Universities for Research in Earthquake Engineering (collectively referred to as SAC) compiled applicable suites of strong motion records (Woodward-Clyde, 1997). Two-dimensional horizontal SAC records exist for various United States locations for hazard levels of 50%, 10%, and 2% in 50 years. ASCE 4 (1998) requires consideration of combined horizontal and vertical seismic effects when there is significant coupling of the horizontal and vertical responses of the structure. For this simplified scoping study, vertical excitation was not considered since the isolation system, by definition, is expected to significantly decouple the structural response from the horizontal input. Therefore, coupling between horizontal and vertical motions is assumed to be small. Although rocking may be a legitimate concern even for isolated structures, the model used is inadequate to capture such a phenomenon. The NRC requires that the correlation of statistically independent motions is less than

0.16 in order to use separate inputs as done in this simplified analysis. Otherwise, the analysis must use excitation in 3-axes simultaneously. A methodology for analyzing and mitigating the effects of high vertical excitation is not presented in this report, but it should be recognized that this is an area of potential vulnerability for base isolated nuclear power plants

A satisfactory analysis encompassing the entire United States involves the inclusion of suites from numerous locations to form a comprehensive loading envelope for code formation. Within the United States, a variety of faulting mechanisms exist, that can result in diverse ground motion characteristics. Of particular interest are strike-slip, reverse, and reverse-oblique events on the U.S. West Coast, as well as less frequent, intraplate U.S. East Coast seismicity. The West Coast events generally represent higher possible seismic intensity events (i.e. larger peak ground accelerations, velocities, and displacements), whereas East Coast events produce motions with broader frequency contents, a separate but important consideration. Additional motion characteristics may also be considered such that the analysis would have worldwide applicability. In this study, a broad range of US regional conditions are sufficiently covered by considering the SAC ground motion suites for sites in Los Angeles, Seattle, and Boston, but no effort was made to cover ground motion characteristics pertinent to non-US sites. A comprehensive list of scaled ground motions, assembled for design of structures based on the aforementioned 2% in 50 years hazard level, along with associated time histories are depicted in Appendices B and C, respectively.

4.2 Aircraft crash loading

Following the terrorist attacks of September 11, 2001, it is now commonly accepted that the effects of deliberate crashes of large commercial aircraft should be considered in the design of nuclear power plant structures. The U.S. Nuclear Regulatory Commission issued a final rule in February, 2009, that requires new reactor applicants to assess the ability of their reactor designs to avoid or mitigate the effects of a large commercial aircraft impact (USNRC, 2007), (USNRC, 2009). The specific aircraft attributes the USNRC requires applicants to consider are considered to be “safeguarded” information and are restricted from public disclosure. Here, to adequately represent the full range of possible impacts, this report considers crashes by two types of aircraft: the Boeing 747-400 and the Boeing 737-900 into a highly idealized and simplified reactor building structure. The 747 is one of the heaviest and fastest commercial airliners currently in use. While significant further evolution of aviation technology will occur over the typical 60 to 80 year lifetime of new nuclear power plants, the 747 provides a reasonable example for a very severe aircraft crash. Conversely, the 737 is one of the lighter commercial airliners in use, providing a reasonable lower bound for commercial aircraft collision loading.

The actual structural loading time history generated by an aircraft crash is a complicated nonlinear function of aircraft mass distribution, crushing strength, and instantaneous velocity. The loading is also a function of the rigidity, strength, and nonlinear inelastic response of the wall segment being impacted, although these effects are smaller because the total deflection of the wall segment should be small in comparison to the crushed length of the aircraft. Under the simplifying assumptions of a

linear-elastic building model and constant aircraft velocity during impact, the loading function becomes a function of three variables: aircraft length, mass, and impact velocity. The loading function is linearized using a method presented by Riera (1968), depicted in Fig. 12, which also served as the basis for impact analysis by Petrangeli and Forasassi (2007) (Petrangeli, 2006). The loading function shape represents the mass distribution over the length of the plane. Because a large percentage of the plane's weight is concentrated in the wing fuel tanks and engines, the force time history resembles the physical shape of the plane.

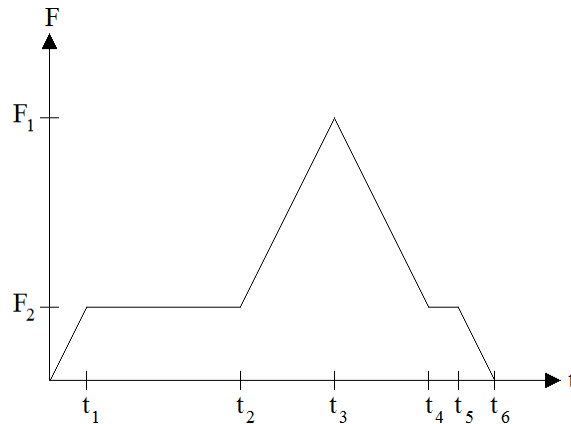


Fig. 12 Impact force linearization (Riera, 1968).

Riera's paper considered accidental impact of a Boeing 707-320, the largest commercial aircraft at the time of publication. This model in its original form is inadequate for current implementation on modular reactors for two reasons. First, the invention and use of larger, faster planes such as the Boeing 747-400 can be expected to impart larger forces on the structure during collision. Second, events like the World Trade Center attacks of September 11, 2001 point to a heightened threat of impact with malicious intent. Whereas Riera considered accidental impacts at much lower speeds (i.e. takeoff and landing speed), the current threat must include analysis of impacts at or exceeding the cruising speed. Together, these effects lead to a more than five-fold increase in the peak force transmitted to the structure.

Time and force scaling of the Riera model is necessary for proper modeling of impact loads from airplanes other than the Boeing 707-320. The time scale factor, X_t , is a function of the aircraft length, L , and velocity, v . Estimation of the airplane crushing time for the previously considered and the newly analyzed aircraft allows direct scaling of the impact time domain as such:

$$t_{crush} = \frac{L}{v} \quad [1]$$

$$X_t = \frac{t_{crush,2}}{t_{crush,1}} = \frac{\left(\frac{L_2}{v_2}\right)}{\left(\frac{L_1}{v_1}\right)} = \frac{L_2 v_1}{L_1 v_2} \quad [2]$$

Force scaling is essential to maintain proper momentum conservation for the larger collision. For conservatism, collisions are assumed to be inelastic and normal to the reactor building surface such that all momentum is transmitted from the plane to the structure. Less momentum would be transferred if the aircraft were to strike the building surface at an angle, or if some fraction of the aircraft missed the building (e.g., the wing tips). Thus, eccentric and incomplete collisions were ignored in order to simplify response and reduce partial airplane impact-induced error. However, it is necessary to note that the worst-case collision would be that due to a complete-collision, eccentric crash such that impact response includes both translation of the center of mass and rotation of the structure about its center of stiffness.

Increase in the plane mass (or weight), m (or W), and velocity, v , tend to linearly amplify the impact force by adding to the momentum transfer. Since the impulse, defined as force acting over some period of time, is equal to the change in momentum, the time scaling factor is also included in the definition of the force scaling factor, X_f .

$$\int F dt_{crush} = p = mv = \frac{W}{g} v \quad [3]$$

$$X_f = \frac{p_2}{p_1} = \frac{\left(\frac{W_2 v_2}{g t_{crush,2}}\right)}{\left(\frac{W_1 v_1}{g t_{crush,1}}\right)} = \frac{W_2 v_2 t_{crush,1}}{W_1 v_1 t_{crush,2}} = \frac{W_2 v_2}{W_1 v_1} X_t \quad [4]$$

The Boeing 747-400 and 737-900 forcing functions used in the analysis are simply the original Riera function for a Boeing 707-320 scaled in each dimension by the proper factors. Figure 13 depicts the 707, 747, and 737 force-time histories graphically, using aircraft data summarized in Table 3. These loading histories have been used as the impact load forcing functions in Section 6.3 to evaluate the global response and acceleration an aircraft would induce in a base isolated structure.

Section 6.4 presents scoping analysis for the inelastic response of a rectangular, decoupled external event shell to aircraft crash. This simplified analysis treats the aircraft impact as an equivalent static load, equal to the maximum force imparted by the aircraft during the crash, with dead loads neglected. Loads from the fuselage and wings are calculated separately, due to the large difference in the time period over which their momentum is imparted to the wall. To calculate the maximum loads, the original Riera forcing time history is scaled in the time dimension by a time scale factor, $X_t = L_{747} v_{707} / L_{707} v_{747}$, which represents the ratio of the crushing times of the Boeing 707 originally considered by Riera and the actual plane (Table 4). Next the force variable is scaled using $X_f = W_{747} v_{747} / W_{707} v_{707} X_t$, in order to preserve the relative momentum

transfer (not the full momentum transfer since the Riera time history only represented about 90% of total momentum transfer of a 707).

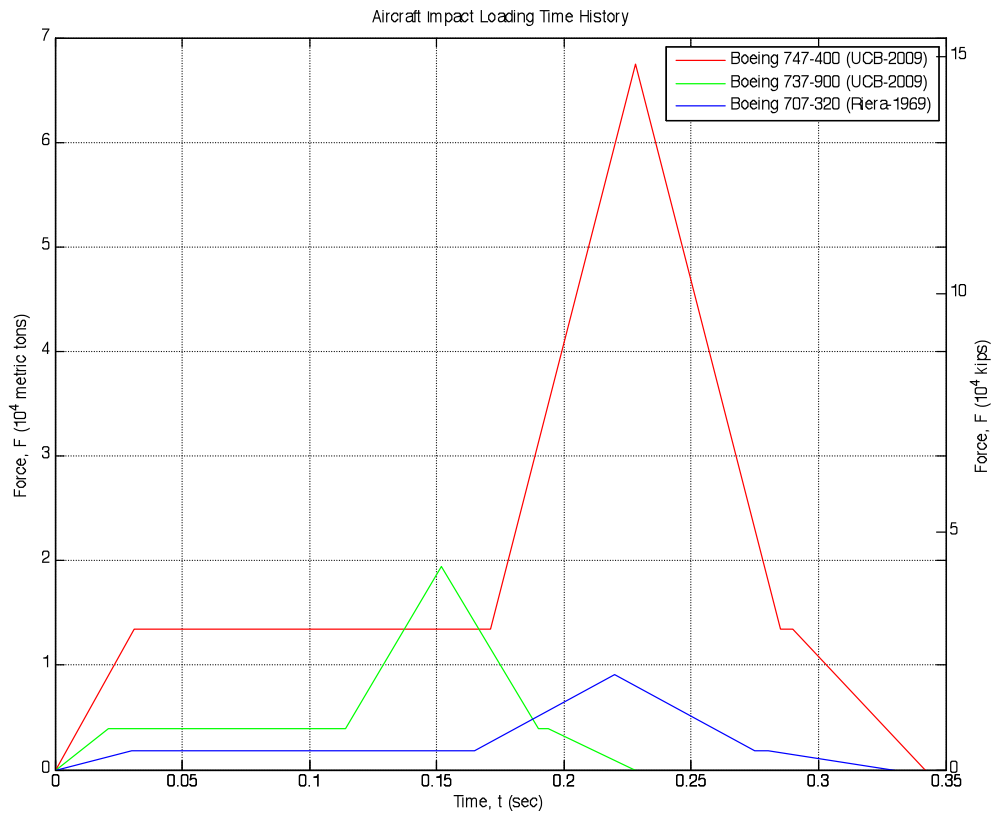


Fig. 13 Impact loading time histories

Table 4. Impact loading linearization parameters.

| | | Riera 1968 | This Study | |
|--|----------------------------|----------------|----------------|----------------|
| Aircraft Type | | Boeing 707-320 | Boeing 747-400 | Boeing 737-900 |
| Aircraft Length, L (m[ft]) | | 34.9 [114.5] | 70.7 [231.8] | 42.1 [138.2] |
| Maximum Weight, W (metric tons [kips]) | | 101 [222] | 397 [875] | 85.3 [188] |
| Impact Velocity, v (m/sec [ft/sec]) | | 103 [338] | 201 [660] | 180 [590] |
| Time Scaling Factor, X_t | | 1 | 1.037 | 0.691 |
| Force Scaling Factor, X_f | | 1 | 7.423 | 2.134 |
| Force Linearization Parameters based on the Riera Linearization (1968) | t_1 (sec) | 0.030 | 0.031 | 0.021 |
| | t_2 (sec) | 0.165 | 0.171 | 0.114 |
| | t_3 (sec) | 0.220 | 0.228 | 0.152 |
| | t_4 (sec) | 0.275 | 0.285 | 0.190 |
| | t_5 (sec) | 0.280 | 0.290 | 0.194 |
| | t_6 (sec) | 0.330 | 0.342 | 0.228 |
| | F_2 (metric tons [kips]) | 1815 [4000] | 13469 [29694] | 3873 [8538] |
| | F_1 (metric tons [kips]) | 9072 [20000] | 67344 [148468] | 19363 [42688] |

4.3 Blast loading

External blast threats typically fall under two categories. One category consists of attacks from a short standoff distance where local deformations will control response and building elements are loaded sequentially. The second category consists of blast waves propagating from a distance, resulting in the entire structure being enveloped in the blast wave, with all exposed members loaded concurrently. Characteristics of these blast loads, as well as their effects on the structure including structural response are discussed in this section, and a more detailed discussion is provided in the report by Wei (2009). Due to the scope of this project as well as the likely method of attack, this blast overview will focus mostly on blast loading to the structure exterior resulting only from physical or chemical explosions such as high explosive bombs and vehicle bombs. A more detailed discussion of the following can be found in Bangash (1993), Smith and Hetherington (1994), and Krauthammer (2008).

Conventional weapons and explosives cause damage through chemical and physical explosions. However, the chemical process is typically the driving mechanism of most modern day explosives. The fuel of a conventional weapon generally consists of a combination of carbon, hydrogen, oxygen, nitrogen, and sulfur which oxidize to form N_2 , NO_x , CO_2 , CO , SO_2 , water vapor, and combustion heat (Krauthammer 2008). The combustion of the fuel components can result in deflagration or detonation depending on the rate at which the explosive materials decompose. Deflagration occurs when the rate of reaction is much lower than the speed of sound, as occurs when low explosives are used to propel projectiles. Detonation occurs when the reaction rate is around 1500-1900

m/s, with the speed of the blast wave increasing as the explosive material becomes denser. High intensity shock waves are then produced in the form of longitudinal pressure (P-wave), longitudinal rarefaction (N-wave), shear (S-wave), and/or surface Rayleigh waves (R-wave). The shockwaves propagate from the explosion site and have high temperature and pressure gradients at the wave fronts, with decaying pressure at larger distances. The properties of the shockwaves such as peak pressure and heat production depend largely on the properties of the explosive materials (Smith and Hetherington 1994).

When designing buildings to be blast resistant, the designer should consider design objectives, site conditions, structural shapes, and the corresponding costs. The design limits describe whether the building needs to remain fully operational at all times or if permanent deformations or even collapse are acceptable (Conrath, et. al. 1999). A nuclear power plant generally needs to resist small blasts without any damage, but after large impact loads such as aircraft crashes or detonation of car or truck bombs, nuclear power plants need only to ensure a controlled safe shutdown. For the modular reactors studied here, it is expected that passive methods will be provided for decay heat removal, and thus that no vital equipment associated with decay heat removal will be located outside of the external event shell, except potentially louver systems located high on the building for intake and exhaust of external ambient air.

Layers of security (defense in depth) can also be created to provide increased standoff distance for car and truck bomb attacks and can manifest as perimeter lines, access and approach control, or even concealed integral structural and nonstructural systems (Conrath, et. al. 1999). Nuclear power plants usually implement barrier systems to provide significant standoff for potential car and truck bombs.

Among the design objectives, structural response to blast loading is the primary concern of structural engineers. In general building design, *ASCE Structural Design for Physical Security: State of the Practice* (Conrath, et. al. 1999) states that site conditions, building performance objectives (eg. fully operation, remain intact and respond elastically, etc.), corresponding costs, and structural shape can have an impact on structural response to blast loading. It is important to note that damage levels due to blast loads cannot be compared to those caused by earthquake loads because although total base shear loads from earthquake loads may be larger than those of blast loads, local effects of the blast loading may induce high local forces as well as significant eccentric loads (that may induce torsion larger than accidental eccentricities considered in earthquake-resistant design), which could cause singular members to fail (Conrath, et. al. 1999), and may further induce progressive collapse of a part or of the entire structure. Krauthammer (2008) provides more detailed discussion of structural response including that of connections and openings.

The pressure-impulse (P-I) diagram is a tool used to determine the failure load for a structure. Maximum displacement or damage level should be defined first and then the P-I diagram can be utilized to find the combination of load and impulse which will cause failure. P-I diagrams differ depending on the shape of the load pulse, the load rise time, material plasticity and structural damping. Though based on the dynamic behavior of a

single-degree-of-freedom model of the structure, P-I diagrams have seen adjustments relating to empirical data due to possible shear failures at the supports (Krauthammer 2008).

With explosions that have duration times much greater than the natural vibration period of the structure a quasi-static or pseudo-static loading can be applied. With smaller explosions that have duration times much shorter than the natural vibration period of the structure, an impulse load may be applied and impulse load static analysis conducted. If the duration of the explosion is between these two categories, a dynamic response will result and a dynamic analysis will need to be performed (Smith and Hetherington 1994). *ASCE Structural Design for Physical Security: State of the Practice* (Conrath, et. al. 1999) further delineates the building response analysis process.

The structural blast loading of a building depends on the location and weight of the explosive as well as the shape and relative size of the building. The resulting pressures on the building surface are derived from static and dynamic overpressures. Typically, progressive collapse analyses are performed to determine the response of a structure under blast loading. In these cases, the elements closest to the explosion site are allowed to fail locally, and the loads are then redistributed to the rest of the structure to evaluate the potential for global failure (Conrath, et. al. 1999). Typical material model assumptions for structures under blast loading are: steel is an elasto-plastic material, and concrete has negligible tensile strength and a finite compression strength. Crushing and elimination of concrete material due to this process should also be considered for reinforced concrete (Krauthammer 2008). It is important to note that, currently, blast design loads are determined through the use of empirical data found in P-I graphs and similar design aids (Conrath, et. al. 1999). It is also important to note that stiff structures can be seen as decoupled from the explosion while flexible structures will interact with the structural loading (Bulson 1997).

To determine the response of above-ground structures, effects from free-field incident pressure, dynamic pressure, and reflected pressures as well as fragmentation need to be taken into consideration. For instance, if a large blast wave hits a structure, such as if the explosion occurred at a distance, the blast wave will surround the building and apply an assumed uniform translational force in the direction of the wavefront. This translational force will push one side of the structure while creating suction on the other side as the blast wave moves over the structure (Smith and Hetherington 1994). Peak pressure is assumed to occur on the closest wall to the explosion at the time the blast wave reaches the wall. Peak pressures for the side walls and roof are assumed to be reached linearly as the blast wave passes over the building. After the blast wave hits the wall, pressures decay bi-linearly in the closest wall and linearly in the side walls and the roof. However, if a small blast charge were placed near a structure, only individual members are affected. Studies have shown that in this situation, the effects from airblast and fragmentation are very large, especially if both of these occur simultaneously (Krauthammer 2008).

Because of the sudden nature of explosive events, local response has a greater effect on the overall response of the building than static loading. Therefore, finite element and finite volume methods are often applied to evaluate these local effects. Quan et.al.

(Quan, et. al. 2005) used AUTODYN, which performs 3d numerical simulations of blast effects on structures based on FEM and finite difference models, to determine the damage to reinforced concrete walls from the detonation of a truck bomb and impact from a Boeing 747 passenger jet. Through these simulations, they found that the interaction and coupling between the blast wave and the reinforced concrete wall occurs primarily within the first 0.25 seconds after the event. During this short period of time pressure differences drive the response of the concrete wall as the blast wave expands, diffracts and propagates through the wall, causing an increase in energy in the wall which later levels off after the blast wave passes beyond the wall. Quan also determined that a Boeing 747 with an impact velocity of 83.3 m/s (273 ft/s) will completely penetrate a conventionally reinforced 1 m thick reinforced concrete wall. Quan suggested a 3-m thick, conventionally reinforced concrete wall to withstand the impact from the airplane (Quan, et. al. 2005). Steel-plate/concrete construction (Section 2.3) has much improved ability to sustain impact loading compared to conventional reinforced concrete due to the membrane action of the steel shell. Therefore, a thinner, lighter, external shield may be adequate. However, detailing of the steel-concrete walls should be done to eliminate the possibility that wall skin coupling bolts or angles might be ejected during an impact and become internal missiles.

To be more specific, however, a number of variables can affect penetration of an object in concrete. For example, the amount of energy required to separate particles in a concrete mass is dependent on the characteristics of the concrete, including aggregate size and concrete density, as well as the reinforcing method (particularly if steel-plate reinforcement is used). Penetration is also affected by projectile variables, such as projectile mass and diameter, and impact incident variables, such as friction coefficient and wall boundary conditions. If one were to assume the missile were rigid, which is not the case in airplane crashes except for the engine turbine rotors, three phases may occur once the missile strikes the surface. The first phase is defined by the penetration of the missile into the concrete target until a certain distance, which is accompanied by the generation, propagation and reflection of stress waves within the concrete mass. Phase II begins at the end of phase I and continues until the missile stops if the missile still has enough kinetic energy after Phase I. Phase III is the occurrence, if any, of perforation of the missile through the target. A more thorough discussion of penetration of concrete by rigid missiles can be found in Guirgis and Guirgis' study (Guirgis and Guirgis 2009). Only certain formulas and methods are approved or accepted by the USNRC for penetration. One can refer to the USNRC Standard Review Plan (SRP) for details.

4.4 Internal and other loads

Loads from containment pressurization (e.g., loss of coolant accidents for water and helium cooled reactors; hydrogen combustion, core-concrete interaction, direct containment heating, and steam explosions for water reactor severe accidents; and sodium combustion for sodium fast reactors) and equipment gravity loads resulting from structural failure or crane operation must also be considered in the design of nuclear reactor buildings. Additional external loads for plant sites required to evaluate certain environmental conditions such as floods or tornado missiles must be considered when designing the external event shell and evaluating the system response.

4.5 References

- American Society of Civil Engineers (ASCE). (2005). "Seismic design criteria for structures, systems, and components in nuclear facilities." ASCE/SEI 43-05, ASCE, Reston, VA.
- American Society of Civil Engineers (ASCE). (1998). "Seismic analysis of safety-related nuclear structures and commentary." ASCE 4-98, ASCE, Reston, VA.
- Beck, P.W. Nuclear Energy in the Twenty-First Century: Examination of a Contentious Subject. *Annual Reviews Energy Environment*, 24, 113-37, 1999.
- Bray, J. "Probabilistic Seismic Hazard Assessment." CE 275 Lecture. University of California, Berkeley. 22 Sept. 2008.
- Bulson, P.S. *Explosive loading of engineering structures: A history of research and a review of recent developments*. E & FN SPON, London, 1997.
- Chopra, Anil K. Dynamics of Structures. New Jersey: Pearson Prentice Hall, 2007.
- Conrath, E.J., Krauthammer, T., Marchand, K.A., and Mlakar, P.F. *ASCE Structural design for physical security: State of the practice*. ASCE, 1999.
- Guirgis, S. and Guirgis, E. An energy approach study of the penetration of concrete by rigid missiles. *Nucl. Eng. Des.* (2009), doi: 10.1016/j.nucengdes.2008.11.016.
- Huang, Y. Performance Assessment of Conventional Base-Isolated Nuclear Power Plants for Earthquake and Blast Loadings. Diss. SUNY Buffalo, 2008
- Kramer, K.L. Geotechnical Earthquake Engineering. New Jersey: Prentice Hall, 1996.
- Krauthammer, T. *Modern Protective Structures*. CRC Press, 2008.
- Nazaroff, W. Lecture #21: Nuclear Power. *UC Berkeley: CE 107 Climate – Change Mitigation Reading Materials*, Spring 2008.
- OpenSees. "OpenSees" <<http://opensees.berkeley.edu/index.php>>. (Accessed May 01, 2009).
- Petrangeli, G. and G. Forasassi, "Large Airplane Crash on a Nuclear Power Plant" (Paper 7081) *ICAPP 2007* 13-18 May, 2007. 1-13.
- Petrangeli, G., "Nuclear safety," Butterworth-Heinemann, Amsterdam, pp. 189-193, 2006.
- Quan, X., Itoh, M., Cowler M., Katayama M., Birnbaum, N., Gerber, B., and Fairlie, G. Applications of a coupled multi-solver approach in evaluating damage of reinforced concrete walls from shock and impact. *SMiRT18-J04-4*, Beijing, China, 2005.
- Riera, Jorge D. "On the Stress Analysis of Structures Subjected to Aircraft Impact Forces." *Nuclear Engineering and Design* (1968): 415 – 426.
- Smith, P.D. and Hetherington, J.G. *Blast and ballistic loading of structures*. Butterworth-Heinemann Ltd, Oxford, 1994.
- U.S. Nuclear Regulatory Commission, "Proposal to Include Aircraft Impact Design Requirements For New Reactors," NRC COMGBJ-07-001, February 27, 2007.

U.S. Nuclear Regulatory Commission, “NRC Issues Final Rule on New Reactor Aircraft Impact Assessments,” NRC News, 09-030, Feb. 17, 2009.

Woodward-Clyde Federal Services (SAC project). “Suites of Earthquake Ground Motions for Analysis of Steel Moment Frame Structures.” National Information Service for Earthquake Engineering. 1997. University of California, Berkeley. 8 March, 2009.
<http://nisee.berkeley.edu/data/strong_motion/sacsteel/ground_motions.html>

World Nuclear Association. Nuclear Power in the World Today. <http://www.world-nuclear.org/info/inf01.html>, accessed April 26, 2009.

5.0 INTEGRATION WITH REACTOR SYSTEMS

This chapter discusses the integration of seismic-base isolation and external event shielding options with reactor safety and operational systems. In particular, the implications of these structural design options on the licensing process are emphasized while also identifying areas of synergistic and competing objectives. The first section provides an overview of the anticipated technology-neutral licensing process being developed by the USNRC. The following section discusses the role of design criteria and the role of system, structure, and component (SSC) safety classification. In particular, the role of performance-based regulation and modular factory construction on maintaining high quality assurance (QA) standards are the main focuses.

5.1 Technology-Neutral Framework (TNF) for Reactor Licensing

The USNRC has developed a preliminary framework for a technology-neutral approach to licensing commercial reactor plants (USNRC, 2004). The current licensing process is LWR-specific and highly prescriptive in its approach for design certification. In order to accommodate fundamentally different reactor technologies, the current licensing process must be modified where it is technology-specific, while demonstrably assuring larger safety margins (USNRC, 1994). The PBMR licensing approach to meeting an evolved licensing process is well described in a series of white papers (PBMR, 2006) and outlines a licensing framework by which Gen IV reactor types can be designed within.

There is little doubt there are significant safety and security implications with the utilization of seismic base isolation technology and fundamental changes to the external event shell configuration. The functional requirements that a SSC must meet are currently codified by the USNRC as general design criteria (GDC) where they are categorized by the following reactor function types: overall requirements, protection by multiple fission product barriers, protection and reactivity control systems, fluid system, reactor containment, and fuel and reactivity control. It is important to note that the development of the current set of GDCs took place over many years of LWR operational experience.

The currently proposed TNF calls for the development of a set of technology-neutral criteria that will capture the same set of requirements for key engineered safety systems while also being technology neutral and performance-based. As an alternative, the PBMR proposed a set of HTGR- specific regulatory design criteria (PBMR, 2004) that are more suitable for Gen IV as listed: (1) control radionuclides in fuel particles, (2) control chemical attack, (3) control heat generation, (4) remove core heat, (5) maintain core geometry, and (6) maintain reactor building geometry. It is this set of design criteria by which the reactor vendor must optimize the design and demonstrate system capability under the entire range of normal and off-normal operational conditions. More on the current role of seismic design criteria is reviewed in the next section while the role of best-estimate plus uncertainty methods for simulation were discussed previously in Section 3.3.

The safety performance of the system will still be measured by a set of technology-neutral quantitative health objectives (QHO's), specified in the Safety Goal Policy Statement of the USNRC, but the demonstration of compliance with these QHO's will require some departure from the traditional LWR-specific Level I, II, and III PRA approaches. This risk-informed approach to reactor safety can be further expanded to identify quantitative performance objectives for seismic design criteria for SSCs.

5.1.1 Event Identification and Reliability Functions

In addition to better understanding what criteria must be met during the design certification process, the question of when the system has to meet this criteria must also be better understood. A comprehensive set of initiating events must be identified using risk-informed methods, and system performance following these events must be analyzed and demonstrated to the regulator. This licensing basis envelope encompasses a set of normal (i.e. within design basis) and off-normal (i.e. beyond design basis) events that are either internally or externally initiated. These events can be categorized by frequency into Anticipated Operational Occurrences (AOOs), Design Basis Events (DBEs), and Beyond Design Basis Events (BDBEs), as shown in Fig. 14.

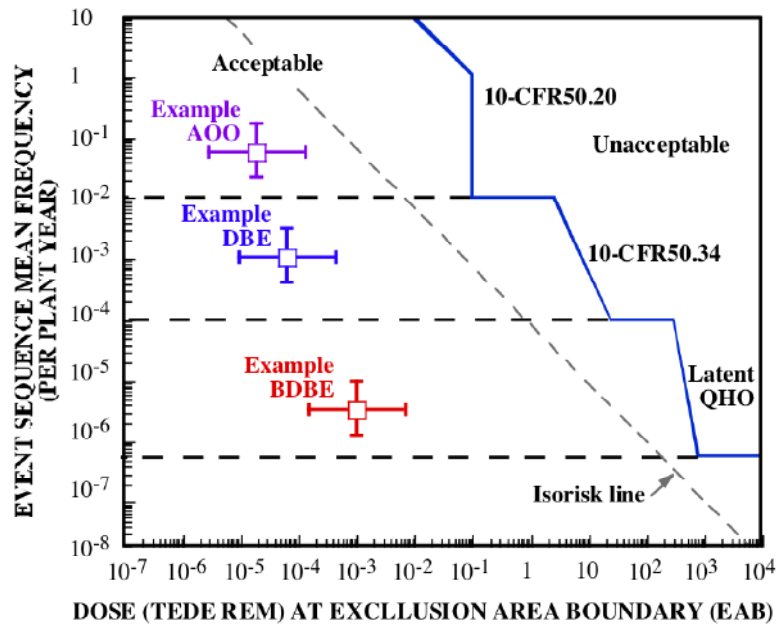


Fig. 14 Event frequency/consequence diagram.

In addition to earthquakes as discussed in Chapter 4, other potential external initiating events must be identified and analyzed, including high winds and naturally generated missiles (tornados and hurricanes); externally initiated fires or floods; accidental aircraft, barge, or ship collisions; nearby truck, train, chemical facility, or pipeline accidents; volcanos; turbine blade missiles; and lightning. Because nuclear facility design considers very rare events with return periods as low as a million years (Fig. 14), empirical information based upon historical experience only provides a starting point for assessing the magnitude and frequency of external events. Due to uncertainties in modeling, designers will commonly adopt relatively conservative assumptions about the severity of external events; this approach also simplifies the development of standardized reactor

designs that can be located at a wide range of sites. However, because earthquake loads are commonly a major driver for reactor core damage frequency in high seismic regions (where the zero period acceleration (ZPA) is greater than 0.2 g), and because seismically qualified structures are expensive, PSHA methods (Section 4.1) are valuable in specifying earthquake hazards.

The frequency of internal initiating events is commonly assessed using event trees and other analysis tools, and depends strongly upon the reliability of equipment. A series of reliability-related activities occur during operations and maintenance (O&M), listed below, that should be considered during the physical arrangement and structural design phase for nuclear facilities:

- Online monitoring
- In service inspection (ISI)
- Predictive maintenance (i.e. structural, conditional monitoring, and operational assessment limit definition)
- Proactive management of material degradation (i.e. effective corrective action program)
- Quality assurance (QA)

The role of each of these functions must be optimized in order to ensure meeting required plant safety margins. One of the reasons that the economic competitiveness and plant availability of the current fleet of plants have improved greatly over the past two decades, while simultaneously the predicted core damage frequency has been driven down, is that significant improvements have occurred in implementing all of these reliability-related activities (EPRI, 2008). For new facility designs, the importance of considering monitoring, inspection, and maintenance during the development of the plant physical arrangement cannot be overemphasized. The availability of adequate space to inspect equipment and to perform maintenance operations, and the availability of appropriate crane and monorail installations to move equipment, can have a major impact on the cost and duration of maintenance activity.

For seismic base isolation an ISI program was developed by GE for the PRISM reactor design and reviewed by the USNRC (USNRC, 1994). The focus of the program was on frequent monitoring of the isolation bearings, however acceptance or failure criteria were not developed.

5.1.2 Physical Arrangement and Reactor Safety

The physical arrangement of the reactor building is closely coupled to the control of radioactivity releases under normal operation and accident conditions. Under normal operation, the reactor building provides multiple ventilation zones that control the migration of radioactive materials, both inside the reactor citadel and in the volume between the citadel and the external event shell.

The physical arrangement of the reactor building also has major implications for worker access control. Access control plays an important role in reducing human errors. For example, the separation of redundant equipment like battery power supplies into physically separated and isolated parts of the reactor building reduces the potential for

operators and maintenance personnel to inadvertently work on the incorrect train of equipment, and also reduces the potential for common-mode failures from large fires or explosions. Positive access control, using card-key access for doors and locks or seals on cabinets and equipment actuators can further reduce the probability of inadvertent mistakes, along with other human performance measures such as two-man rules, procedure adherence, and appropriate training.

Under emergency conditions, emergency access and egress become important design issues that are affected by plant physical arrangement. The requirements for emergency access and egress may conflict with the requirements for positive access control for safety and security. In general, the trend toward passive safety systems, which do not require routine access for operator surveillance, help to reduce this source of conflict, since this equipment can be located in inaccessible locations without concern about personnel access and egress issues.

In severe reactor accidents, the consequences of a radiological release due to fuel damage will depend on how effectively the reactor building provides hold up and scrubbing of radionuclides, to limit their release into the environment. Thermal damage to fuel can release volatile fission products, including noble gases and other volatiles. Other volatiles, including cesium, iodine, and ruthenium, condense onto surfaces or into aerosols upon reaching cooler regions away from thermally degraded fuel.

The physical arrangement of the reactor building, including the geometry of the containment or confinement volume located inside the citadel structure, plays a major role in affecting the hold up, removal, transport, and release of fission-product aerosols. A key concern relates to the potential for structural failure of these structural boundaries that could provide a pathway for a large, early release, before the various mechanisms that remove aerosols (gravitational settling, diffusiophoresis and thermophoresis) have had sufficient time to reduce aerosol concentrations. Structural failures may be driven by internal sources, particularly the release of stored energy from high-pressure coolants (water, helium), from chemical reactions (sodium), or from interactions of high-temperature molten fuel with volatile coolants (water). Structural failures may also be driven by external events, in particular external missiles and earthquakes.

When structural integrity is maintained, the release of fission product aerosols occurs primarily through leakage paths associated with piping and electrical penetrations. Leakage requires a pressure differential, and will be different for high-pressure, low-leakage structures versus low-pressure, low-leakage or filtered volumes. In base isolated structures, this leakage from the citadel is likely to act as the containment or confinement, so leakage will occur into the volume between the citadel and the external events shell. This volume is normally ventilated, to assure that any release is directed through an exhaust stack that can be monitored for flow rate and radionuclide concentration, to provide the basis for predicting plume concentrations and making off-site protective action decisions.

5.1.3 Physical Arrangement and Physical Security Functions

Reactor structures and physical arrangement must be closely integrated with the design of the plant physical protection system (PPS). The design of the physical protection system starts with systematic identification of potential targets for radiological sabotage and for theft of material. For reactors, fresh and spent fuel is generally sufficiently unattractive for theft that the PPS design is determined principally by considerations of radiological sabotage. The exception is reactors that use mixed oxide (MOX) fuel, since the plutonium in fresh MOX fuel is substantially more attractive for theft due to the lack of significant radiation levels from fission products.

For radiological sabotage, the identification of targets starts with the same probabilistic risk assessment (PRA) models used for safety assessment. These can be used to identify target *cut sets*, that is, combinations of different equipment and structural items that, if damaged, could result in a radiological release. Likewise, these models can be used to identify *success sets*, that is, combinations of equipment that, if protected from damage, are capable of preventing a radiological release.

With information about cut sets and success sets, optimal physical arrangements can reduce the required size of the physical protection force. First, to the extent that there exists a success set or sets that are comprised primarily or exclusively of passive components, that can be placed in inaccessible locations, physical protection force requirements can be reduced. Non-passive systems are typically comprised of redundant equipment items to increase reliability, and typically the protection of only a single equipment item is needed for a success set. Therefore, as with safety, there are physical protection benefits from providing physical isolation of redundant equipment, with separate access pathways for each equipment train.

The physical arrangement of a facility must also consider the defensive strategy of the protective forces. In general, the arrangement should provide protected locations for security force personnel, while forcing intruders to move through exposed locations. For effective response to occur, unauthorized access must first be detected. For external intruders, systems for detection and delay should be provided outside the reactor building, at the perimeter of the plant protected area.

Physical arrangement and access control also contribute to reducing risks associated with potential insider threats. From the perspective of safety, positive access controls reduce the potential for inadvertent errors, and they can likewise be effective to detect and prevent malicious actions (along with other human performance methods such as two-man rules, supervisor observations, and personnel background checks).

Nuclear facilities already require substantial physical barriers to provide biological shielding, radionuclide containment, and external event exclusion, structures are already in place that can provide effective barriers for physical protection, as long as physical protection requirements are considered early in design.

In base isolated structures, the isolated citadel can provide areas with effective access control, including highly inaccessible areas, where passive components can be located. Examples can include equipment that is located in normally inaccessible space below

heavy crane-movable hatches. Likewise, the volume between the citadel and external event shell may provide an appropriate place to locate redundant trains of equipment, since significant physical separation can be achieved by locating the trains at different positions around the periphery of the building. In this case, for physical security, it is important to assure that the physical arrangement provides physically separate access paths to each equipment train location.

5.1.4 Major SSCs Requiring Design Integration

An incomplete list of the major SSCs that must be integrated in to the external event shell and base-isolated citadel design and be evaluated with respect to the system seismic response are listed below. In addition, all supportive systems for safety-related SSCs in the primary system must be factored when finalizing the design of the external event shell. Some affected SSCs include but are not limited to the following:

- Cranes
- Snubbers
- Piping
- Electrical (multiple sources)
- HVAC
- I&C
- Fire protection system
- Component cooling systems

Seismically-based isolated structures can present issues for important building penetrations between gaps. It is desirable to minimize the number of safety-related SSC's requiring these umbilical connections across structure gaps where overall system structural integrity must be maintained.

5.2 Reactor System Seismic Design Criteria

The General Design Criteria (GDC) 2 of Appendix A to Title 10, Part 50, of the *Code of Federal Regulations* require that nuclear power plant SSCs important to safety must be designed to withstand the effects of earthquakes without loss of capability to perform their safety functions. Since each reactor system can be decomposed into a set of SSCs, the USNRC staff developed a seismic design classification system (Regulatory Guide 1.29, USNRC) establishing a Seismic Category I for SSCs that must be designated to be functional in the event of the design basis seismic event (i.e. safe shutdown earthquake). The AP-1000 Design Control Document (Westinghouse, 2008) defines a safety-related function as one that is relied upon during or following a design basis event to provide for the following:

- The integrity of the reactor coolant pressure boundary,
- The capability to shut down the reactor and maintain it in a safe shutdown condition,
- The capability to prevent or mitigate the consequences of accidents that could result in potential offsite exposures comparable to the guideline exposures of 10 CFR 100,

The design options for base-isolation and external event shells discussed in Chapter 2 are intended to meet functional requirements with respect to seismic and external event load considerations.

5.2.1 SSC Seismic Classification

After extensive regulatory experience with issuing permits and operating licenses for LWRs, the NRC staff developed a seismic design classification based on three categories for SSCs. Each category is briefly discussed below. In addition, buildings are also assigned a classification based on the contained equipment. Codes and standards for design and construction of each building are contingent upon this classification. The role of modular construction in meeting these criteria is further discussed in the following section.

5.2.1.1 Seismic Category I (SC-I)

Most safety-related SSC's are classified as SC-I with only a few exceptions. It is expected that a technology-neutral licensing approach for Gen IV designs will implement risk-informed and performance-based regulatory methods in order to ensure sufficient safety margins are being met. For smaller pool-type Gen IV reactors that rely heavily on passive safety systems, it is expected that the overall number of SSCs will be significantly less than LWR and ALWR designs however the ratio of SC-I to other SSCs will be greater. According to the PRISM PSID (NUREG 1368, NRC), the design of SC-I structures include specifying and complying with the following:

- Applicable codes, standards, specifications, and regulations
- Methods and criteria for loads and load combinations
- Design and analysis procedures
- Structural acceptance criteria
- Materials
- Testing and in-service inspection requirements

SC-I structures, systems, and components must meet the quality assurance requirements of 10 CFR 50, Appendix B. An example of a building that would meet SC-I category of building codes and standards would be the reactor building of the modular reactor.

5.2.1.2 Seismic Category II

Seismic Category II applies to plant structures, systems, and components which perform no safety-related function. Seismic Category II includes SSCs designed to prevent structural failure during a SSE or interaction with SC-I items that could impact the functioning of a safety-related SSC to an unacceptable level, or could result in incapacitating injury to plant operators in the control room. SC-II fluid systems require a higher level of pressure boundary integrity if located near safety-related equipment. Systems, structures and components that are classified as SC-II are also subjected to QA requirements requiring that these components will not cause unacceptable structural failure of or interactions with SC-I items. An example of a building that would meet SC-II category of building codes and standards might be the plant vent stack and stair structure.

5.2.1.3 Non-seismic

Non-seismic (NS) structures, systems, and components are those that are not classified SC-I or SC-II. Non-seismic equipment and piping are typically routed outside of safety-related buildings and rooms to avoid potential safety issues. In general, it is required that even complete failure and collapse of NS structures not affect an nearby safety-related structures.

5.2.2 Implications for Plant Construction

Improved construction methods are essential in improving the quality and reducing the construction schedules and costs of small modular reactor concepts. It is essential that these best-practice methods are fully integrated into the reactor design process early on in order to reduce expected capital costs. A study by the Nuclear Energy Agency stated that the total cost reduction due to modularization is estimated to be between 1.4 to 4% of the total construction cost (OECD, 2000). In this section, the role of plant arrangement and modular construction methods in driving down construction costs is discussed.

5.2.2.1 Improved Plant Arrangement and Reduction in Safety-Related SSCs

Recent experience with the licensing and construction of the AP-1000 plant illustrates the value in improving the overall plant arrangement. By significantly reducing the footprint while maintaining equivalent generation capacity, Westinghouse is able to drive down the expected capital cost of the AP-1000. The overall reduction in plant volume was achieved by optimizing the overall plant arrangement and reducing the amount of safety-related equipment using passive safety systems. In Figure 15, the drastic reduction in volume of the nuclear island (the only SC-I category building in the plant) can be seen. According to Westinghouse, reducing the amount of SC-I building volume can have significant cost savings since seismic structures cost as much as three times as more than non-seismic structures (Westinghouse, 2009).

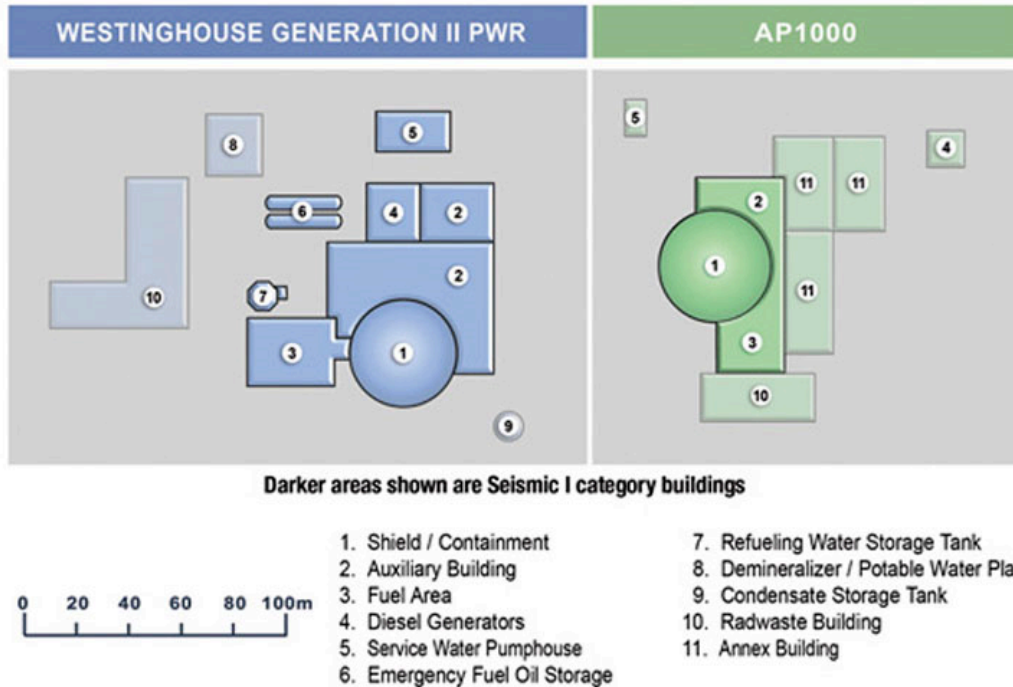


Fig. 15 Comparison of Seismic Category I Buildings for AP-1000 and previous generation PWR (Westinghouse, 2009).

This recent experience is a useful reminder that a viable next generation reactor concept should aim to provide even greater volume reduction without compromising operational efficiency or plant safety. It also shows that rational building and key common SSC arrangement can have a significant impact on cost.

5.2.2 Modularization

With the overall reduction in size and complexity of the pool-type reactors considered, modular construction methods discussed in Section 2.3 are expected to play an even greater role than the recent experience with ALWRs such as the AP-1000. Modular construction allows for offsite factory construction where it is typically much easier to maintain high QA standards while improving and standardizing fabrication processes using computer aided manufacturing. Additionally, modular reactor designs with passive safety systems are very amenable to factory optimization due to the reduction in key safety-related SSCs and increased plant compactness. Reactor modules can be pre-fabricated for structural assemblies, mechanical equipment, piping, tubing, cable trays, electrical panels etc.. Perhaps one of the most attractive advantages of modular construction is the ability to perform much of the fabrication in parallel with other activities onsite, which can have a large impact on construction schedule while maintaining high levels of quality assurance. It should be noted that one must incorporate the transportation cost and factory-unique costs into the net savings resulting from modularization.

Following the lead from the AP-1000, it is expected that future Gen IV reactors will house all safety-related equipment in a nuclear island rated seismic category I structure where volume reduction is optimized with respect to accessibility issues.

5.3 References

- U.S. NUCLEAR REGULATORY COMMISSION, “Regulatory Structure for New Plant Licensing, Part 1: Technology Neutral Framework,” Working Draft Report, Revision a, December 2004.
- U.S. NUCLEAR REGULATORY COMMISSION, Title 10, U. S. Code of Federal Regulations, Part 50. Policy Statement on Advanced Reactors. 59 FR 35461, July 12, 1994.
- US Design Certification: Licensing Basis Event Selection for the Pebble Bed Modular Reactor,” PBMR Document Number 040251, Rev. 1, June 30, 2006.
- US Design Certification: Probabilistic Risk Assessment Approach for the Pebble Bed Modular Reactor,” PBMR Document Number 039144, Rev. 1, June 13, 2006.
- US Design Certification: Safety Classification of Structures, Systems and Components for the Pebble Bed Modular Reactor,” PBMR Document Number 043553, Rev. 1, August 24, 2006.
- US Design Certification: Defense-in-Depth Approach for the Pebble Bed Modular Reactor,” PBMR Document Number 043593, Rev. 1, August 12, 2006.
- Electric Power Research Institute, “Safety and Operational Benefits of Risk-Informed Initiatives”, EPRI White Paper, 1016308, February, 2008
- U.S. NUCLEAR REGULATORY COMMISSION, NUREG-1368, “Preapplication Safety Evaluation Report for the Power Reactor Innovative Small Module (PRISM) Liquid-Metal Reactor”, February, 1994.
- U.S. NUCLEAR REGULATORY COMMISSION, Regulatory Guide 1.29, “SEISMIC DESIGN CLASSIFICATION”, Revision 4, March, 2007.
- Westinghouse. *AP1000 Design Control Document Rev. 17*. Submitted to U.S. Nuclear Regulatory Commission September 22, 2008.
- Source OECD Nuclear Energy, OECD Documents Reduction of Capital Costs of Nuclear Power Plants (ISBN 9264171444), 2000, pp. 1-110(110).
- Westinghouse. Westinghouse AP-1000: AP-1000 at a Glance http://www.ap1000.westinghousenuclear.com/ap1000_glance.html, accessed September 18, 2009.

6.0 PARAMETRIC ANALYSIS

This chapter presents the results of modeling and simulation of seismic and aircraft impact response of base-isolated nuclear power plant structures and their external shields.

The seismic and aircraft crash analysis of base isolated structure response considers structures with several different weights and isolation periods, to study safety and other performance requirements according to general base isolation design guidelines and base isolation provisions in IBC 2006 (International Code Council, 2006) (Kelly and Naeim, 1999). The models and the simulations were implemented and executed using Matlab and OpenSees (<http://opensees.berkeley.edu>). Response of the underlying soil was not modeled explicitly, but earthquake records from sites with various soil conditions were used. The selection of earthquakes and aircraft impact loads was performed as described in Chapter 4.

The analysis of the inelastic response of an external event shell to aircraft crash was conducted using the state-of-the-art structural analysis research software framework OpenSees. This finite element modeling and analysis framework is capable of modeling both the expected non-linear response and added damping of the isolation systems as well as the unexpected but possible non-linear response of the structural elements of the building structure. The structural models were developed considering the guidelines presented in ASCE 4-98 (ASCE, 2000).

6.1 Base-isolated NPP Model for Seismic Analysis: Assumptions and Parameters

The base-isolated NPP models used for the analysis in Section 6.3 (seismic response) are fashioned after base-isolated NPP models used in seismic analyses by Huang, et al (2007). These one and two-node models represent rigid or lollipop 68,000 metric ton (150,000 kip) superstructure atop a base-isolated layer. When the superstructure is considered rigid (one-node models), the mass is lumped at the top of the isolator element and no amplification due to superstructure elasticity is considered. Contrarily, when the superstructure is considered linear-elastic, the mass is split between the two ends of the superstructure element (lollipop), and the element stiffness is chosen such that the non-isolated period is 0.22 seconds. Viscous damping for this element is assumed to be 2% and the motion above the isolation layer is taken into account. Both these superstructure models are assumed to be accurate since the purpose of base-isolation is to minimize superstructure interstory drifts and eliminate inelasticity.

Multiple isolator models were used in order to compare and contrast the response when inelasticity in the isolator is considered. The Matlab model for equivalent linear-elastic isolation bearings considers 10% viscous damping and a stiffness chosen to make the isolated period approximately 3.0 seconds. The OpenSees model for bilinear isolation bearings uses the elastomeric bearing element which defines the response hysteresis using the initial stiffness (k_c), post-yield stiffness ratio (α), and yield strength (F_y). In accordance with the Huang model, these parameters were set to 2,300 metric tons (5,000 kips), 0.1, and 3000 metric tons/cm (17000 kips/in), respectively, such that the post-yield tangent stiffness (αk_c) would produce a model with an isolated period of approximately 3.0 seconds. Because of high-frequency acceleration response “spikes” which occur as a

result of abrupt stiffness changes (Wiebe and Christopoulos, 2010), the raw data from the OpenSees model was augmented using a low-pass filter which removed the high frequency component. Only the filtered data is considered in the results and conclusions.

A parametric analysis of variables affecting the seismic response of the isolation system is not presented in this paper due to an abundance of literature correlating the efficacy of isolation systems with their ability to significantly increase the fundamental frequency of the structure. Instead, the seismic analyses will be used to demonstrate the level of modification of desired response quantities (namely accelerations and displacements), compare results from models with various refinements, as well as comment on the geographic and geologic applicability of base-isolation.

6.2 Base-isolated NPP Model for Impact Analysis: Assumptions and Parameters

The base-isolated structural model of a base-isolated nuclear power plant (Figure 9A) used for the analysis presented in 6.4 (global aircraft response) was developed in Matlab. A number of assumptions made during the modeling process should be considered when viewing the results. The most important assumption is that both the structure above the isolation level and the isolation devices in the isolation layer remain elastic. In conjunction with this assumption is the simplification that structural and isolation damping are viscous and remain constant at 5% and 10% of critical, respectively. The total mass of the superstructure is distributed over the height as follows: 43.3%, 33.3%, and 23.3% of the total structural mass is assigned to the first, second, and third floor, respectively. The model of the base isolated nuclear power plant is, thus, a three degree-of-freedom shear beam model with the bottom shear beam representing the base isolation layer and the top two shear beams representing the stiff superstructure. Finally, the horizontal stiffness of superstructure is selected such that the fundamental vibration period of the non-isolated structure is approximately 0.34 seconds. Thus, superstructure properties are chosen such that the un-isolated structure is very stiff, as would be expected for bulky nuclear structures.

The consequence of these assumptions is a model that gives conservatively high estimates of accelerations of the superstructure, while the displacements of the superstructure are likely to be smaller than those obtained using a more accurate non-linear model of the isolation devices. Additionally, the model will fail to show any inelasticity in the structure, which is expected to be extensive, although acceleration levels will give an estimate of the level of damage. Despite the restrictive modeling assumptions, an analysis of the superstructure response to impact loading will enable a comparison of different design alternatives discussed in Section 2.2.

Two principal properties of the isolated structure govern its dynamic response to aircraft impact loads. They are: the total structural weight, W , and the fundamental vibration period of the isolated structure, T (which essentially is directly related to the stiffness of the isolation layer, K_{iso} , since the weight, or mass, of the structure is already a parameter). Analysis of nine separate design options is accomplished by considering a matrix of three distinct structural weights (20,000 metric tons [44,000 kips], 50,000 metric tons [110,000 kips], and 100,000 metric tons [220,000 kips]), and three different building periods (1.35, 2.00, and 2.99 seconds). Damping ratios of the structure and the

isolation layer were kept constant in this parametric analysis, and were not considered as design parameters in this study. This was done because increasing damping in the isolation layer may change the dynamic response of the superstructure by inducing higher-mode response, which is not desirable.

6.3 Earthquake Response of the Base Isolated NPP Model

Each of the four base-isolated NPP models was subjected to 30 two-horizontal-component ground motion records (each direction considered independently) in order to ascertain the effect of considering isolation inelasticity and superstructure elasticity on the peak acceleration and displacement response. A summary of the resulting peak response data is available in Appendix C. The acceleration response is essential in estimating the seismically induced damage in the structural and non-structural elements of the superstructure. However, because nearly all the displacement in the isolated structure is concentrated in the isolation layer, the absolute displacements are not a useful barometer for damage assessment; instead they are used to design the size of the isolators and the width of the isolation gap.

Figures 16 and 17 show the peak acceleration response of each isolated model versus the peak isolation response of the non-isolated linear-elastic model subjected to the same groundmotion. In all cases, the non-isolated structure is given a period of 0.22 seconds and a damping ratio of 2% to match the properties in the elastic superstructure models. Each ground motion group has been differentiated by color and regression lines constrained to go through the origin were fit to each group. Despite noticeable scatter in the data, the slopes of these lines describe the ability of each model to effectively reduce accelerations as input magnitudes increase. It is clear that for reducing structural accelerations, each model is most effective in response to the Boston motions, and is least effective in response to the Los Angeles motions. This result is due to two factors: soil mechanics and faulting conditions. The Boston motions were chosen to depict stiffer soil conditions and intraplate faulting, resulting in higher-frequency ground accelerations which are easily filtered out by the flexible, long-period isolation system. Conversely, the west coast motions represent poorer soil conditions (poorest in Los Angeles) and plate-boundary faulting mechanisms (e.g. strike-slip and reverse faulting) which can cause low-frequency, pulse-like records capable of resonating with isolation systems. Thus, base-isolation systems require application at stiffer soil sites for full efficacy. Nevertheless, by reducing the response accelerations, base-isolation systems reduce the range of anticipated forces thereby increasing the ability for one system to be applicable over a wider range of building sites.

Comparisons of the various modeling options depicted in Figures 16 and 17 enable comment on the most-appropriate methods for analysis. The effect of superstructure elasticity is seen by comparing the 1-DOF models (Figure 16) to the 2-DOF models (Figure 17). Reviewing the data shows that inclusion of superstructure elasticity changes regression line slopes by 0.4 – 5.7%. Consequently, the rigid superstructure analysis is considered to be sufficiently accurate. Observation of the results also show that bilinear model regression line slopes increase in Boston, Seattle, and Los Angeles by 122%, 50%, and 22%, respectively, over those associated with the linear-elastic models. At large input

magnitudes, these changes can be drastic, demonstrating the importance of considering inelasticity in isolation analysis.

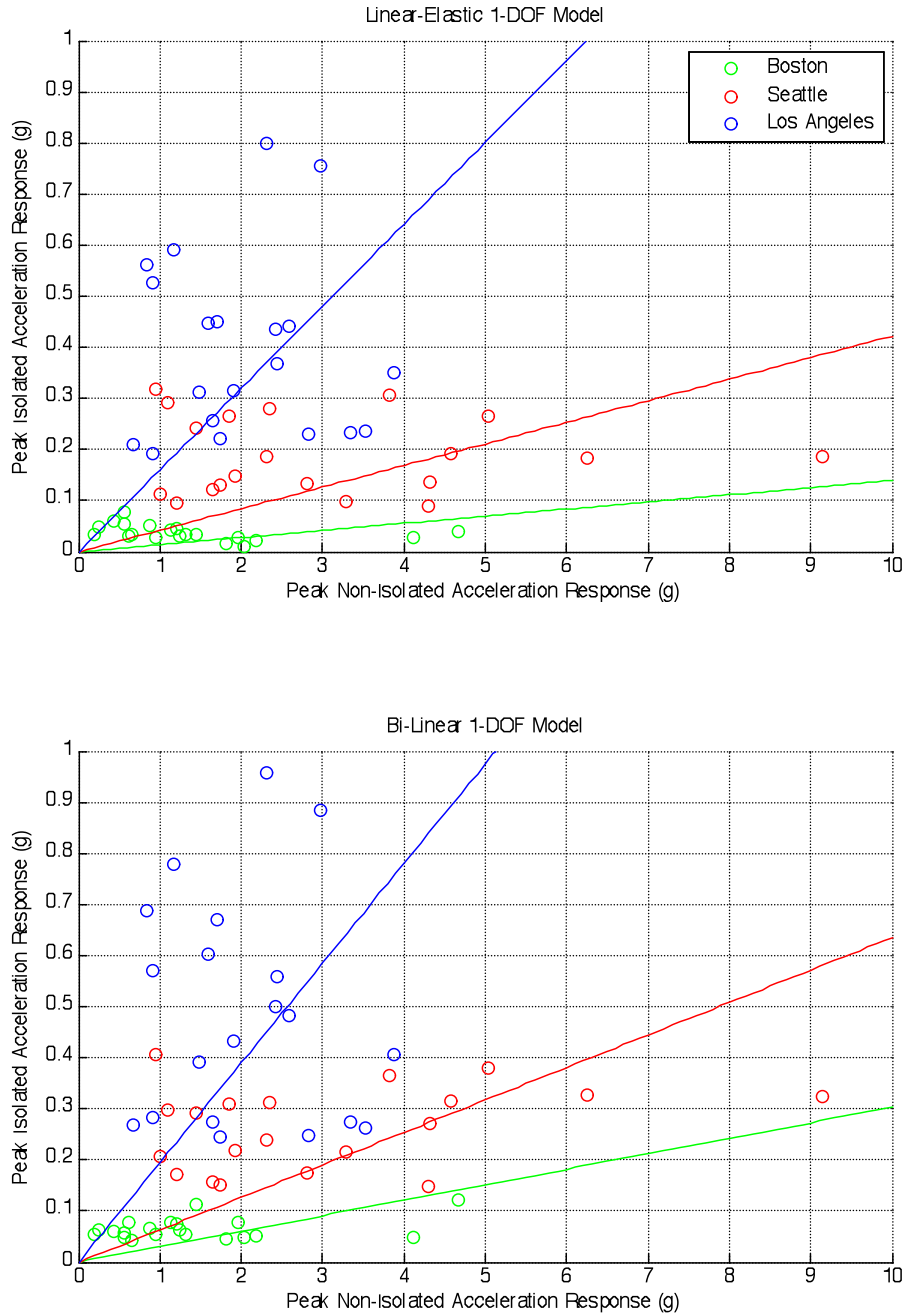


Fig. 16 Peak acceleration response of linear-elastic and bilinear isolator models with rigid superstructures

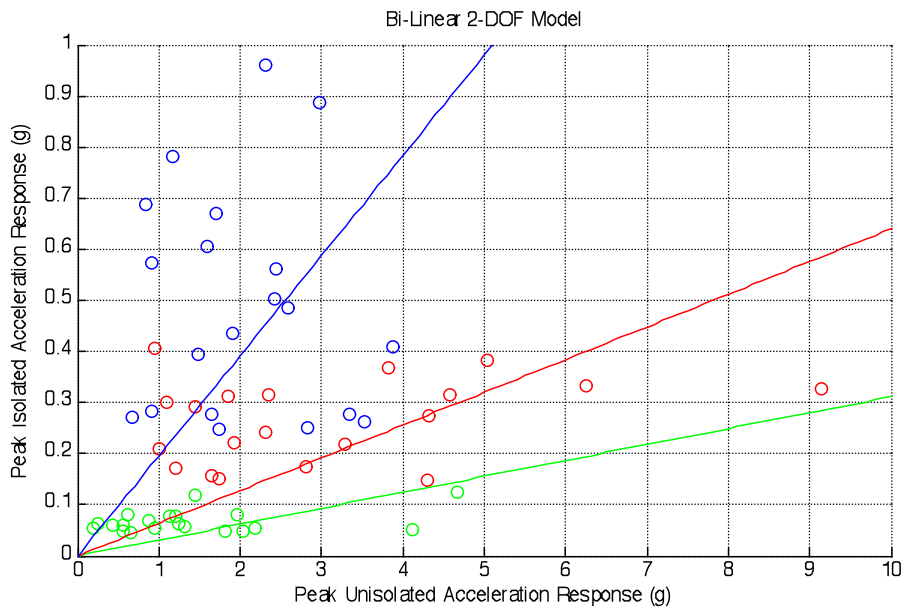
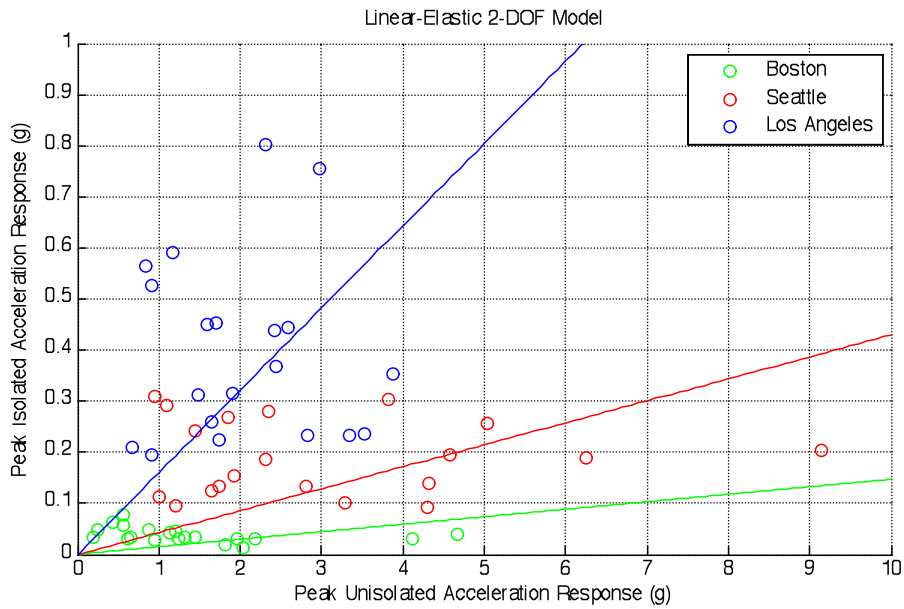


Fig. 17 Peak acceleration response of linear-elastic and bilinear isolator models with linear-elastic superstructures

Figure 18 shows the peak displacement response of each 2-DOF isolated model as a function of the peak ground displacement (PGD). The 1-DOF model was found to have regression line slopes within 2% of those shown in Figure 17, again showing the close approximation of the rigid model, and therefore have not been plotted. The data for this model is presented in Appendix C. The peak displacement is often larger than the PGD of the input groundmotion, an expected result since spectral displacements increase approximately linearly in the velocity sensitive period-range containing most base-isolated structures. However, this is not problematic since this displacement is localized in the isolation layer and can be designed for by creating an isolation gap with a width equal to the largest anticipated 2-dimensional displacement (found to be 2.8 m, or 9.1 ft, from the 2-DOF bilinear model in response to the ground motion of LA25 and LA26) times a factor of safety.

An interesting result of Figure 18 is that some of the regression lines for the displacement data increase in slope from the linear to the bilinear case, while others decrease. Once again the range of data from the bilinear model appears to be larger, so this model is recommended for a conservative analysis; however, both models are relatively close and show far less scatter than the acceleration data. Thus more confidence can be inferred from the displacement analysis.

Although not directly analyzed within, the effect of period choice on the response of base-isolation systems is an important concept for the designer. Figure 19 shows acceleration response spectra for two of the ground motions used in this study. For the LA 21 record, it is evident that lengthening the base isolation period will have a substantial effect, reducing the PGA-normalized spectral acceleration to approximately 0.20 at a period of 4.0 seconds (an 80-90% reduction depending on the original period of the superstructure). On the other hand, the LA 24 record only reduced the PGA-normalized spectral acceleration to 0.75 at the same period. Although this can be as much as an 80% reduction depending on the initial period of the superstructure, it is still a very large percentage of the original PGA. It should be emphasized that although peak isolated response accelerations are sometimes large fractions of the ground motion PGA (i.e. small reductions), they are almost invariably small fractions of the peak non-isolated response accelerations, especially when the structure in question is very stiff like most NPPs. Furthermore, the efficacy of an isolation system to significantly reduce peak response accelerations below the PGA is predicated on soil type and faulting mechanisms, as previously mentioned, since these variables control the frequency content of the resulting ground motion.

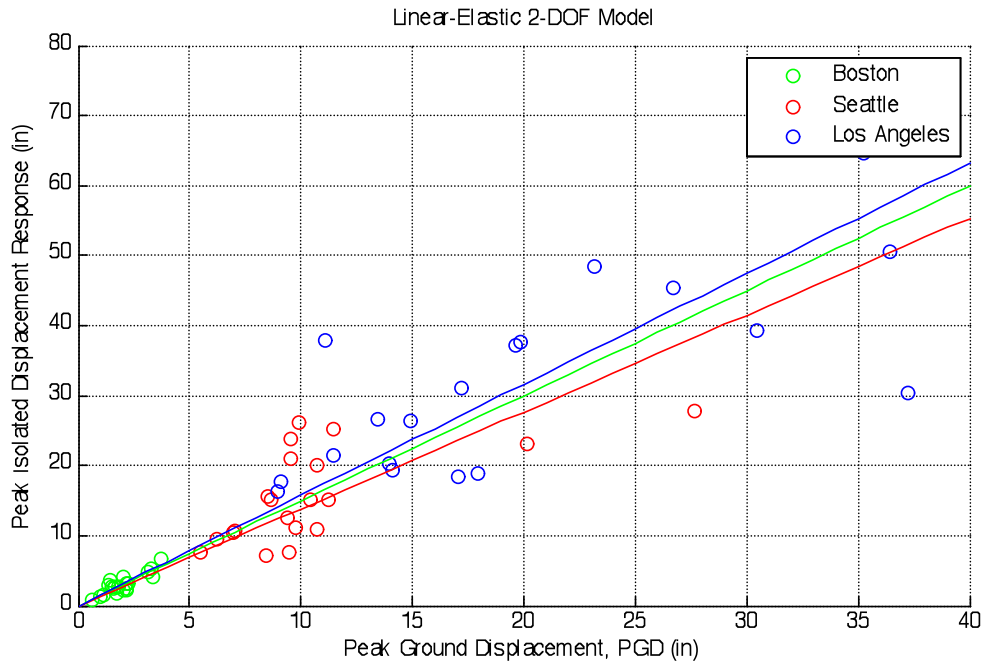


Fig. 18 Peak displacement response of linear-elastic and bilinear isolator models with linear-elastic superstructures

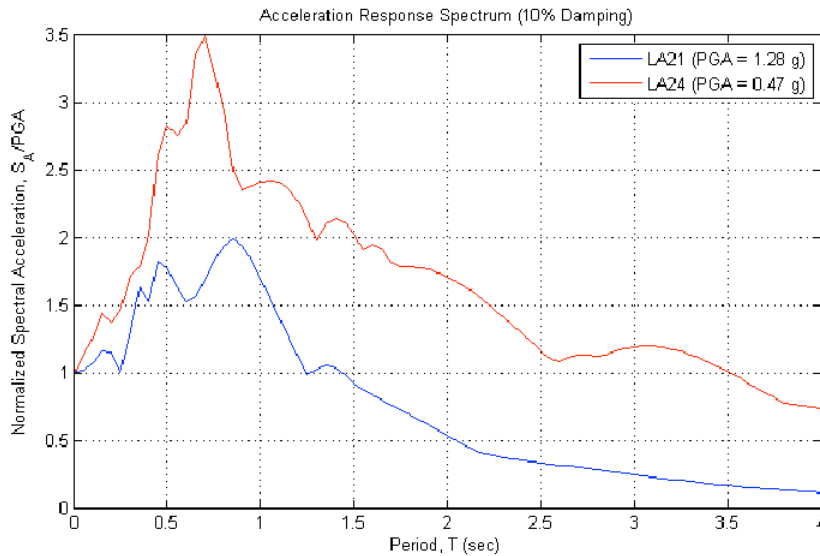


Fig. 19 Normalized spectral accelerations for two ground motion records from the SAC Project Los Angeles ground motion suite.

6.4 Response of Base-Isolated NPP Model to Aircraft Impact

The three-story simplified model of a base-isolated nuclear power plant was analyzed to compute its response to impulse loads resulting from aircraft impact. Two aircraft types, Boeing 747-400 and Boeing 737-900 aircraft (Table 2) were chosen to represent the upper and lower bounds for possible impact cases, respectively. This loading is applied over a relatively small surface area of the nuclear power plant: therefore, there are two principal concerns. The first concern is the local behavior of the structure at the point of impact, including possible local collapse and penetration of the aircraft. This concern is addressed in Section 6.4. The second concern is how these forces are transferred down the structure and ultimately to the ground, as well as the global consequences of such motion. This section addresses the global response of the structure to airplane impact, including transfer of momentum and global motion of the base isolate structure and deformation of isolation devices.

The nine models of base-isolated nuclear power plant described in Section 6.1 were subjected to two aircraft impact load histories. Dynamic analysis was conducted as an impact load analysis, where the impulse load histories shown in Figure 13 were applied to the top-level mass of the three-degree-of-freedom base isolated nuclear power plant model. The loading is applied assuming on-center impact without eccentricities.

Figure 20 presents the dependence of the impact-induced peak roof acceleration on the weight and the fundamental vibration period of the base isolated structure. Because this peak acceleration is attained early on, before the end of the impulse load, peak acceleration response is essentially independent of the fundamental vibration period and depends only on the weight of the structure (i.e. its ability to admit and respond to the momentum transfer during impact). As the weight, or inertia, of the structure is increased, its peak accelerations are decreased. Thus, base isolated structures subjected to aircraft

impact should be made as heavy as possible to minimize impact-induced accelerations. Alternatively, the nuclear power plant can be configured as shown in Figure 7B, with the base isolated citadel decoupled from its external event shield such that aircraft impact loads are not transmitted into the base isolated citadel structure in the first place.

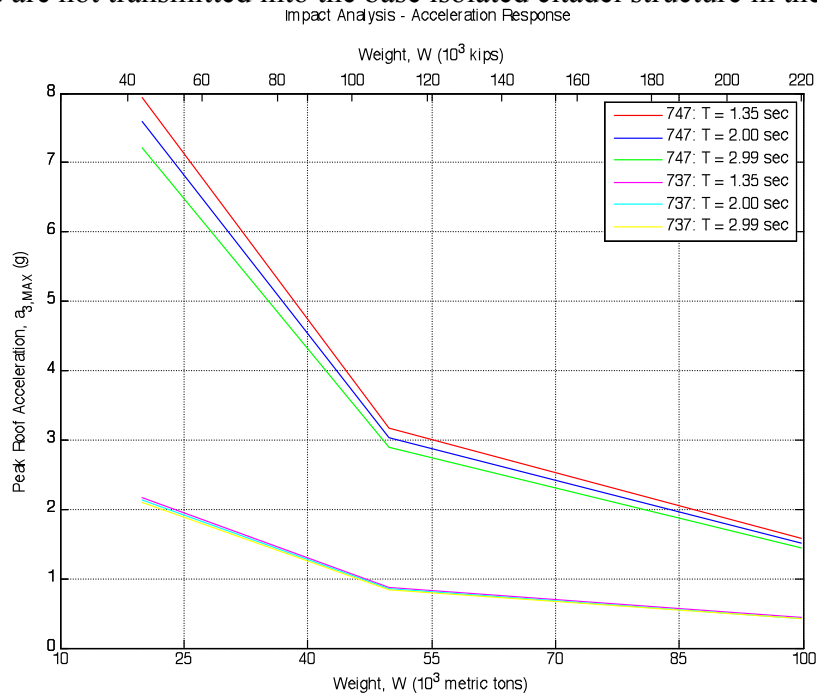


Fig. 20 Effect of structure weight and period on aircraft impact response.

Appendix D presents the time histories of acceleration and displacement response of the model masses to aircraft impact for the nine analyzed cases. Inspection of displacement time histories for the three masses suggests that, in addition to deformation in the fundamental vibration mode (deformation of the isolators), the superstructure also shows significant deformation due to the second vibration mode (superstructure masses moving differently). The peak displacement of the isolators is as high as 60 inches (for the case when the lightest and softest structure is impacted by the heavier aircraft): this may limit the type and the size of the isolation devices that can be used. The peak relative story displacement of the superstructure is approximately 5 inches: significant damage to structural walls is expected at this level of interstory drift.

More importantly, peak roof accelerations are significantly larger than those induced by earthquake loading. Furthermore, the aircraft impacts the superstructure directly, requiring a redundant load path that can sustain the applied force despite local failures and inducing high-frequency vibration in the entire superstructure. The resulting response is very unfavorable for the structure, its components, and equipment, which now must be qualified for the full spectrum of frequencies, as opposed to only the low frequency end from the isolation-filtered earthquake response.

Although not directly analyzed, we can infer that consideration of eccentric impact and torsion it induces would lead to larger peak acceleration and displacement responses, especially at the perimeter of the superstructure and the isolation layer. If friction pendulum bearings were to be used, differential horizontal displacement of individual bearings would also induce differential vertical lift at each isolator. This could induce uplift at interior bearings, inducing higher stresses in grade beams (which now have to span longer distances) and under perimeter foundations.

6.5 Decoupled Event Shell Response to Aircraft Crash

This section examines the local and global effects of aircraft impact on the external event shield structure that is decoupled from the base isolated citadel structure, as shown in Figure 8B. For such above-grade structures, two major categories of external event shells can be considered, those with cylindrical or those with rectangular geometries. The AP-1000 (Fig. 9A) uses a cylindrical external event shell, which is physically decoupled from the internal containment vessel. The cylindrical event shield configuration was not examined in this report. As a part of a scoping study (Wei, 2009), the response of a simplified rectangular external events shell was studied, where the shell is reinforced on its interior by a honeycomb lattice of beams and columns. Results from this study are summarized in this section.

The reference external event structure, shown in Fig. 21, was designed as a grillage structure that acts as a 3-dimensional diaphragm under airplane impact loads. The overall structure has a footprint of 60 m x 60 m (192'x192') and a height of 45 m (144 ft). These dimensions are required to span the above-grade portion of a typical LWR reactor building. A 3-D model was created using the OpenSees structural analysis framework to capture the expected 3-dimensional response of the external shell structure. A non-linear static pushover analysis was performed to determine the response of the external events shell to a direct impact by a Boeing 747-like hypothetical airplane (BHA), with length, weight, and velocity parameters given in Table 4. While orthogonal beam-column grill structure was selected based on structural engineering considerations, in an actual base-isolated reactor building, the volume between the beam and column lattice could be used to house equipment and provide access for operations and maintenance.

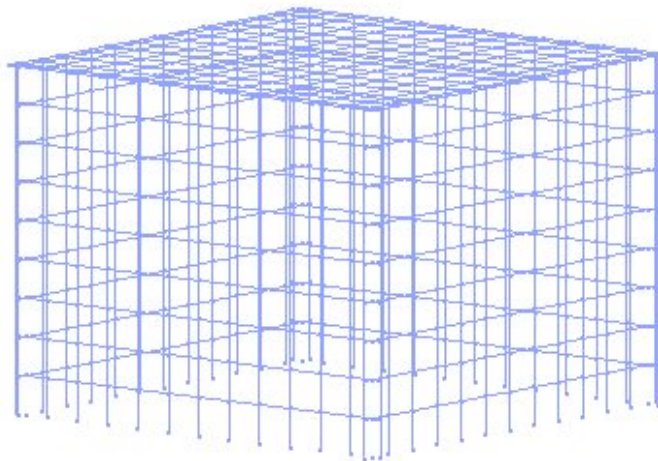


Fig. 21 Rectangular external event shell model geometry.

To determine the response of an external event shell, airplane crash loads can be applied either dynamically or statically. Dynamic analysis is required to capture the peak dynamic response values amplified by the impact pulse, to determine the participation of different structural vibration modes in the motion of the structure after impact, and to investigate the interaction between the structure and the impacting aircraft. However, the goal of this scoping study was to evaluate the behavior and examine the failure modes of the three-dimensional external event shell structure grillage decoupled from the internal citadel structure that is base-isolated. This limited goal can be achieved by conducting a non-linear static pushover analysis using a point-load pattern to represent the impacting aircraft, because the results of such non-linear pushover analysis are indicative of the response envelope of the dynamic response of the external shield structure.

As shown in Fig. 22, the BHA fuselage was estimated to generate a force of 375,000 kN (84,400 kips) and the wings a force of 142,000 kN (32,000 kips), creating a total force of 631,000 kN (148,400 kips). Event shell deformations and element forces and deformations due to this static force loading were calculated to determine structural performance. By allowing the lattice structure of the external event shell to resist and soften the impact, and by providing a sufficient isolation gap, the inner, base-isolated citadel structure will be able to respond elastically and remain undamaged. It is important to note that the function of the external event shell is to prevent unacceptable damage to safety-related structures and components inside the decoupled, base-isolated citadel. Restarting of the reactor was not taken as the post-impact performance goal, so relatively large inelastic deformations of the external event shell are tolerated.

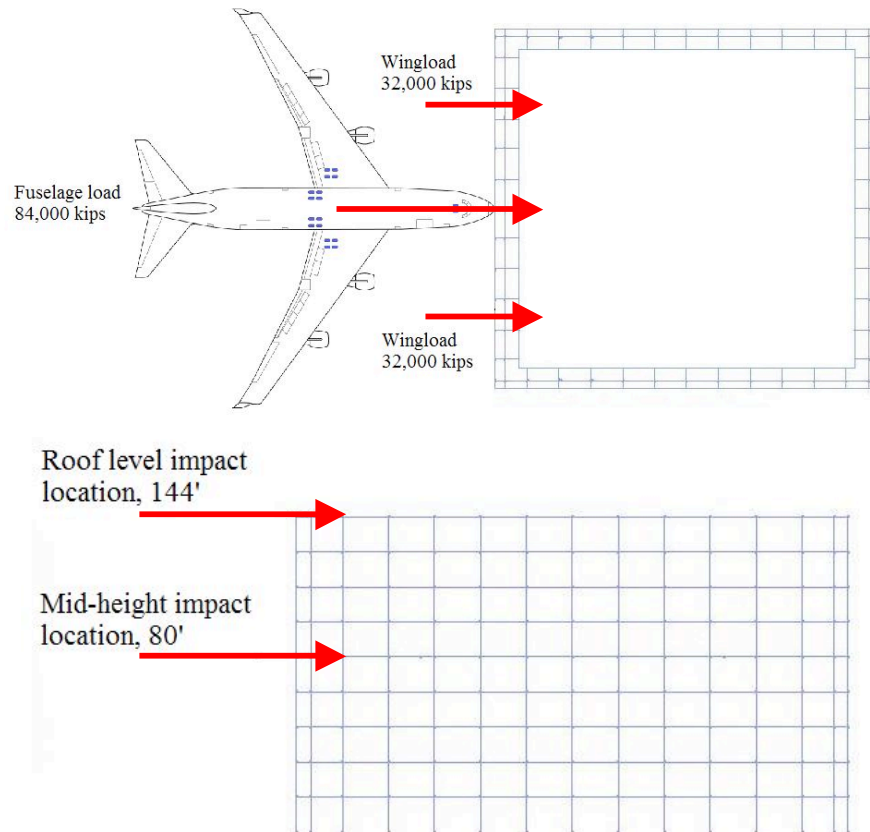


Fig. 22 BHA impact load locations into rectangular decoupled external event shell.

The lattice structure of the external event shell was designed to take advantage of diaphragm action. The beams and columns of the external shield structure are made using conventional reinforced concrete. The cross-section design iteration process started by conducting a pushover analysis, using the initial beam and column dimensions and strengths (material strength factor of 1). The pushover analysis of the initial model failed to converge at load levels well below the BHA load level was reached. The design was modified in subsequent iteration by observing where and how the model was failing and by increasing the size and strength of the sections until the shell was capable of sustaining the aircraft load as follows

Material strength for the external events shell elements was determined iteratively. The first iteration started with a concrete strength of 27.6 MPa (4 ksi) and reinforcing steel strength of 345 MPa (50 ksi). These material strengths were then multiplied by a material factor ranging from 1 to 8. This helped evaluate the elastic response of the external event shell, determine the general failure modes, and find if beams or columns govern the behavior and if the failure of the cross-sections is due to exceeding steel (in tension) or concrete (in compression) limits.

Once a design was identified that was capable of sustaining the entire airplane load applied at the mid-height of the side wall of the external shell structure, further iterations were made because some sections that worked for a mid-height airplane impact location

failed when the airplane load was applied at the roof level. This was due to the interaction between the roof grid and the loaded wall. When the load was applied at the roof, the roof grid beams acting as a diaphragm need to have a sufficiently large amount of reinforcement to transfer (drag) a large axial loads from the loaded wall to the other walls of the external shell structure. However, if the amount of reinforcement was too high, the roof grid became too stiff and prevented successful distribution of the impact load to the entire structure causing a localized failure at the point of mid-height impact. Therefore, a balance was struck between increasing the amount of reinforcement in the wall columns and beams to prevent local failure and the stiffness and strength of the roof grid.

The final lattice structure walls for the reference external event shell design are shown in Fig. 23. They are designed as a grid of equally spaced beams and columns. The columns have a depth of 4.57m (15.0') and a width of 1.22 m (4.0') and are spaced 4.88 m (16.0') apart on center. The beams span between the columns and have a width of 4.57 m (15.0'), a depth of 1.22 m (4.0'), and a length of 4.88 m (16.0'). A roof diaphragm grid was created using beams with the same sections as those in the walls of the external shell structure placed at the grid spacing defined by the columns. Table 5 shows the reinforcing selected for the beams. Conventional reinforcing bar was used in this study. However, the event shell may be constructed using composite steel-plate/concrete construction (Section 2.3) due to improved inelastic response and strength compared to conventional reinforcing.

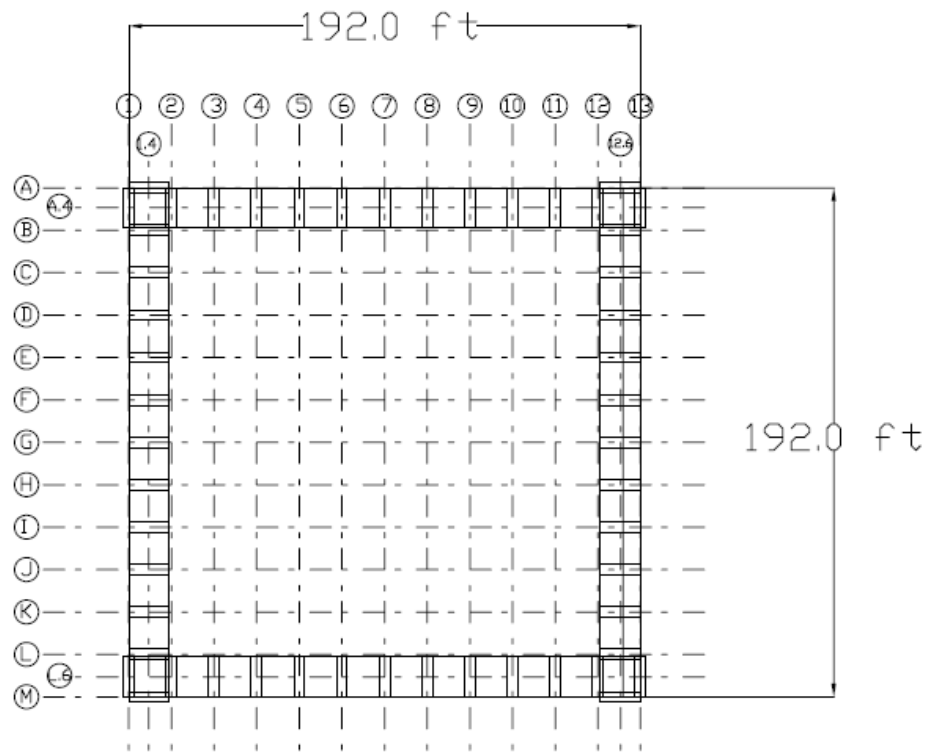


Fig. 23 Rectangular event shield plan view.

Table 5 Element section dimensions.

| Element | Section height (ft) | Section width (ft) | Element length (ft) | Top reinf. | Bottom reinf. | Intermediate reinf. |
|----------------|----------------------------|---------------------------|----------------------------|-------------------|----------------------|----------------------------|
| Column | 15 | 4 | 16 | (50) #18 | (50) #18 | (40) #18 |
| Beam | 4 | 15 | 16 | (45) #18 | (45) #18 | (24) #18 |
| Roof grid | 15 | 4 | 16 | (50) #14 | (50) #14 | (40) #14 |

Because the space within the lattice walls of the external shell structure will ideally be used for equipment storage, a superimposed dead load of 4.8 kPa (100) psf and a live load of 0.96 kPa (20 psf) were assumed in addition to self weight. This load was also included in nodal mass calculations because most of the load is assumed to be long term. A perimeter load was also added to represent the structural cladding. This cladding was assumed to be a sandwich steel/concrete composite construction with a 0.40 m (1.3') thick concrete section between two 0.152-m (6.0") thick steel plates to aid in reducing local missile penetration. Note that the structural action of the cladding was not taken into account in this study. Instead the cladding dimensions were used to conservatively assess its weight. Additional detailed analysis is warranted to determine the optimal (likely smaller) plate thickness to resist penetration.

The BHA model was described in Chapter 4. In the analyses of the external event shell structure, the aircraft impact loads are applied horizontally at two locations, at roof level (144' above ground) and at mid-height of a wall (80' above ground), as shown in Fig. 25. The aircraft was assumed to impact the structure in horizontal flight along one of its principal axes. This maximizes the impact normal force. Eccentric load effects in the horizontal and vertical planes due to an off-axis impact were not considered.

The model built in this study was built using the OpenSees framework. The Open System for Earthquake Engineering Simulation (OpenSees) is a software framework created at the NSF sponsored Pacific Earthquake Engineering Research (PEER) Center that can simulate seismic response of structural and geotechnical systems. The framework is object oriented and open source, which allows users, typically earthquake engineering researchers, to influence how OpenSees operates. OpenSees' framework includes computation, modeling, and information technology components. OpenSees capabilities include modeling and analysis of nonlinear response using a wide array of materials and beam column elements. The model can be defined at an element, section or fiber level (OpenSees 2009).

In the reference model material strengths were assumed to be with a concrete strength of 55.2 MPa (8 ksi) and reinforcing steel strength of 414 MPa (60 ksi), assuming that the steel reinforcement was Grade 50 with an over strength factor of 1.1. The material types used in the model are OpenSees' Concrete01 and Steel01. Concrete01 is a uniaxial Kent-Scott-Park concrete material that assumes negligible tensile strength and has a degraded linear unloading/reloading stiffness based on the Karsan-Jirsa model. Steel01 is a uniaxial bilinear steel material with kinematic hardening (OpenSees, 2009). A force based nonlinear beam column element was used to model the behavior of the columns

and beams. This element considers distributed plasticity along the element, the integration of which is based on the Gauss-Lobatto quadrature rule. This model used five integration points along the element, with two integration points located at the element ends and the three intermediate points spaced evenly along the element.

The model of the external events shell has a total of 1338 elements. Of these elements 502 are beams, 364 are roof grid beams, and 468 are columns. The external diaphragm is neglected in the analysis. The loading, including both self weight and superimposed dead load and live load, on the beam is 17.6 k/ft and on the roof grid beam, 18.9 k/ft. The total weight of the external events shell is 145,000 metric tons (320,000 kips). The natural vibration periods for the first three modes are 0.89 seconds, 0.72 seconds, and 0.69 seconds, respectively.

The loaded wall undergoes significant local yielding when the BHA load is applied at mid-height. However, once the forces are transferred to the rest of the external events shell structure through the roof diaphragm action, the structural elements in the roof and the other three walls behave elastically. Note that local failure and possible elimination of the beam and column lattice structure at the point of impact was not modeled, nor were the effects of local penetration through the diaphragm of the external event shell building analyzed.

The deformed shape of the front wall under the BHA mid-height impact load is shown below in Fig. 24. Profile views of the deformed shapes along different reference planes, and results for roof-height impact, are given elsewhere (Wei, 2009).

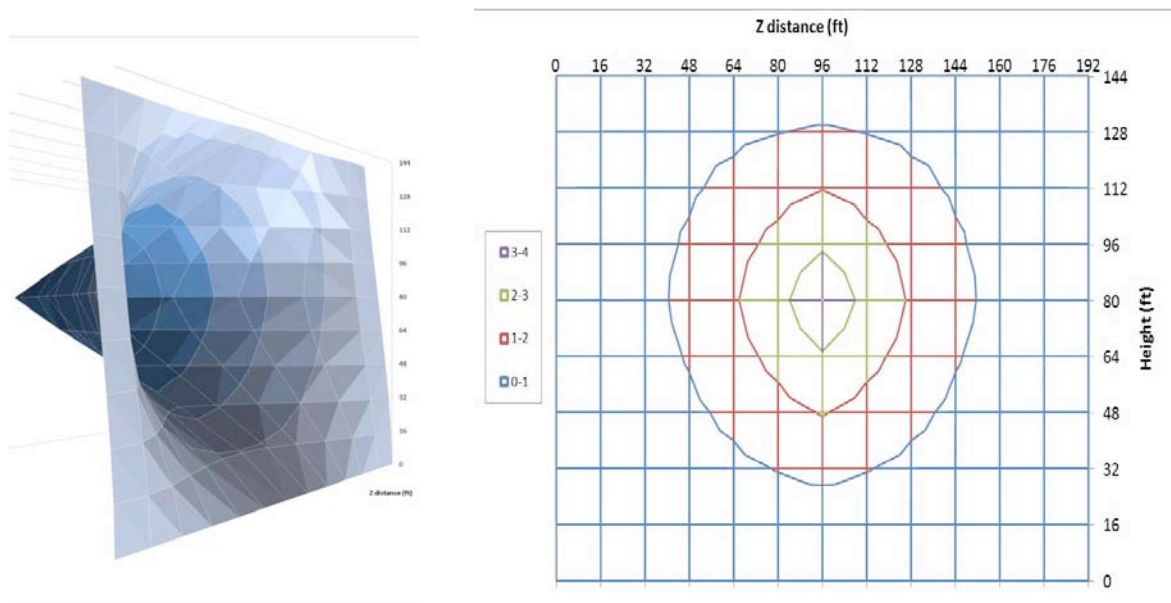


Fig. 24 Deformed shape of the loaded wall for mid-height BHA impact into the rectangular decoupled external event shell (displacements in feet).

The maximum displacement occurs at the node where BHA impacts the loaded wall and is approximately equal to 1.13 m (3.7 feet). The maximum induced interstory drift ratio is approximately 6%. Such interstory drift values indicates that the locally impacted

beams and columns will sustain sever damage but may be able to survive the airplane crash and still carry some load. The loaded wall is the only wall that deforms inelastically. The mid-height BHA impact causes a “bunching up” of the external events shell roof near the loaded wall. This transfers an outward horizontal force on the side walls as well as the back wall. However, the resulting maximum displacements on these walls are not large: the maximum horizontal displacement at the top of the back wall is approximately 0.15 m (0.5’), and only 0.0091 m (0.03’) on the side walls. The maximum vertical displacement of the roof is approximately 0.15 m (0.5’). This results in a maximum interstory drift ratio of 0.5% in the back wall and 0.2% in the adjacent walls. Such interstory drift levels indicate mild to moderate damage in the external event shield structure.

The maximum moment, in the vertical column with maximum loading in the impacted wall, occurred at the 6th story and the top story for the mid-height and roof-level BHA impact cases, respectively. The column yield moment was approximately 250,000 kip-in. This moment was attained at a relatively small displacement of 0.061 m (0.2’) in the mid-height BHA impact case. In contrast, the column did not fail in moment under the BHA roof-level impact. The column attains its shear strength (of approximately 45,000 kN (10,000 kips)) at approximately the same time when it yields in bending in the mid-height BHA impact case. This suggests that the column likely fails locally. The column yielded in the case when BHA impacts at roof level, but just barely.

The highest-loaded horizontal beam in the impacted wall was selected to investigate its failure mode. The maximum moments and shears for the mid-height and roof-level BHA impact cases occurred in the beam in between J and K (Fig. 24) on the 6th story and in between K and L on the top story on the loaded side of the event shell, respectively. The beam yield moment is approximately 1.0×10^6 kN-m (6000 kip-inches). The maximum-loaded beam yielded in the mid-height BHA impact case but remained elastic in the roof-level BHA impact case. The column attains its shear strength (of approximately 71,300 kN (16,000 kips)) slightly before it yields in bending in the mid-height BHA impact case. Shear strength of the beam was never exceeded in the roof-level BHA impact case, even though it was assumed the beam shear reinforcement was only the minimum required by ACI Code (4GR60 #4 hoops every 0.152 m (6.0”) on center).

Based on this simplified scoping study, it can be concluded that decoupled external events shell structures can likely be designed to withstand a BHA impact load. The mid-height BHA impact case was found to be more critical than the roof level BHA impact case. In the mid-height BHA impact case the loaded wall responded inelastically, with beams and columns in the zone corresponding to the load pattern extent (approximately 30 m (100 feet)) yielding in bending and approaching or exceeding their shear strength. Generally, the vertical column behavior was controlled by bending, while the horizontal beam behavior was controlled by shear. The rest of the external event shell structure remained elastic. Given the beam and column sections adopted for the external event structure in this study, the waffle slab construction of the rectangular external events shell allowed the loaded wall to resist and transfer resultant forces from the airplane crash to

the rest of the external events shell. Dynamic analysis, and significantly greater design optimization, would be required in the design of an actual external event shell.

6.5 References

- American Society of Civil Engineers, “Design of Blast Resistant Buildings in Petrochemical Facilities”, ASCE report, p. 280, 1997.
- American Society of Civil Engineers, “Seismic Analysis of Safety Related Nuclear Structures”, ASCE Standard No. 4-98. p. 136, 2000.
- International Code Council, 2006 International Building Code, p. 679, March 2006.
- Huang, Y, A. Whittaker, M. Constantinou, and S. Malhushte. “Seismic demands on secondary systems in base-isolated nuclear power plants”, *Earthquake Engineering and Structural Dynamics* 2007. John Wiley, New York, 2007.
- Kelly, J.M. and F. Naeim, “Design of Seismic Isolated Structures”, John Wiley, New York, 1999.
- OpenSees. “OpenSees” <<http://opensees.berkeley.edu/index.php>>. (Accessed May 01, 2009).
- Wei, J., “Utilization of Decoupled External Events Shield for Blast Load Protection of Nuclear Power Plants,” UCBTH, Dept. of Civil and Environmental Engineering, U.C. Berkeley, May 21, 2009.
- Wiebe, L. and C. Christopoulos, “Characterizing acceleration spikes due to stiffness changes in nonlinear systems”, *Earthquake Engineering and Structural Dynamics* 2010. John Wiley, New York, 2010.

7.0 FINDINGS AND CONCLUSIONS

Advanced technologies for structural design and construction have the potential for major impact not only on nuclear power plant construction time and cost, but also on the design process and on the safety, security and reliability of next generation of nuclear power plants. In future Generation IV (Gen IV) reactors, structural and seismic design should be much more closely integrated with the design of nuclear and industrial safety systems, physical security systems, and international safeguards systems. Overall reliability will be increased, through the use of replaceable and modular equipment, and through design to facilitate on-line monitoring, in-service inspection, maintenance, replacement, and decommissioning. Economy will also be improved, through integrated engineering efforts to optimize building arrangements to minimize building heights and footprints. Finally, the licensing approach will be transformed by becoming increasingly performance based and technology neutral, using best-estimate simulation methods with uncertainty and margin quantification.

In this context, two structural engineering technologies, *seismic base isolation and modular steel-plate/concrete composite structural wall*, are investigated in this report. These technologies have major potential to (1) enable standardized reactor designs to be deployed across a wider range of sites, (2) reduce the impact of uncertainties related to site-specific seismic conditions, and (3) alleviate reactor equipment qualification requirements. However, the benefits of these new technologies can be amplified if the physical arrangement of the structures, systems and components in the nuclear power plant is re-examined. Use of base isolation provides an opportunity to divide the nuclear power plant structure into three distinct portions: the base isolation layer, the citadel, containing the power generation unit, and the external event shield.

We considered three fundamental configurations of these systems, designed to respond to the two principal hazards: earthquake loading and malicious aircraft impact loading. Thus, we considered two configurations where both the external event shield and the citadel are base isolated: one completely underground and the other above-ground, and one configuration where the external shield is decoupled from the base isolated citadel and firmly attached to the ground. After characterizing the earthquake and aircraft loads and developing simplified load models, we developed a simplified dynamic model of the above-ground integrated configuration and simplified static model of the decoupled external event shield. We analyzed these models to compute a rough estimate of the response of the structure to the earthquake and aircraft loadings focusing on the response quantities pertinent to an evaluation of feasibility of the three considered physical configurations of base isolated nuclear power plant structures.

This report concludes that a base isolated nuclear power plant is feasible. Modern base isolation devices, namely lead-rubber bearings or friction-pendulum bearings, are capable of supporting the weight and providing the displacement capacity required to isolate the typically heavy and stiff nuclear power plant superstructure. Typical optimal base isolation periods will be in the range of 1.5 to 3.0 seconds. The displacements imposed on the base isolation layer in this period range can be easily accommodated using currently available devices. While impact between the structure and the

surrounding soil (closing of the isolation gap) that may occur in beyond design basis situations was not analyzed, this report recognizes the potentially serious consequences of such event and recommends further studies. Similarly, the effect of vertical motion on the base isolated structure was not investigated. However, this report recognizes the potentially serious effects of vertical earthquake-induced vibrations on the structures, systems and components of the citadel and recommends further studies to clarify this issue.

The nature of underlying soils must be considered for base isolated designs. This is because the ground motion frequency content on soft soil sites tends to have a significant amount of energy in the period range of the isolated structure. This has the potential to induce higher (resonant) deformations in the isolation layer and higher accelerations in the isolated structures. This report recommends further studies to investigate the interaction between soil, structure and base isolation layer. Given the expected non-linear behavior of base isolation devices, it is likely that such investigations will need to be conducted using time-domain analysis methods, in departure of the current frequency-domain soil structure interaction practice.

A base isolated structure will affect the physical arrangement and connectivity between different plant equipment. The “umbilicals” include electrical and steam power conduits, coolant conduits and control and communications lines. The most challenging umbilicals to design and qualify will be large-diameter pipes to carry high-temperature and/or high-pressure fluids. For plants that use closed gas cycle power conversion that can be located on the same isolated foundation as the reactor, so that no high-temperature piping needs to cross the base isolation gap, the problem of umbilicals crossing the isolation gap is significantly simplified. This report concludes that base-isolated structures should be decoupled from the reactor external event shell structure, departing from earlier practice. This conclusion was made because aircraft impact induces deformations and accelerations that are significantly larger (approximately half-order-of-magnitude) than those induced by earthquake loading. Thus, a decoupled external shield structure is needed to separate the aircraft and earthquake protection functions of the structure. This report also concludes that a separate external shield structure is feasible. This conclusion is based on a pilot design and non-linear aircraft response analysis of a prototype rectangular reinforced concrete external event structure.

Steel-plate/concrete construction methods provide particularly high promise for reducing cost, accelerating schedules, and improving the performance of reactor structures, particularly base-isolated structures with or without the decoupled external shield. In case of decoupled external shields, composite steel/concrete construction is particularly attractive because of the high resistance to local damage and penetration and excellent structural strength, stiffness and ductility properties required to span long spans, form structural diaphragms and resist aircraft impact and earthquake loading. In addition, composite steel/concrete construction allows for large-scale pre-fabrication in a factory-like environment of ship-yard-type plants, which simplifies and improves quality control and accelerates construction.

Structural designs must be closely integrated with the design of reactor safety and security systems. With early design integration, the reactor building structures can serve multiple functions, including providing multiple barriers for radionuclide release and transport, enabling a zoned ventilation system, and providing for effective access control.

The most significant change in the modeling and simulation of base-isolated reactors will be the shift of many verification and validation tasks from the software vendor to the designers to justify modeling assumptions of isolator responses. Designers will be required to demonstrate both confidence in the isolator response model, which should require some non-linear analysis, and competence in predicting the response of isolated structures. Despite these additional efforts, we anticipate that the modeling and simulation of isolated structures will have the distinct advantage over non-isolated structures in that the response of the reactor systems and components will be much simpler to analyze under reduced accelerations under earthquake loading.

Finally, there remain several important verification and validation issues that will need to be addressed for base-isolated structures as new designs proceed through the USNRC general design certification process. Designers currently have few actual structural responses to use as benchmarks and shake table experiments of representative systems will be needed until more historical data becomes available. The best case for modelers of lead-rubber bearings to model will be the response of the USC Teaching Hospital in the 1994 Northridge earthquake. Historical experiences with isolated structures also demonstrate the importance of quality assurance to verify that the modeled structure accurately represents the as-built structure, especially potential compromises of the isolation gap.

There is very strong feedback between the design approaches taken to achieve seismic base isolation, to accommodate new requirements for aircraft crash resistance, to accelerate construction using steel-plate/concrete structural modules, to achieve physical security and access control, to control reactivity and decay heat removal, and the design of the balance of plant systems including power conversion. These choices impact design, regulatory review and permitting, as well as construction materials quantities, and construction time, and ultimately affect construction cost.

8.0 NOMENCLATURE

α = isolation post-yield stiffness ratio
 a_i = i^{th} level floor acceleration (g)
 $a_{i,\text{max}}$ = maximum floor acceleration of level i (g)
 a_p = maximum floor acceleration due to impact based on momentum conservation (g)
 $F(t)$ = force at time, t , in the Riera linearization (metric tons [kips])
 F_1 = plateau force parameter in the Riera linearization (metric tons [kips])
 F_2 = peak force parameter in the Riera linearization (metric tons [kips])
 f_{iso} = isolation frequency (Hz)
 F_y = isolation system yield strength
 g = acceleration due to gravity (981 cm/sec² [386 in/sec²])
 k_e = initial isolation stiffness
 K_{iso} = isolation plane stiffness (metric tons/m [kips/in])
 L_i = length of airplane i (m [ft])
 p_i = momentum transferred by airplane i
PGA = peak ground acceleration of a seismic record (g)
PGD = peak ground displacement of a seismic record (cm [in])
PGV = peak ground velocity of a seismic record (cm/sec [in/sec])
 S_A = spectral acceleration (g)
 $t_{\text{crush},i}$ = crushing time of airplane i (sec)
 t_i = i^{th} time parameter in the Riera linearization (sec)
 T = isolation period (sec)
 u = floor displacement (cm [in])
 u_{MAX} = maximum floor displacement (cm [in])
 u_p = maximum floor displacement due to impact based on momentum conservation (cm [in])
 v_i = velocity of airplane i (m/sec [ft/sec])
 v_p = airplane velocity (cm/sec [in/sec])
 v_s = idealized initial structural velocity due to momentum transfer (cm/sec [in/sec])
 v_{MAX} = maximum structural velocity response (cm/sec [in/sec])
 W_i = weight of airplane i (metric tons [kips])
 W_p = weight of plane (metric tons [kips])
 W = weight of structure (metric tons [kips])
 X_t = time scaling factor
 X_f = force scaling factor

APPENDIX A: GROUND MOTION

Table B-1. SAC Ground Motions

| SAC Ground Motion Suite for 2% in 50 Years Hazard | | | | | | | |
|---|------|-----------------------|-----------|------|---------------|----------------|---------|
| Group Area | Name | Earthquake | Magnitude | Year | Distance (km) | Scaling Factor | PGA (g) |
| Los Angeles | LA21 | Kobe Japan | 6.9 | 1995 | 3.4 | 1.15 | 1.25 |
| | LA22 | Kobe Japan | 6.9 | 1995 | 3.4 | 1.15 | 0.92 |
| | LA23 | Loma Prieta, CA, USA | 7.0 | 1989 | 3.5 | 0.82 | 0.42 |
| | LA24 | Loma Prieta, CA, USA | 7.0 | 1989 | 3.5 | 0.82 | 0.47 |
| | LA25 | Northridge, CA, USA | 6.7 | 1994 | 7.5 | 1.29 | 0.87 |
| | LA26 | Northridge, CA, USA | 6.7 | 1994 | 7.5 | 1.29 | 0.94 |
| | LA27 | Northridge, CA, USA | 6.7 | 1994 | 6.4 | 1.61 | 0.93 |
| | LA28 | Northridge, CA, USA | 6.7 | 1994 | 6.4 | 1.61 | 1.33 |
| | LA29 | Tabas, Iran | 7.4 | 1974 | 1.2 | 1.08 | 0.81 |
| | LA30 | Tabas, Iran | 7.4 | 1974 | 1.2 | 1.08 | 0.99 |
| | LA31 | Elysian Park, CA, USA | 7.1 | * | 17.5 | 1.43 | 1.30 |
| | LA32 | Elysian Park, CA, USA | 7.1 | * | 17.5 | 1.43 | 1.19 |
| | LA33 | Elysian Park, CA, USA | 7.1 | * | 10.7 | 0.97 | 0.78 |
| | LA34 | Elysian Park, CA, USA | 7.1 | * | 10.7 | 0.97 | 0.68 |
| | LA35 | Elysian Park, CA, USA | 7.1 | * | 11.2 | 1.10 | 0.99 |
| | LA36 | Elysian Park, CA, USA | 7.1 | * | 11.2 | 1.10 | 1.10 |
| | LA37 | Palos Verdes, CA, USA | 7.1 | * | 1.5 | 0.90 | 0.71 |
| | LA38 | Palos Verdes, CA, USA | 7.1 | * | 1.5 | 0.90 | 0.78 |
| | LA39 | Palos Verdes, CA, USA | 7.1 | * | 1.5 | 0.88 | 0.50 |
| | LA40 | Palos Verdes, CA, USA | 7.1 | * | 1.5 | 0.88 | 0.63 |
| Seattle | SE21 | Mendocino, CA, USA | 7.1 | 1992 | 8.5 | 0.98 | 0.76 |
| | SE22 | Mendocino, CA, USA | 7.1 | 1992 | 8.5 | 0.98 | 0.49 |
| | SE23 | Erzincan, Turkey | 6.7 | 1992 | 2 | 1.27 | 0.61 |
| | SE24 | Erzincan, Turkey | 6.7 | 1992 | 2 | 1.27 | 0.54 |
| | SE25 | Olympia, WA, USA | 6.5 | 1949 | 56 | 4.35 | 0.90 |
| | SE26 | Olympia, WA, USA | 6.5 | 1949 | 56 | 4.35 | 0.82 |
| | SE27 | Seattle, WA, USA | 7.1 | 1965 | 80 | 10.04 | 1.76 |
| | SE28 | Seattle, WA, USA | 7.1 | 1965 | 80 | 10.04 | 1.39 |
| | SE29 | Vaparaíso, Chile | 8.0 | 1985 | 42 | 2.90 | 1.64 |
| | SE30 | Vaparaíso, Chile | 8.0 | 1985 | 42 | 2.90 | 1.57 |
| | SE31 | Vaparaíso, Chile | 8.0 | 1985 | 42 | 3.96 | 1.27 |
| | SE32 | Vaparaíso, Chile | 8.0 | 1985 | 42 | 3.96 | 0.90 |
| | SE33 | Deep Interplate | 7.9 | * | 65 | 3.84 | 0.80 |

| | | | | | | | |
|--------|------|-----------------------------|-----|------|-----|------|------|
| | SE34 | Deep Interplate | 7.9 | * | 65 | 3.84 | 0.65 |
| | SE35 | Miyagi-oki, Japan | 7.4 | 1978 | 66 | 1.78 | 0.61 |
| | SE36 | Miyagi-oki, Japan | 7.4 | 1978 | 66 | 1.78 | 0.78 |
| | SE37 | Shallow Interplate | 7.9 | * | 15 | 0.94 | 0.56 |
| | SE38 | Shallow Interplate | 7.9 | * | 16 | 0.94 | 0.53 |
| | SE39 | Shallow Interplate | 7.9 | * | 17 | 1.49 | 0.58 |
| | SE40 | Shallow Interplate | 7.9 | * | 18 | 1.49 | 0.75 |
| Boston | BO21 | Foot Wall | 6.5 | * | 30 | 0.99 | 0.32 |
| | BO22 | Foot Wall | 6.5 | * | 30 | 0.99 | 0.36 |
| | BO23 | Foot Wall | 6.5 | * | 30 | 0.84 | 0.34 |
| | BO24 | Foot Wall | 6.5 | * | 30 | 0.84 | 0.24 |
| | BO25 | Foot Wall | 6.5 | * | 30 | 0.63 | 0.29 |
| | BO26 | Foot Wall | 6.5 | * | 30 | 0.63 | 0.31 |
| | BO27 | Nahanni, Canada (Station 1) | 6.9 | 1985 | 9.6 | 0.27 | 0.25 |
| | BO28 | Nahanni, Canada (Station 1) | 6.9 | 1985 | 9.6 | 0.27 | 0.24 |
| | BO29 | Nahanni, Canada (Station 2) | 6.9 | 1985 | 6.1 | 0.56 | 0.17 |
| | BO30 | Nahanni, Canada (Station 2) | 6.9 | 1985 | 6.1 | 0.56 | 0.21 |
| | BO31 | Nahanni, Canada (Station 3) | 6.9 | 1985 | 18 | 2.63 | 0.38 |
| | BO32 | Nahanni, Canada (Station 3) | 6.9 | 1985 | 18 | 2.63 | 0.39 |
| | BO33 | Saguenay, Canada | 5.9 | 1988 | 96 | 4.48 | 0.57 |
| | BO34 | Saguenay, Canada | 5.9 | 1988 | 96 | 4.48 | 0.78 |
| | BO35 | Saguenay, Canada | 5.9 | 1988 | 98 | 9.21 | 1.50 |
| | BO36 | Saguenay, Canada | 5.9 | 1988 | 98 | 9.21 | 0.71 |
| | BO37 | Saguenay, Canada | 5.9 | 1988 | 118 | 9.30 | 0.52 |
| | BO38 | Saguenay, Canada | 5.9 | 1988 | 118 | 9.30 | 0.65 |
| | BO39 | Saguenay, Canada | 5.9 | 1988 | 132 | 9.58 | 0.51 |
| | BO40 | Saguenay, Canada | 5.9 | 1988 | 132 | 9.58 | 0.78 |

* Denotes a simulated ground motion record

APPENDIX B: EARTHQUAKE GROUND MOTION

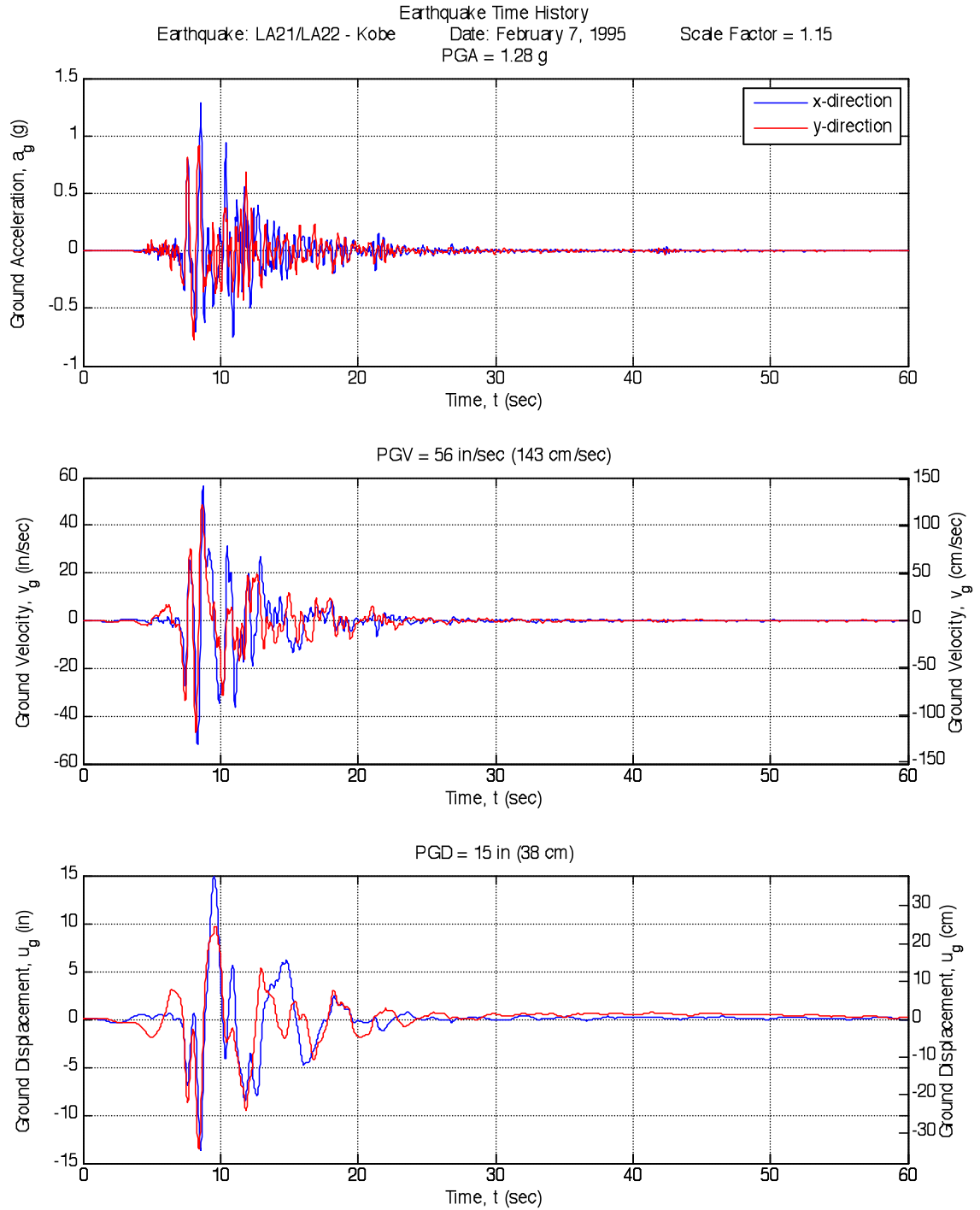


Fig. B-1. LA21/LA22 – Kobe Earthquake

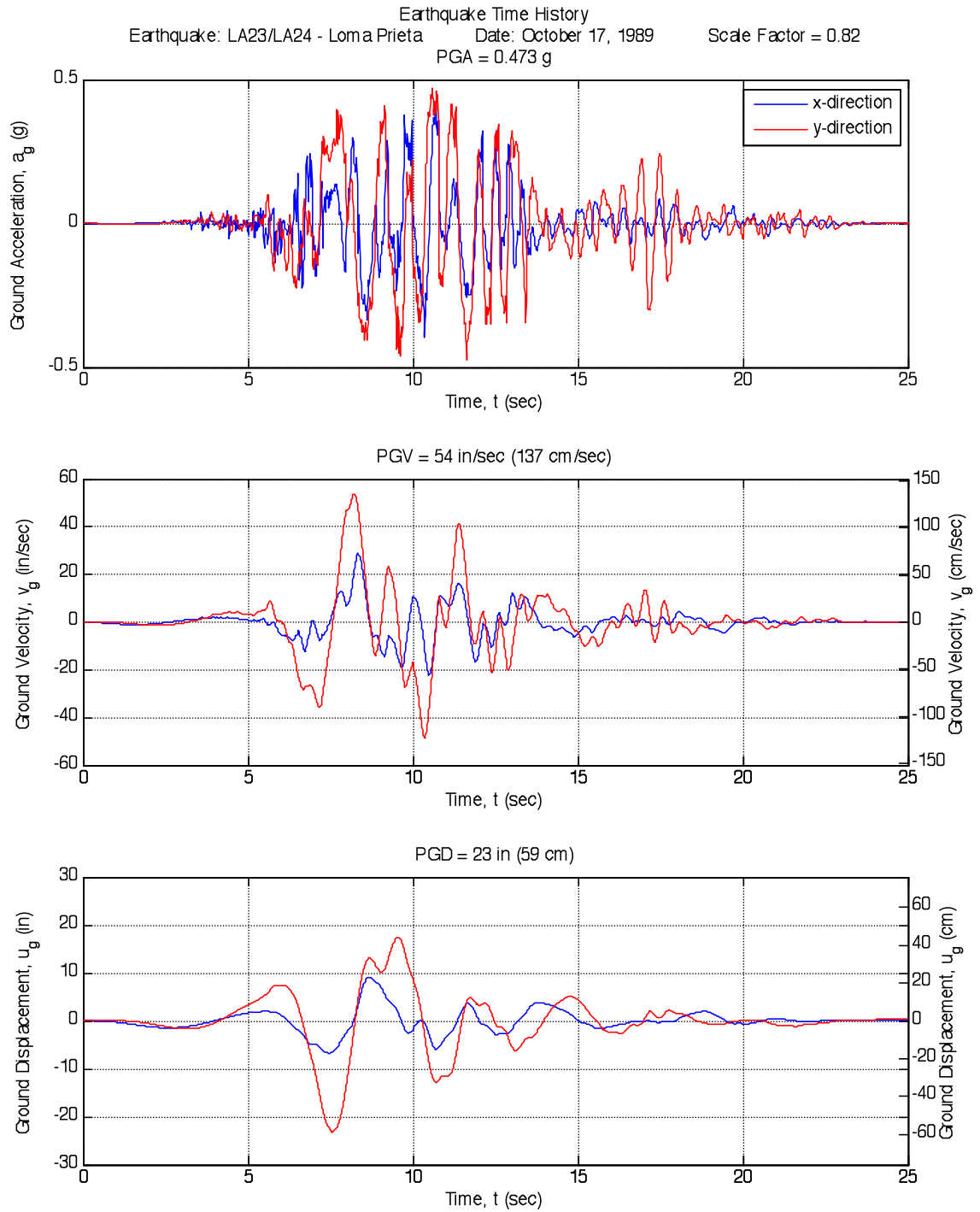


Fig. B-2. LA23/LA24 – Loma Prieta Earthquake

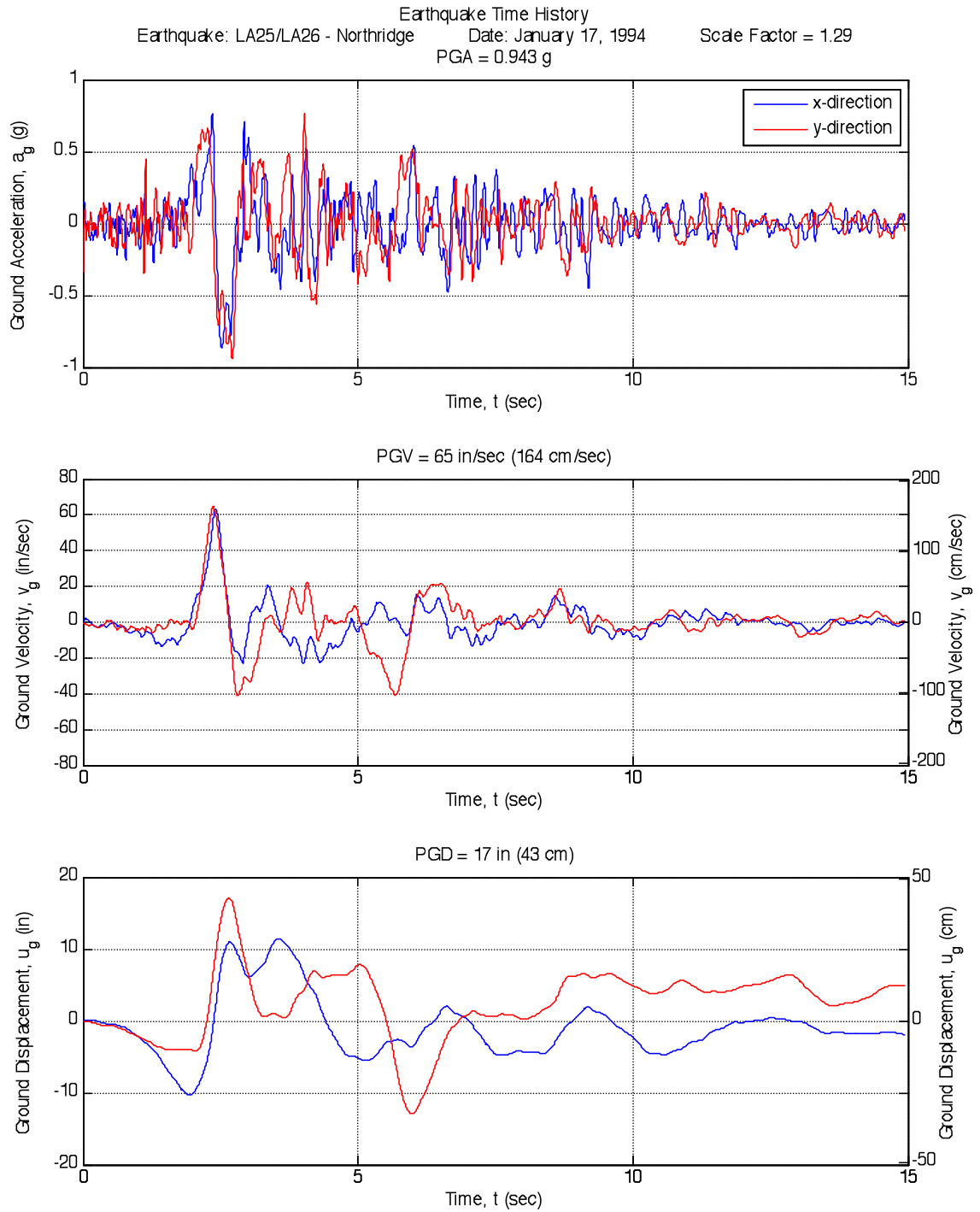


Fig. B-3. LA25/LA26 – Northridge Earthquake

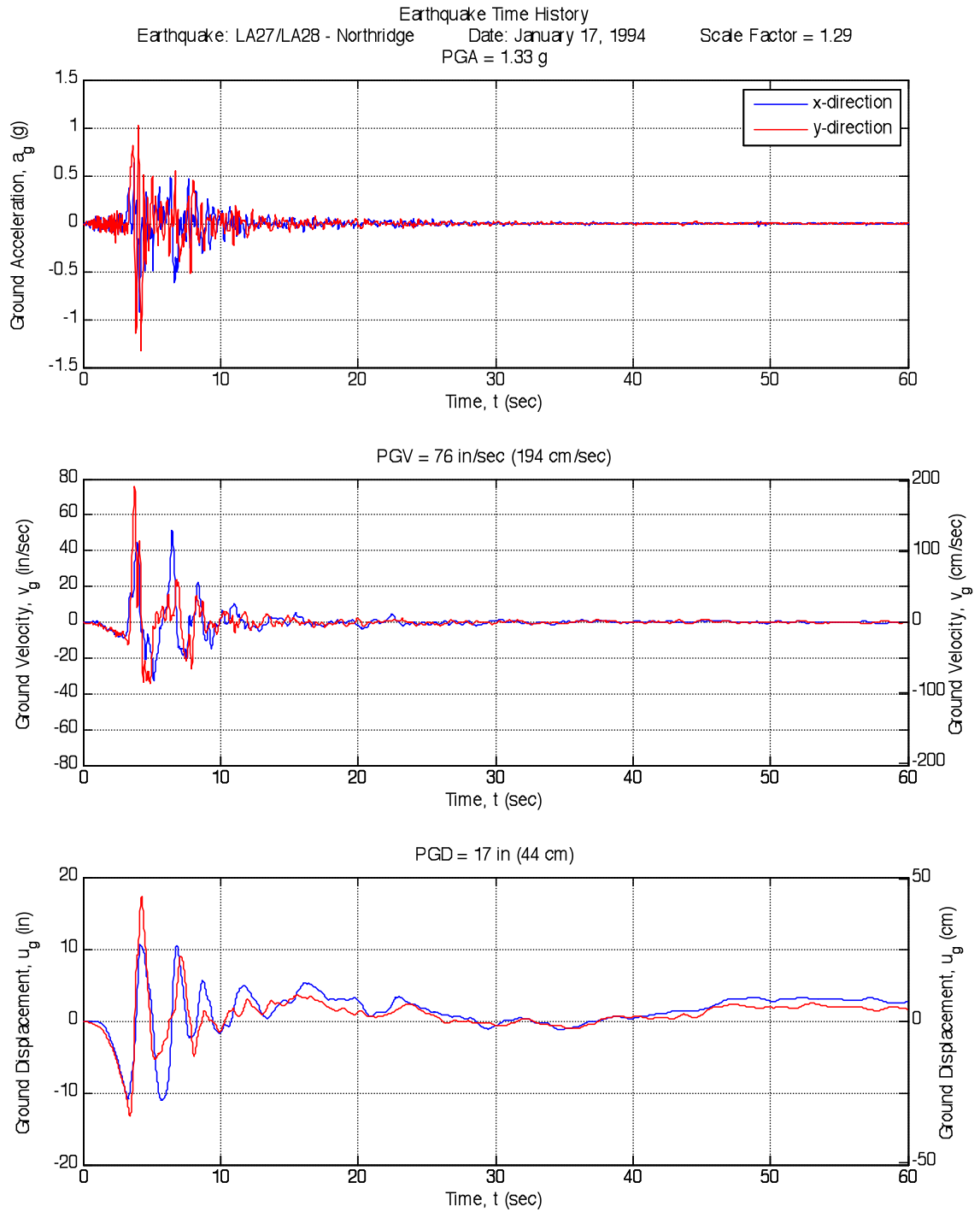


Fig. B-4. LA27/LA28 – Northridge Earthquake

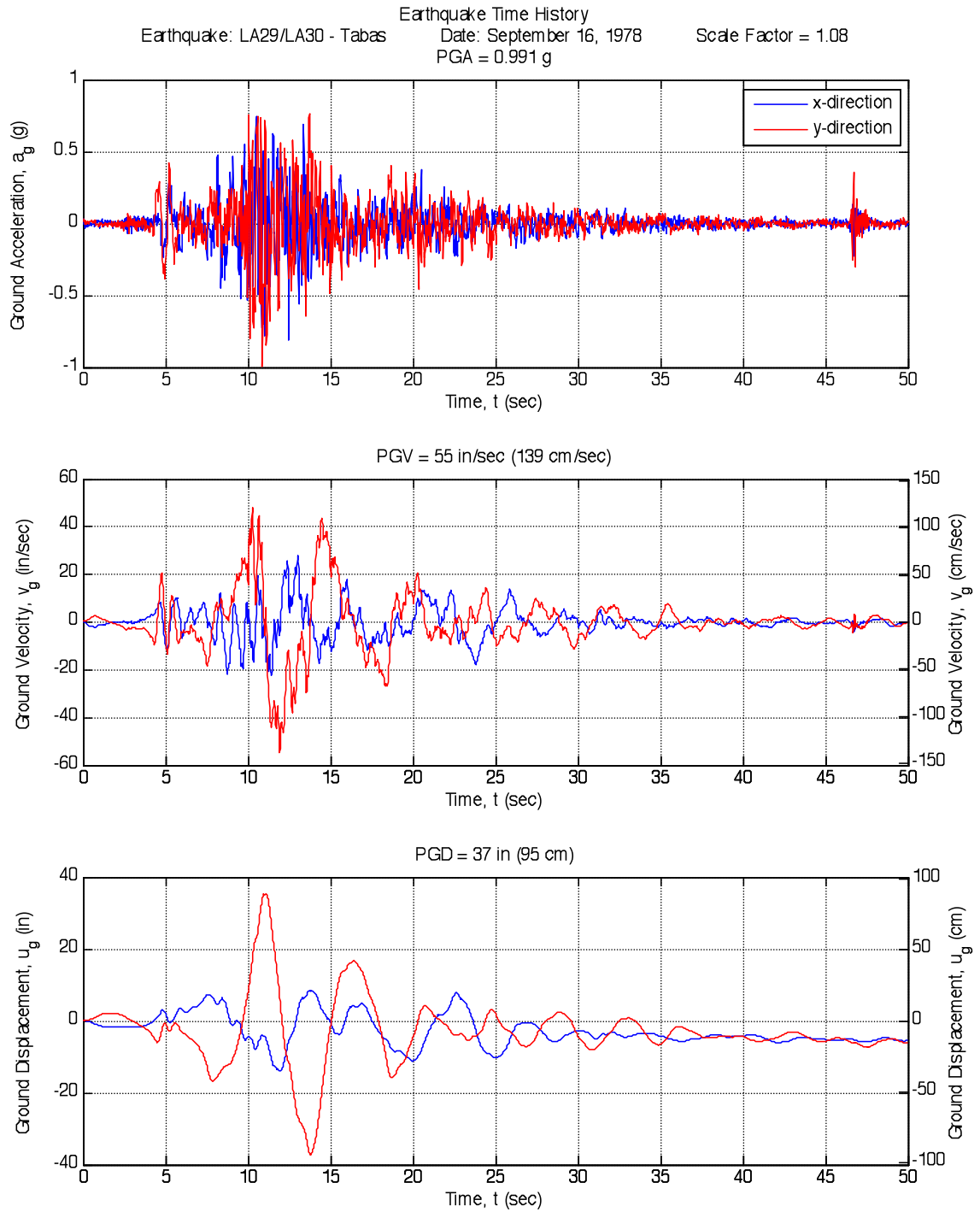


Fig. B-5. LA29/LA30 – Tabas Earthquake

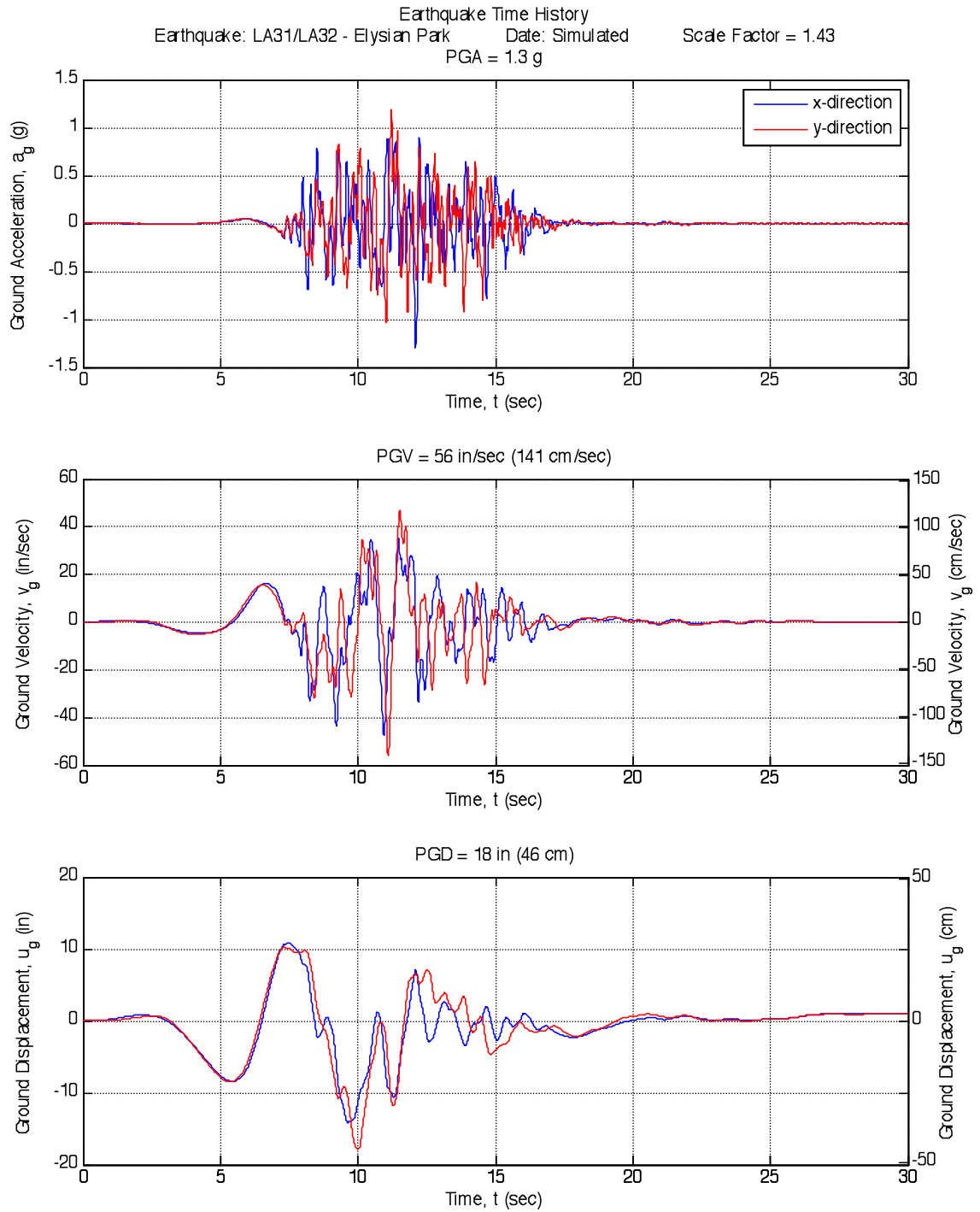


Fig. B-6. LA31/LA32 – Elysian Park Earthquake

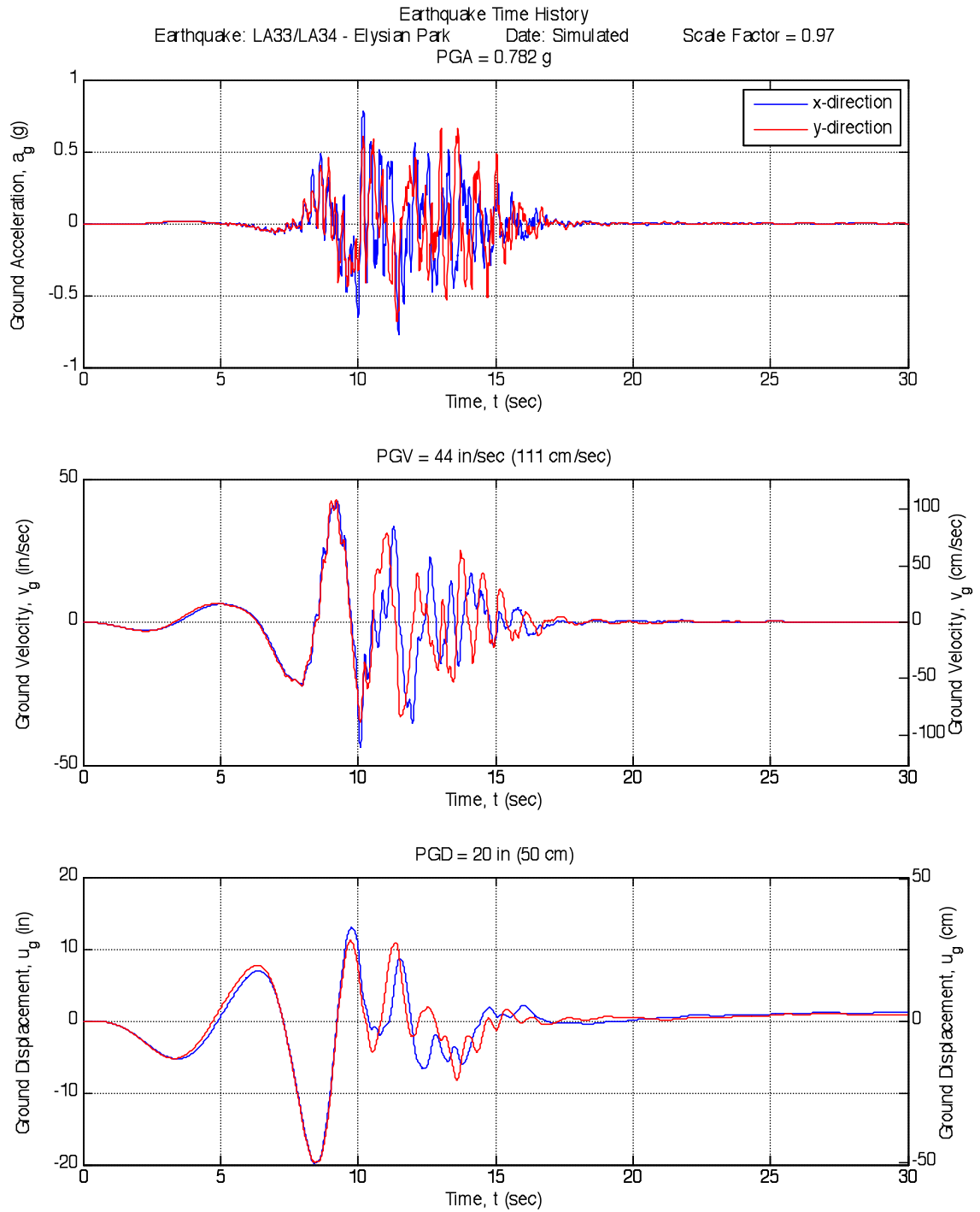


Fig. B-7. LA33/LA34 – Elysian Park Earthquake

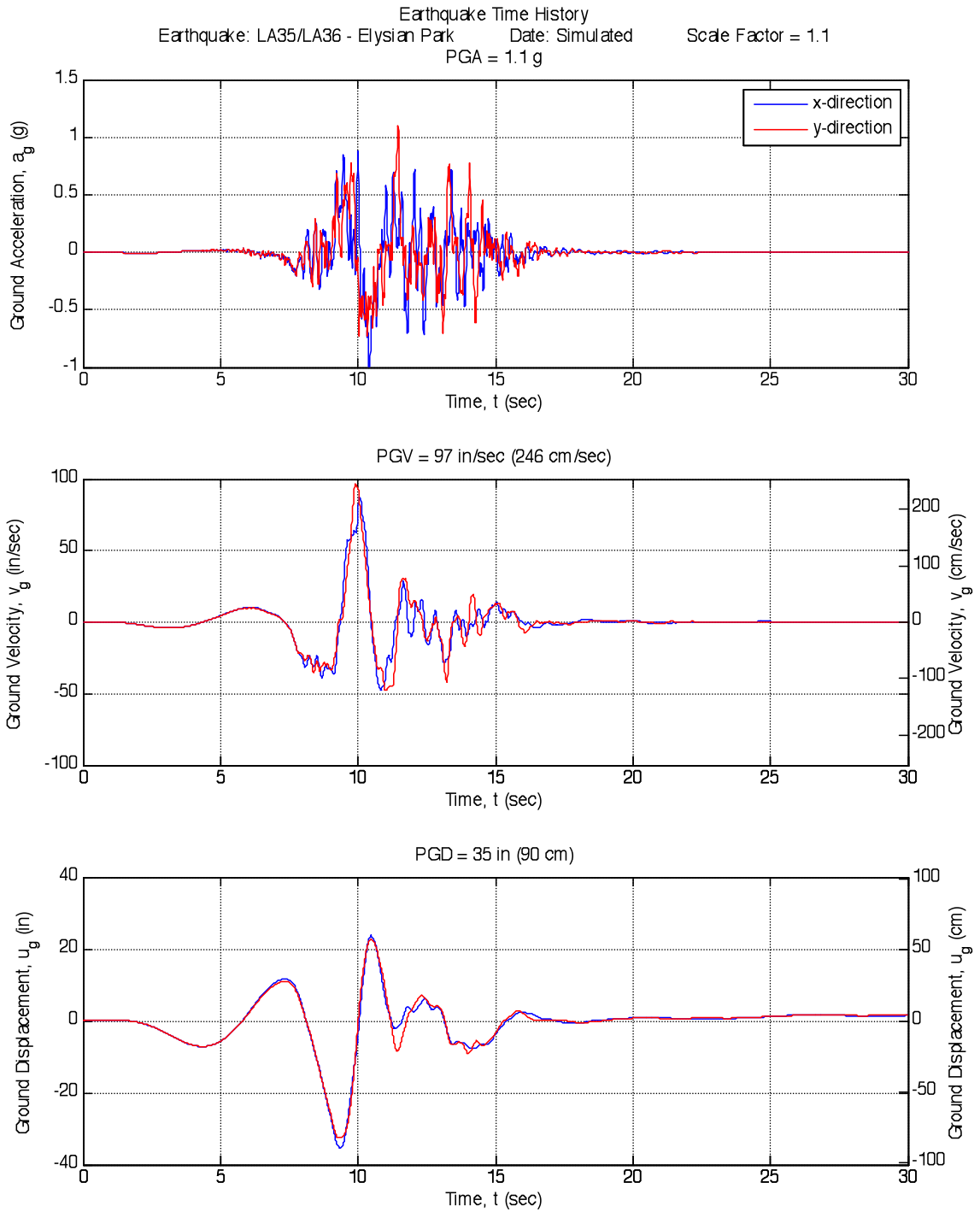


Fig. B-8. LA35/LA36 – Elysian Park Earthquake

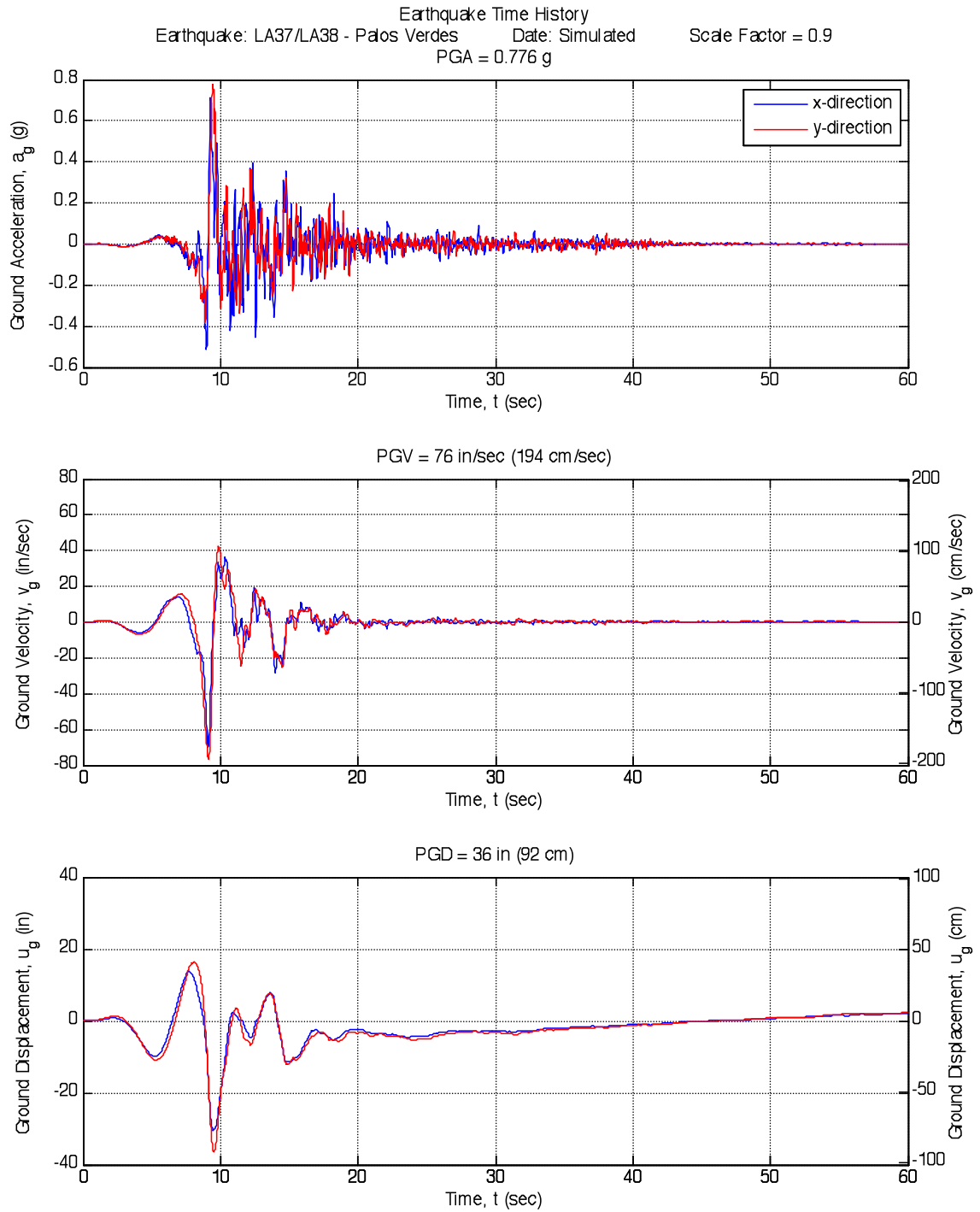


Fig. B-9. LA37/LA38 – Palos Verdes Earthquake

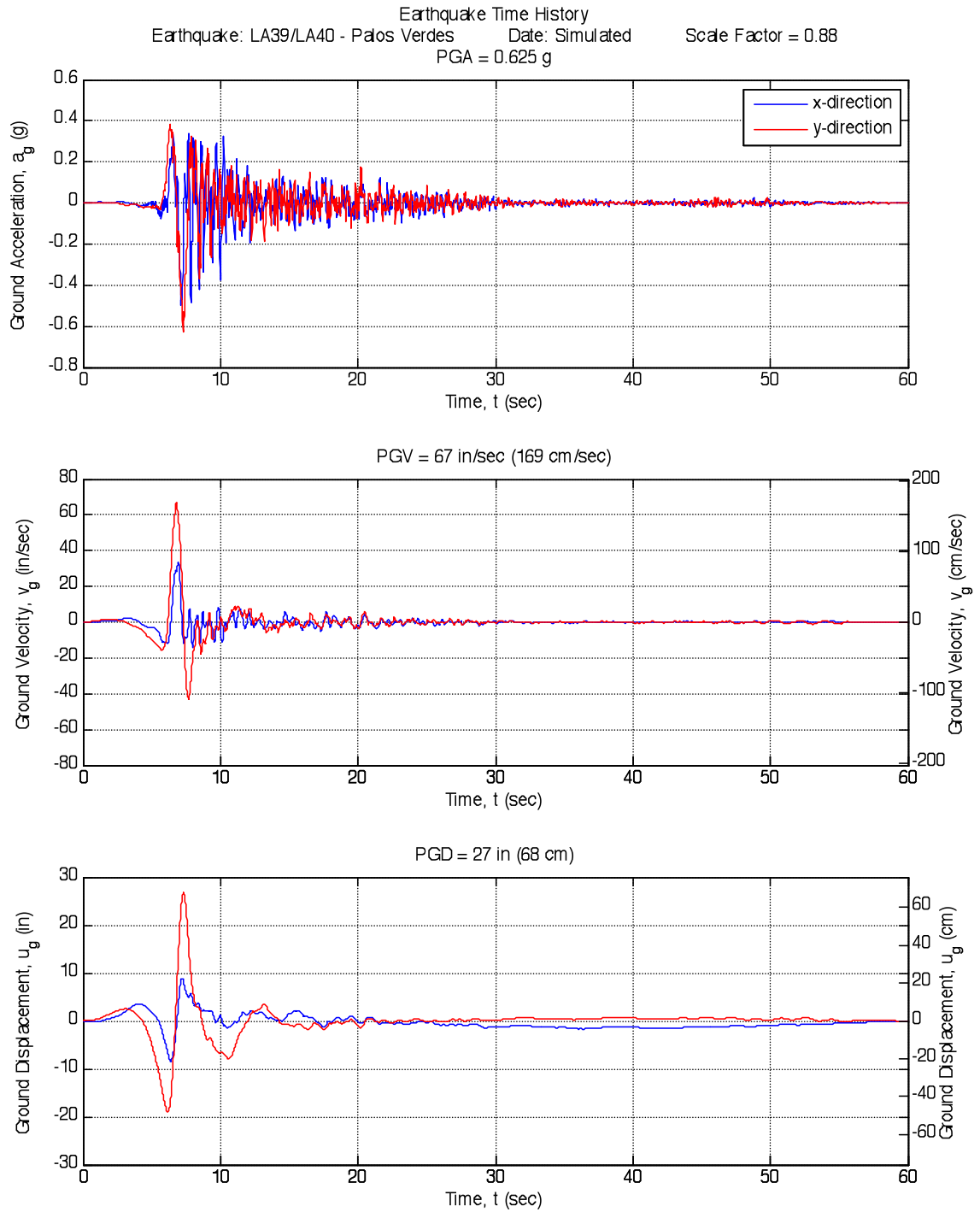


Fig. B-10. LA39/LA40 – Palos Verdes Earthquake

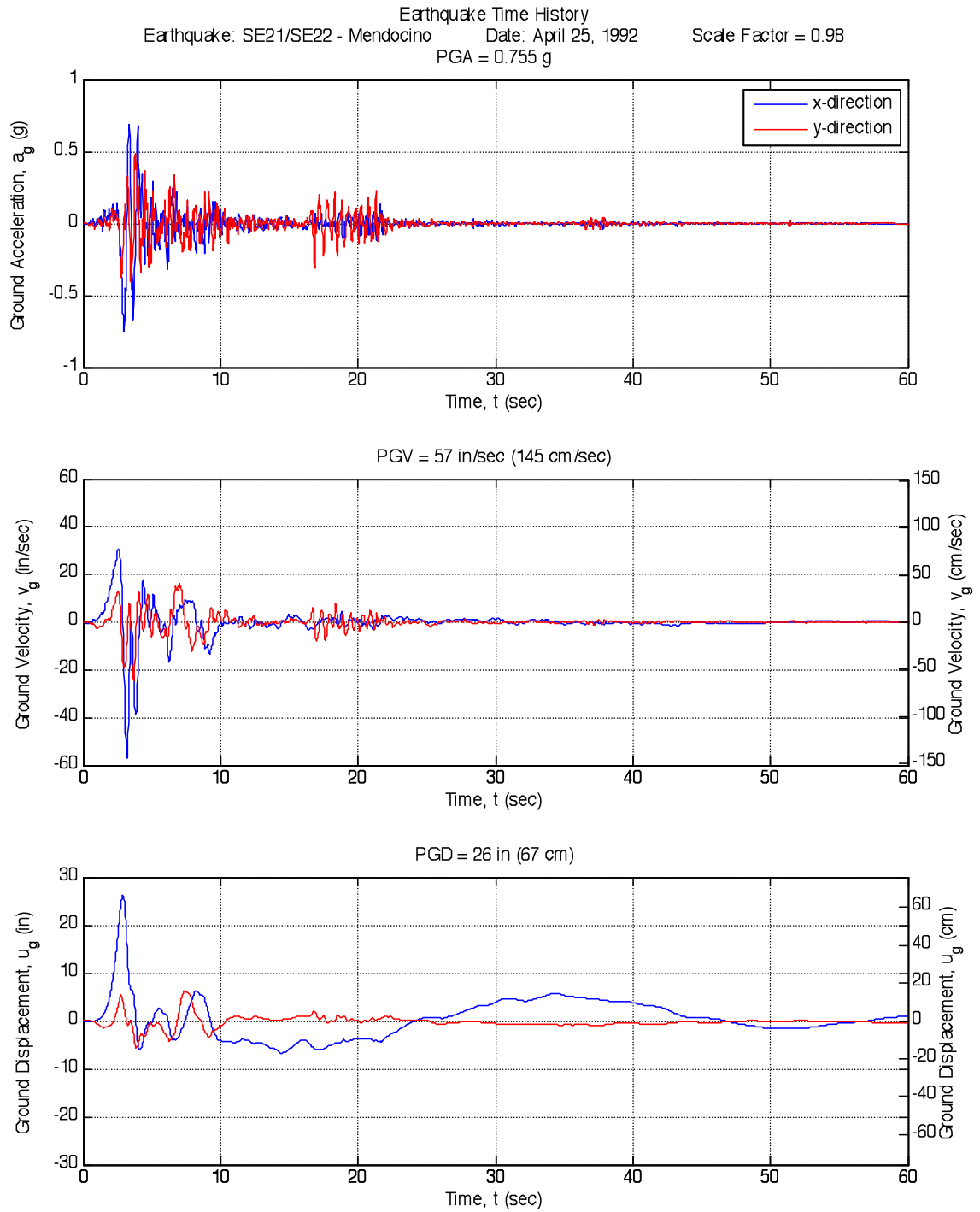


Fig. B-11. SE21/SE22 – Mendocino Earthquake

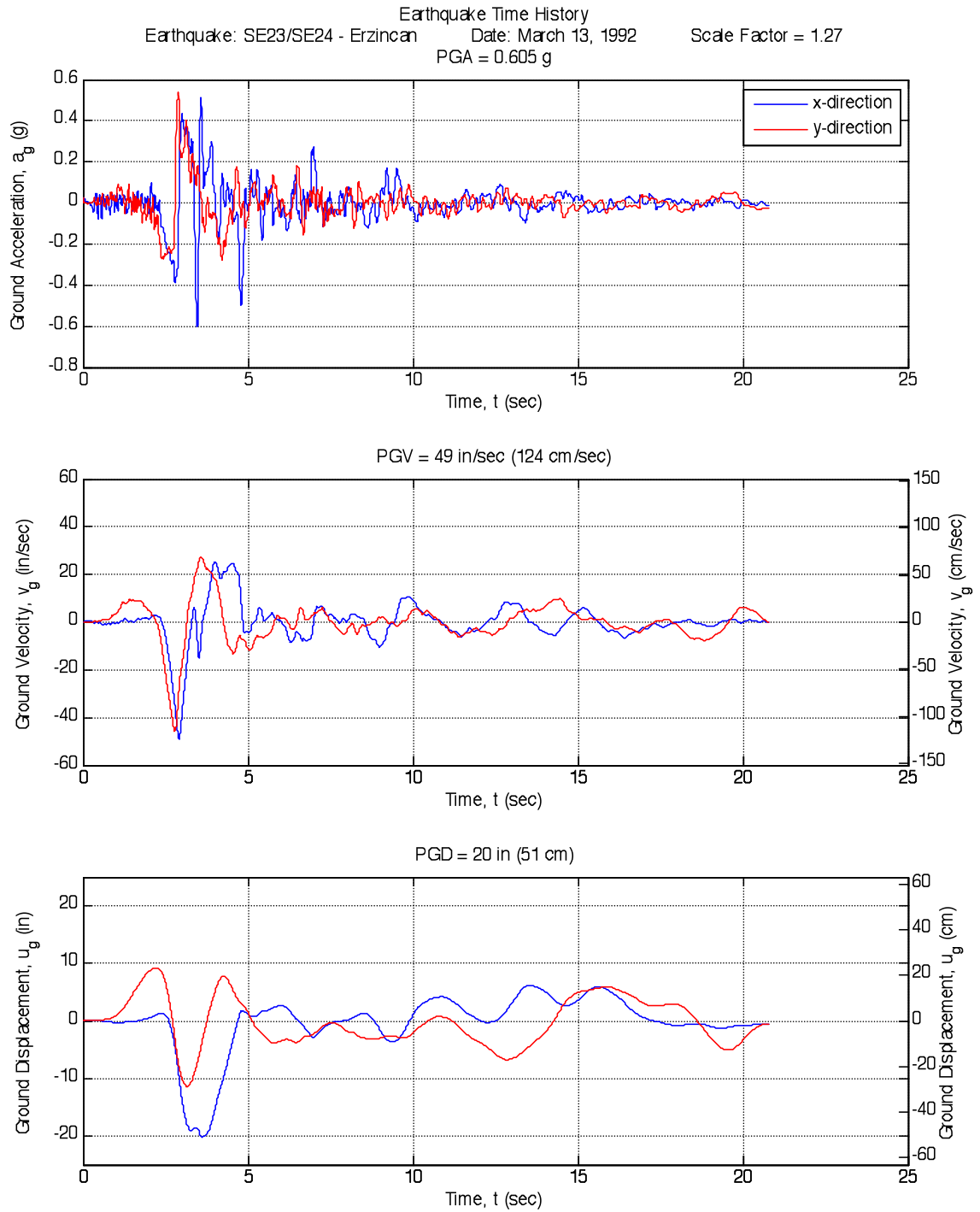


Fig. B-12. SE23/SE24 – Erzincan Earthquake

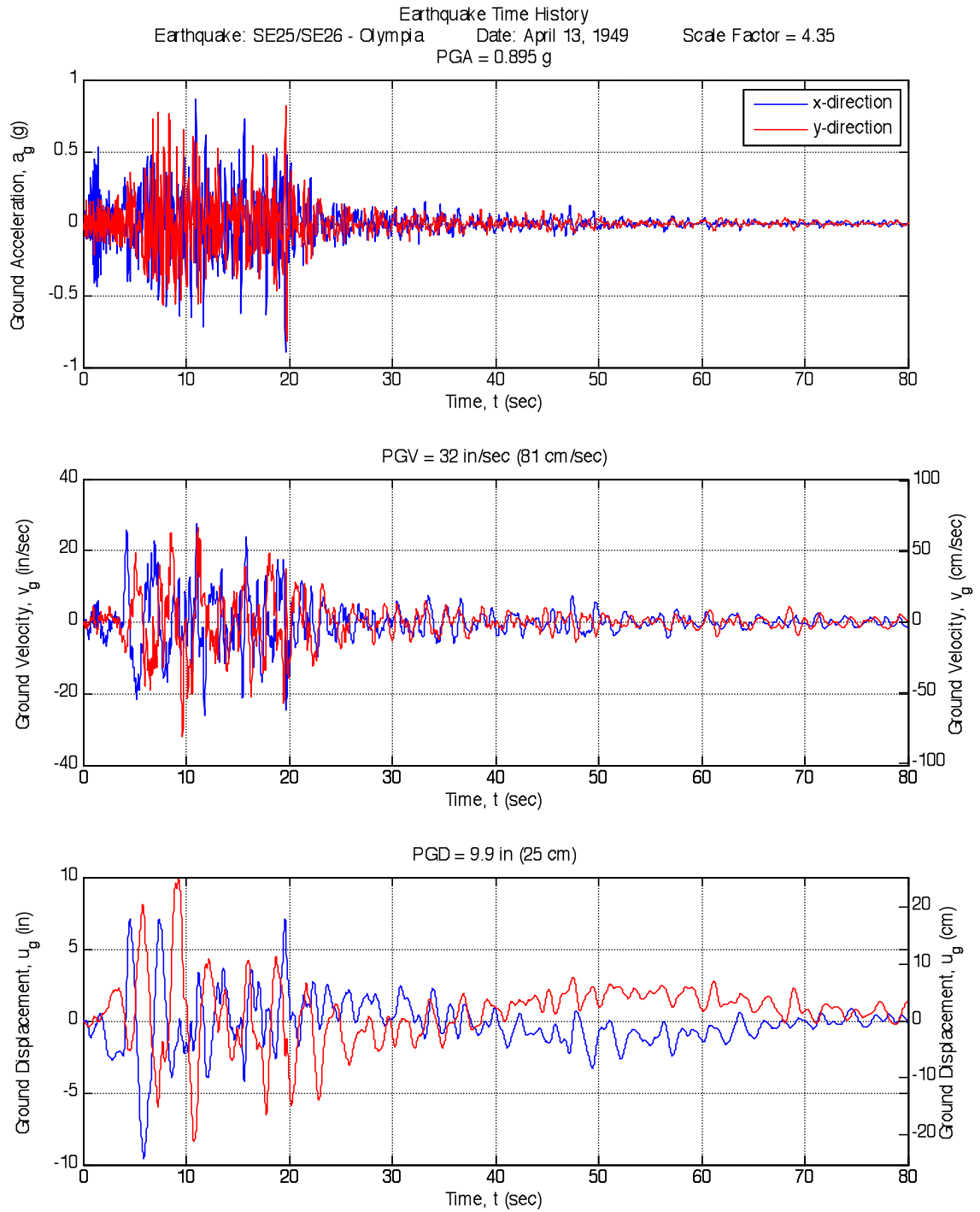


Fig. B-13. SE25/SE26 – Olympia Earthquake

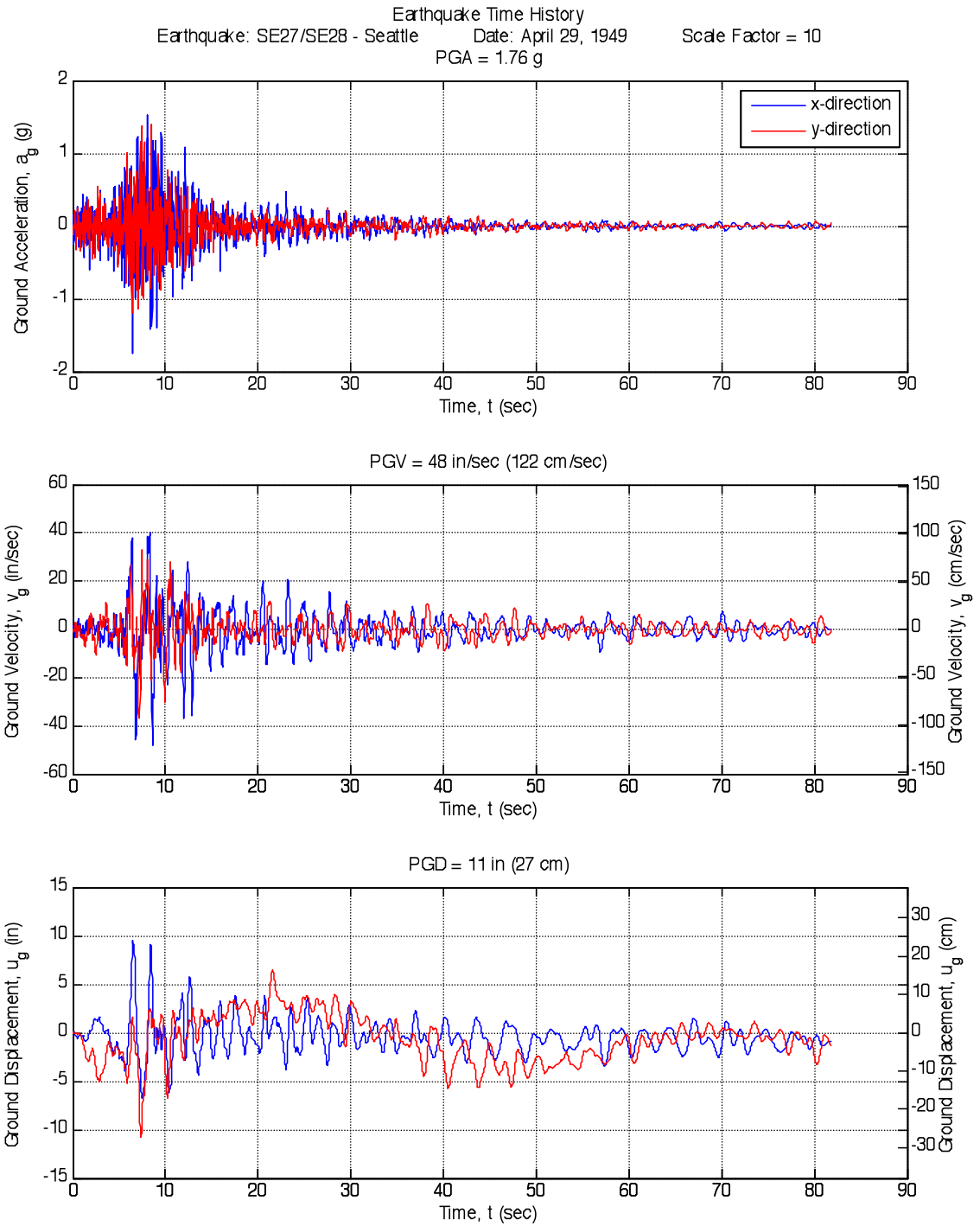


Fig. B-14. SE27/SE28 – Seattle Earthquake

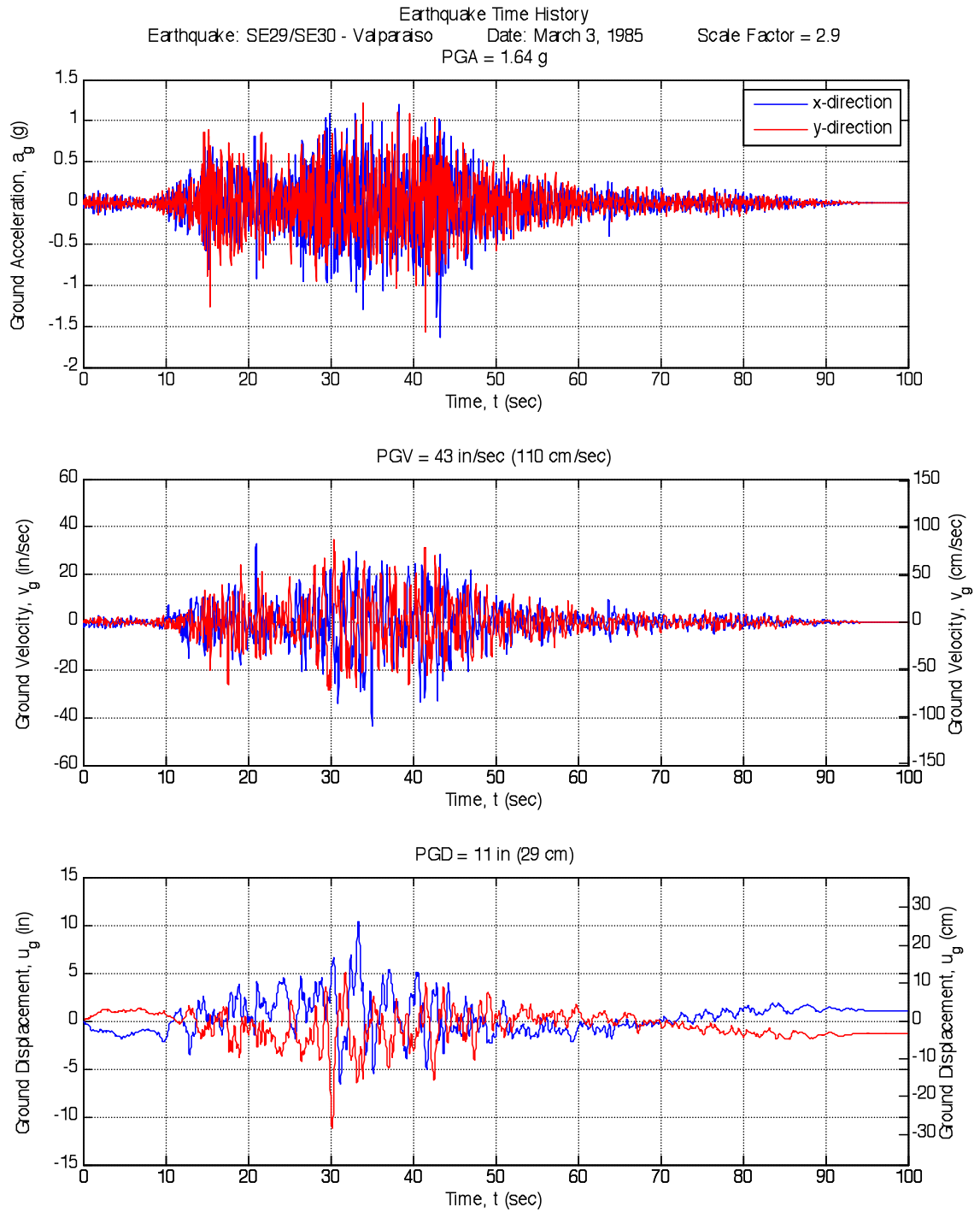


Fig. B-15. SE29/SE30 – Valparaiso Earthquake

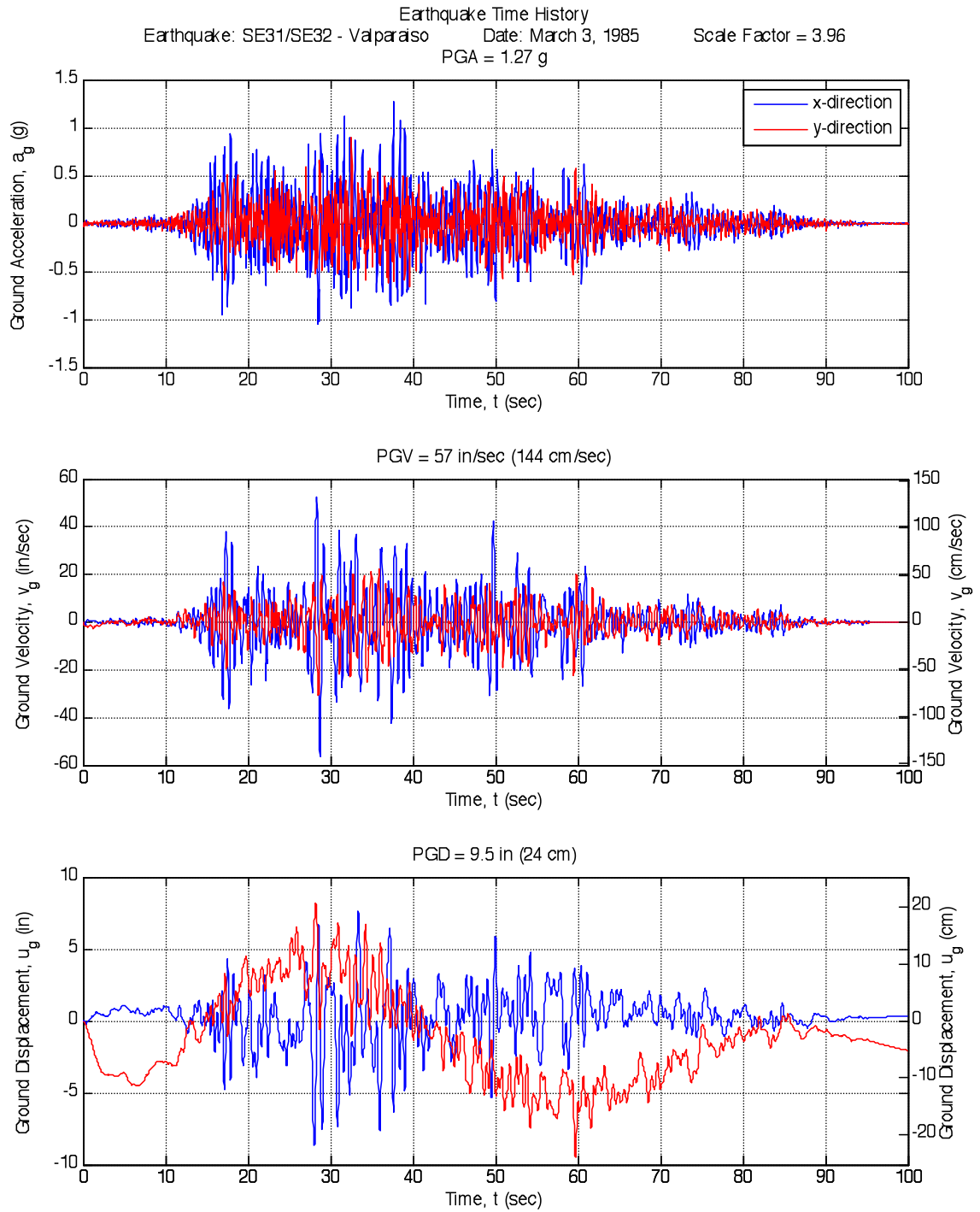


Fig. B-16. SE31/SE32 – Valparaiso Earthquake

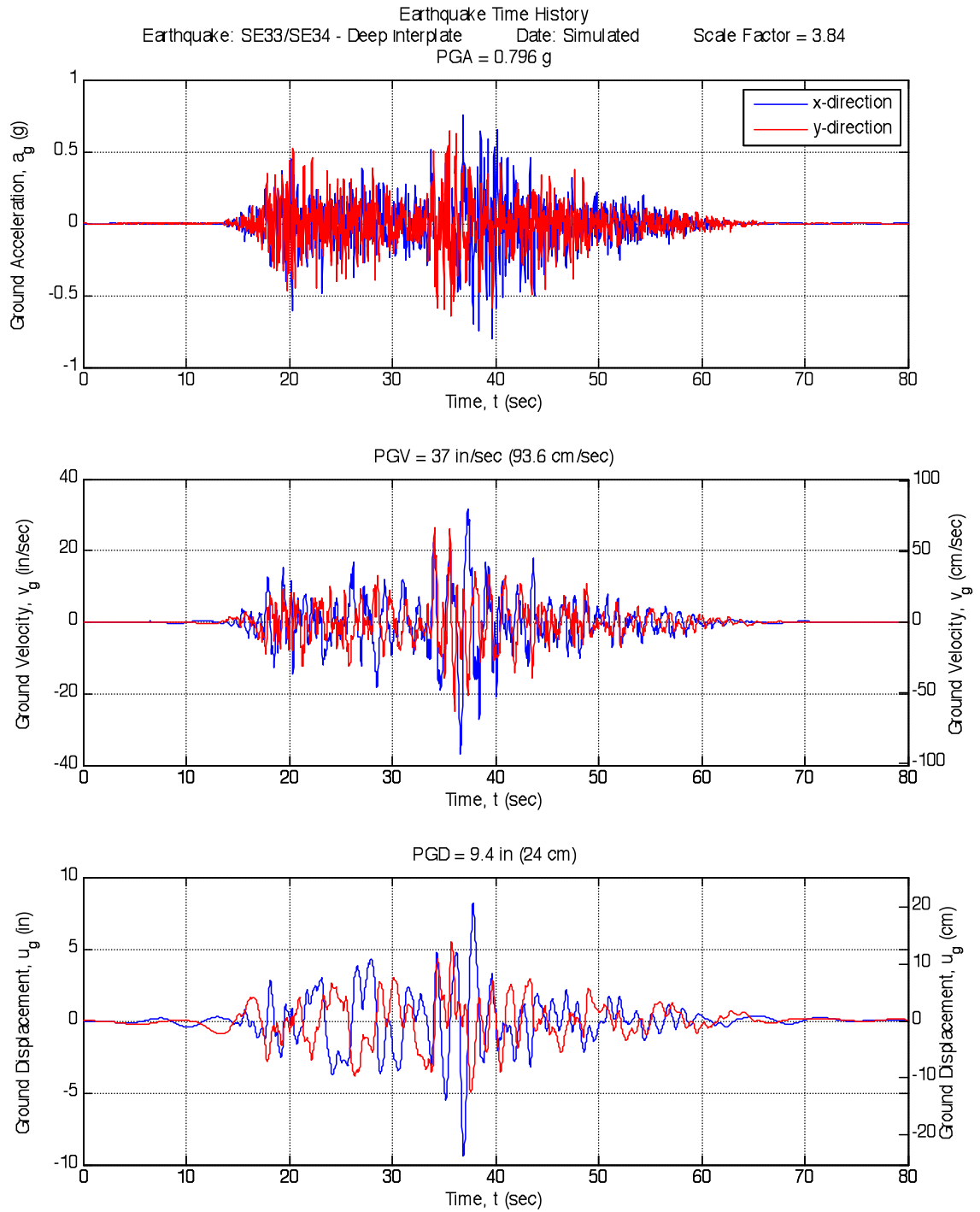


Fig. B-17. SE33/SE34 – Deep Interplate Earthquake

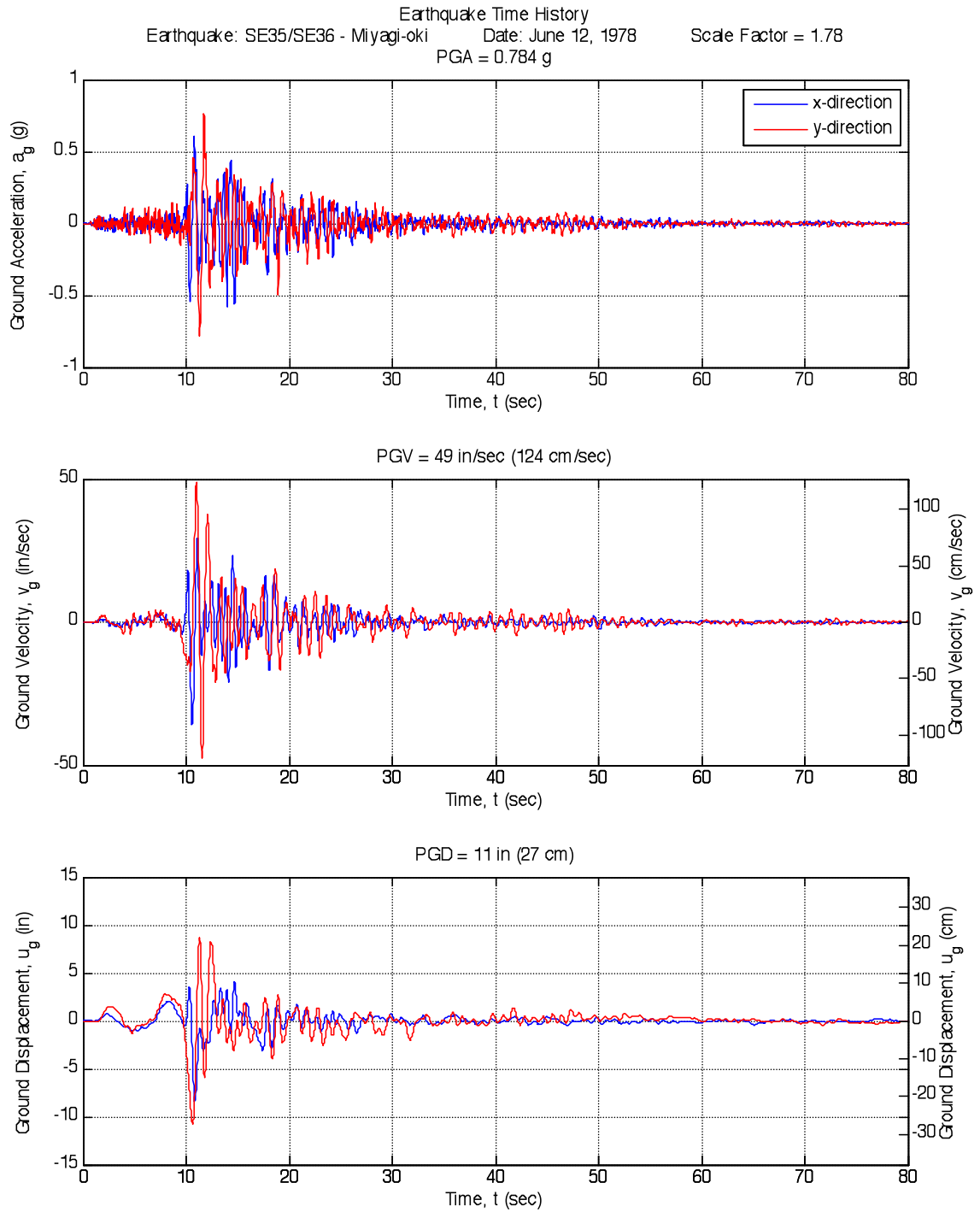


Fig. B-18. SE35/SE36 – Miyagi-oki Earthquake

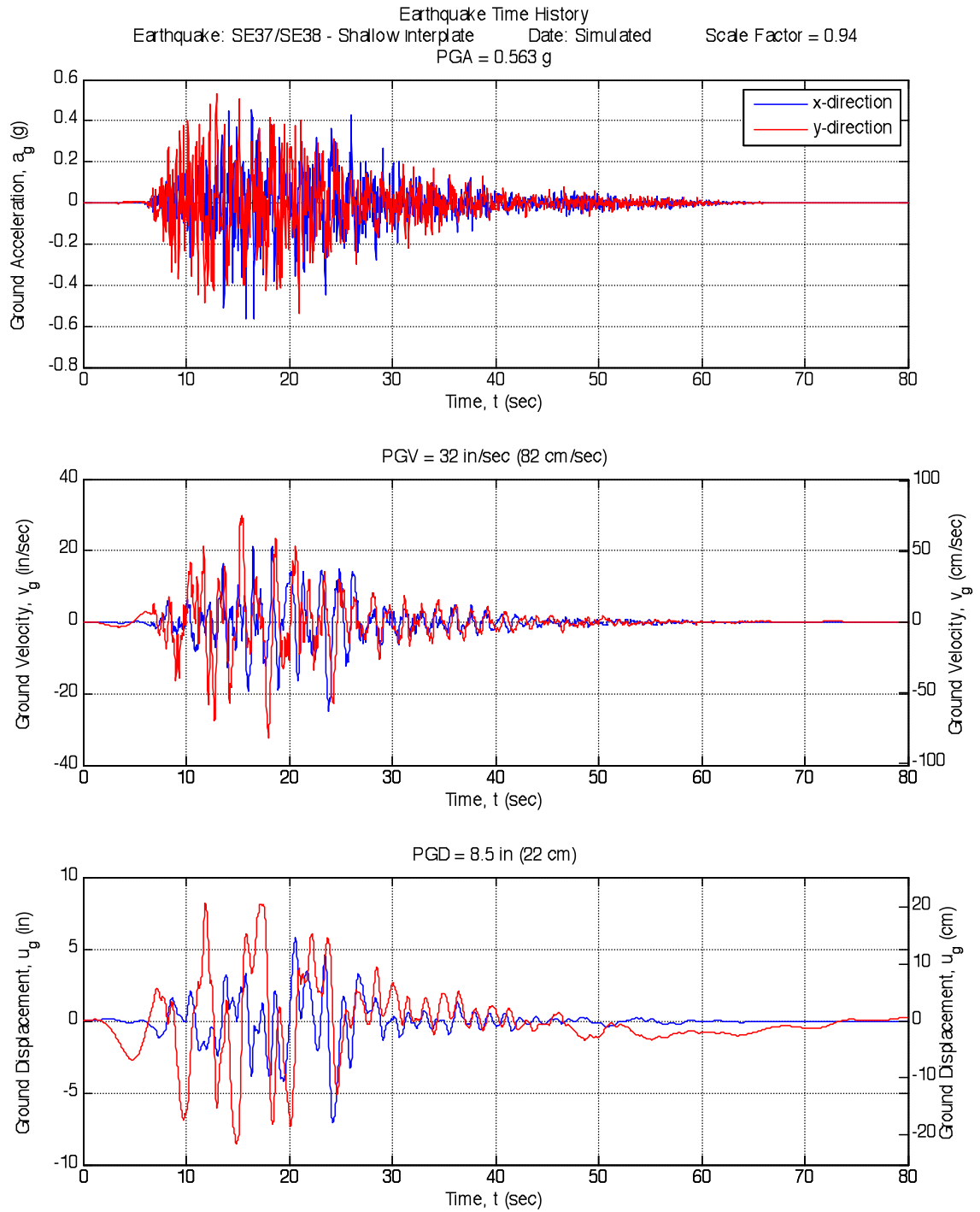


Fig. B-19. SE37/SE38 – Shallow Interplate Earthquake

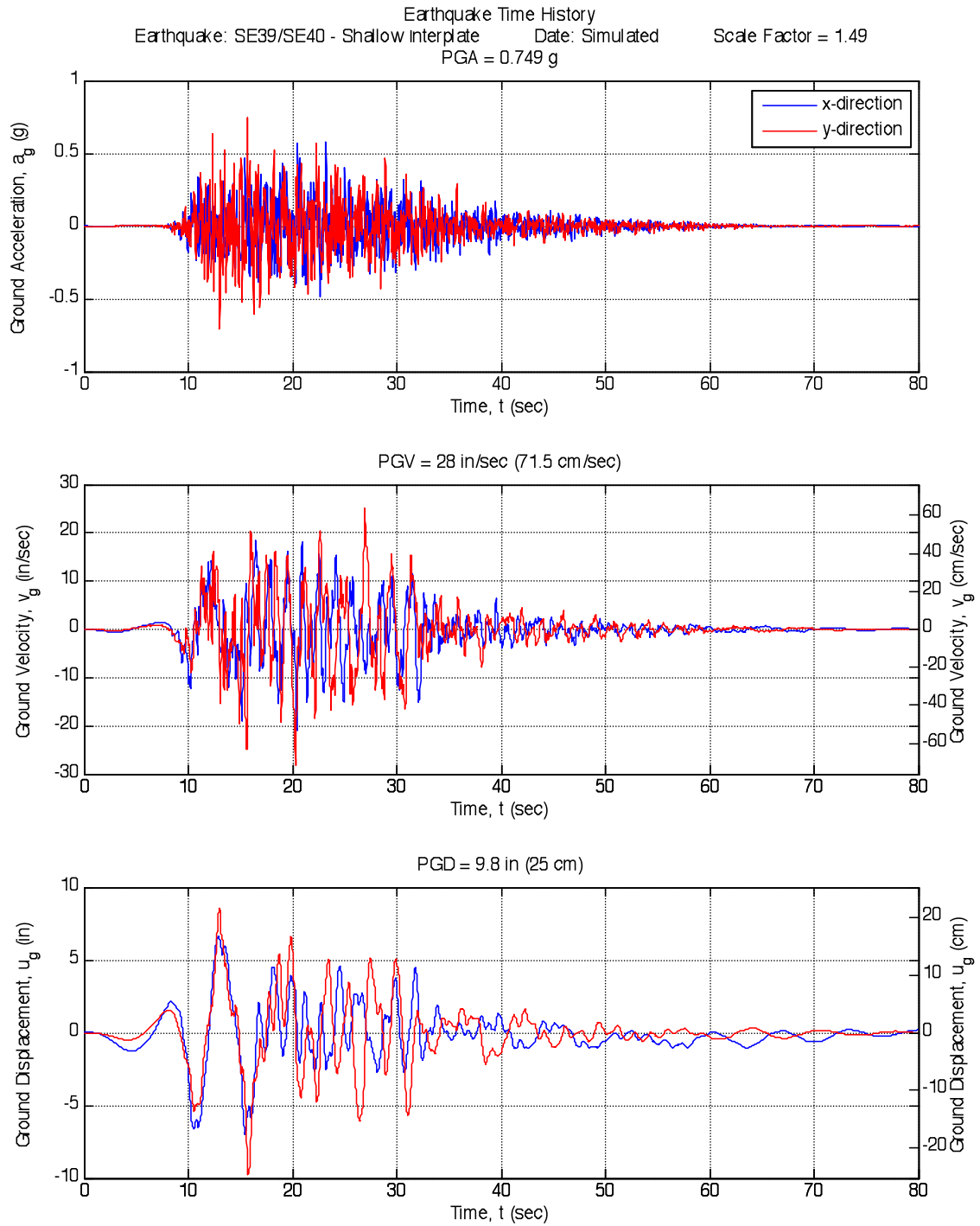


Fig. B-20. SE39/SE40 – Shallow Interplate Earthquake

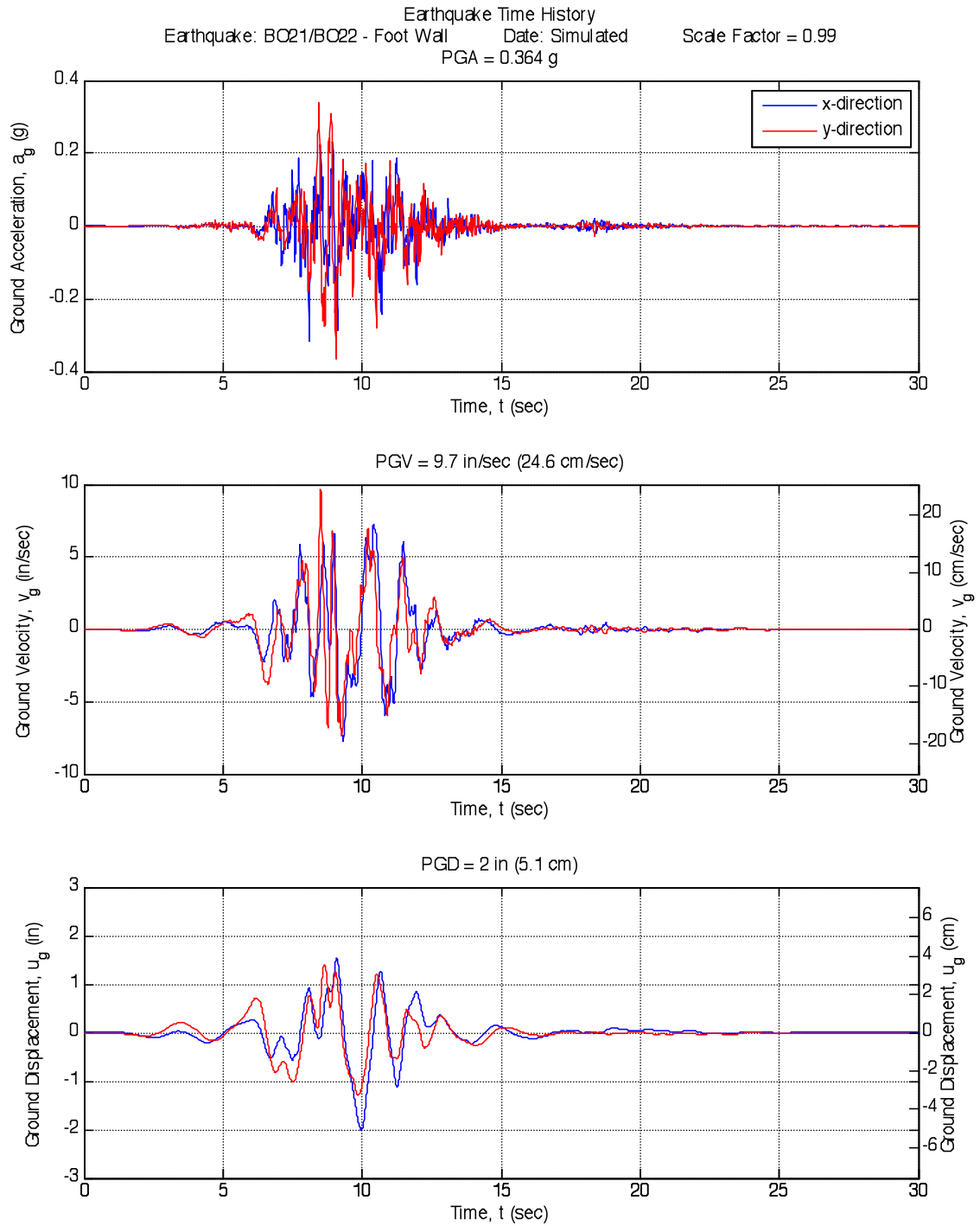


Fig. B-21. BO21/BO22 – Footwall Earthquake

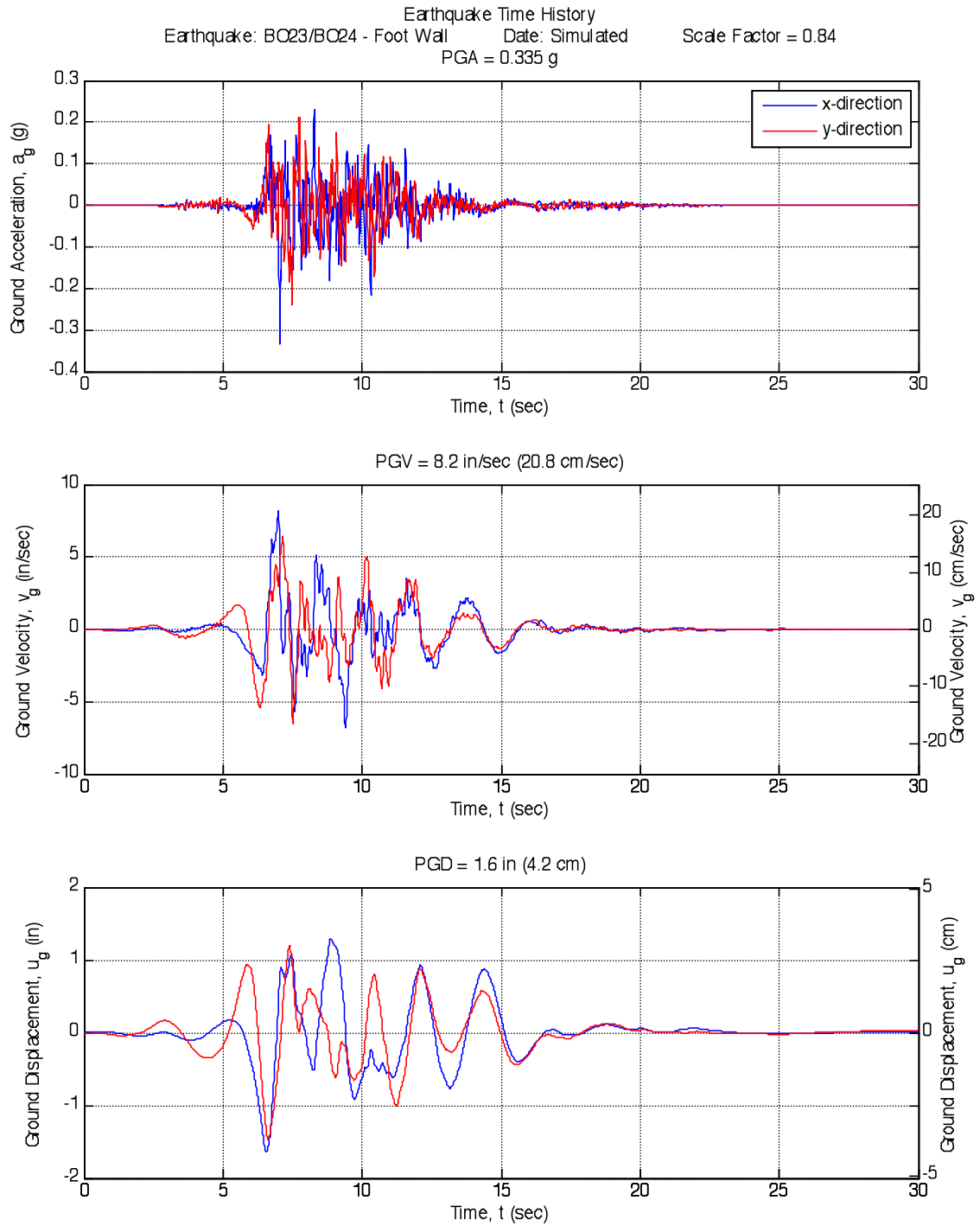


Fig. B-22. BO23/BO24 – Footwall Earthquake

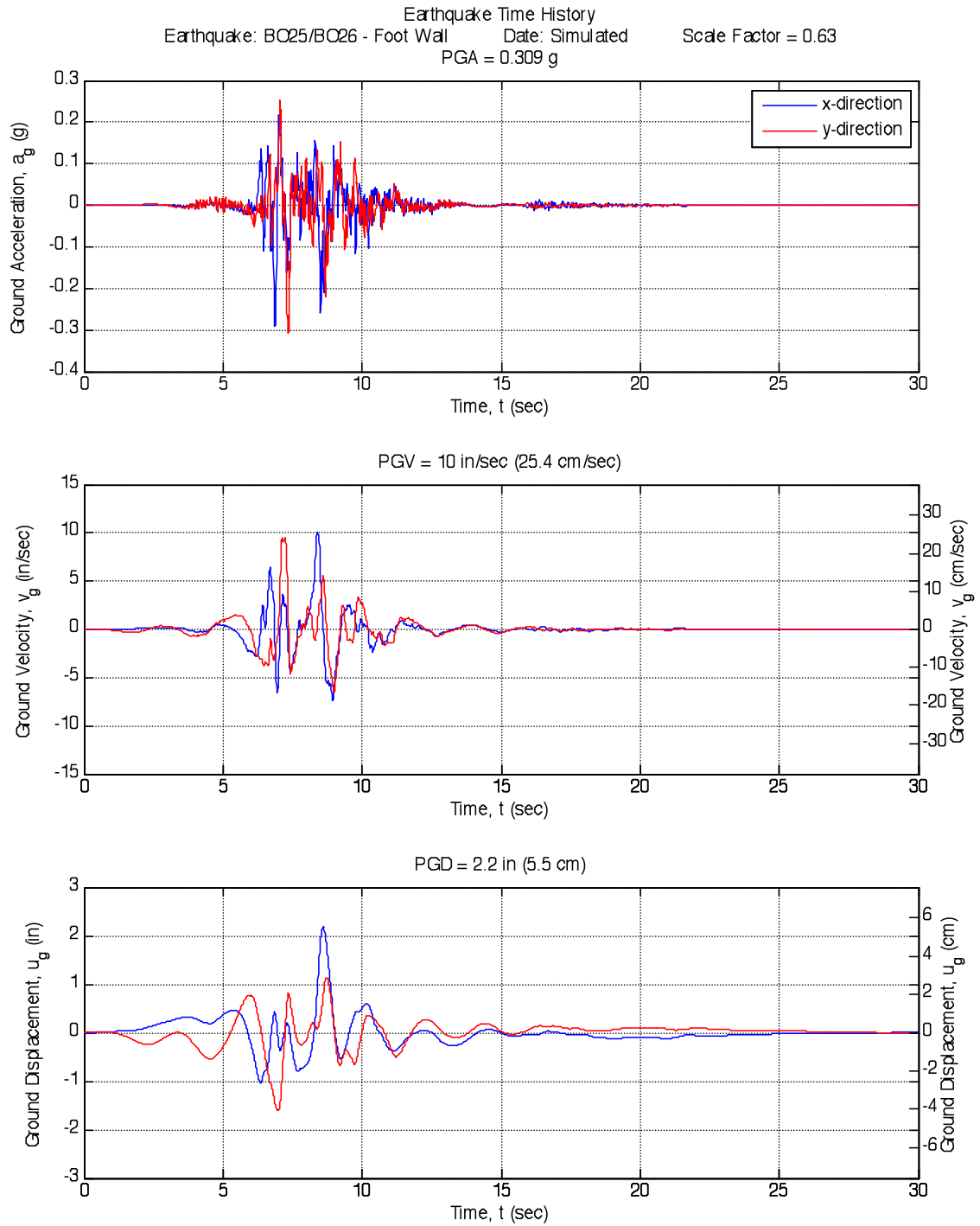


Fig. B-23. BO25/BO26 – Footwall Earthquake

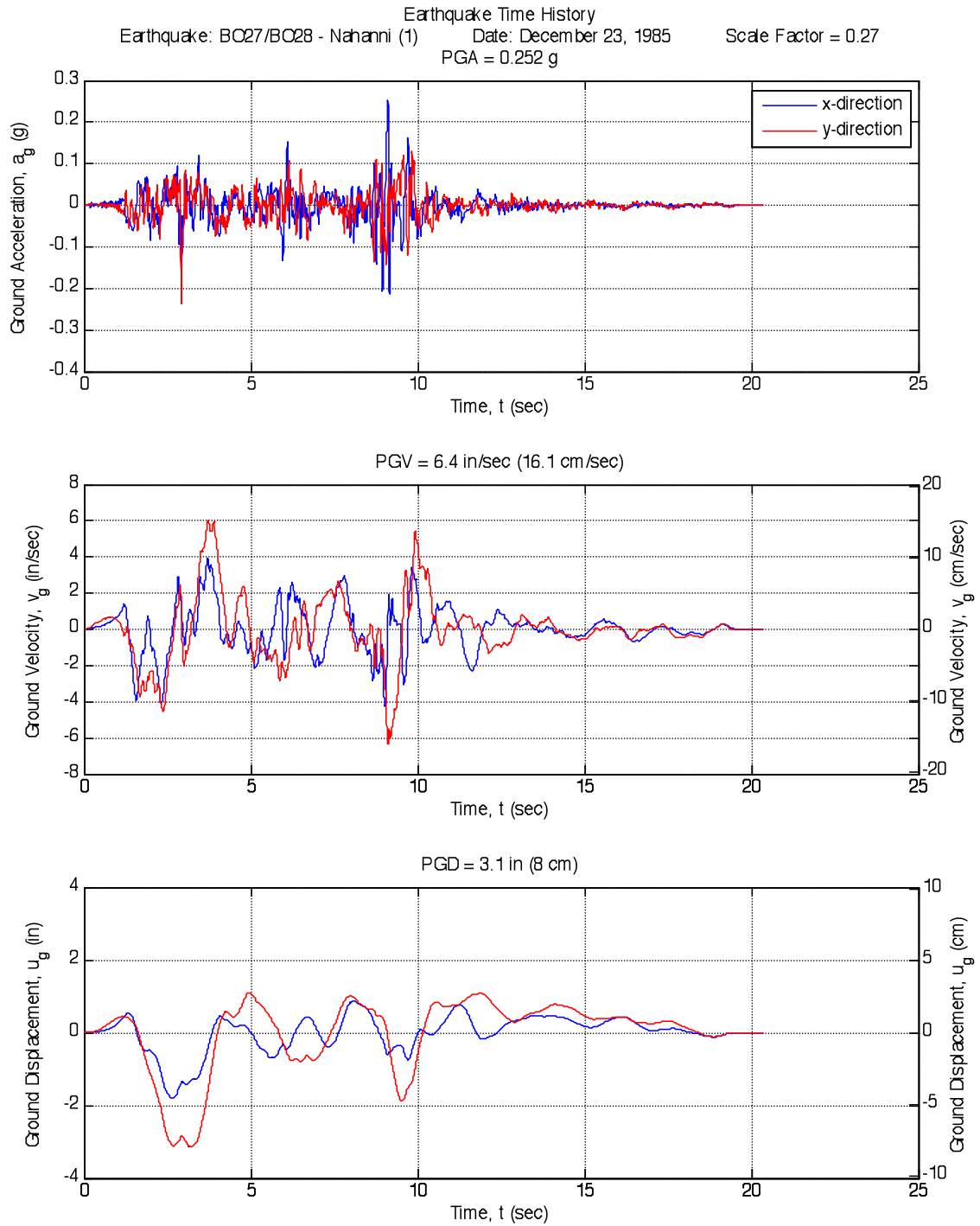


Fig. B-24. BO27/BO28 – Nahanni (Station 1) Earthquake

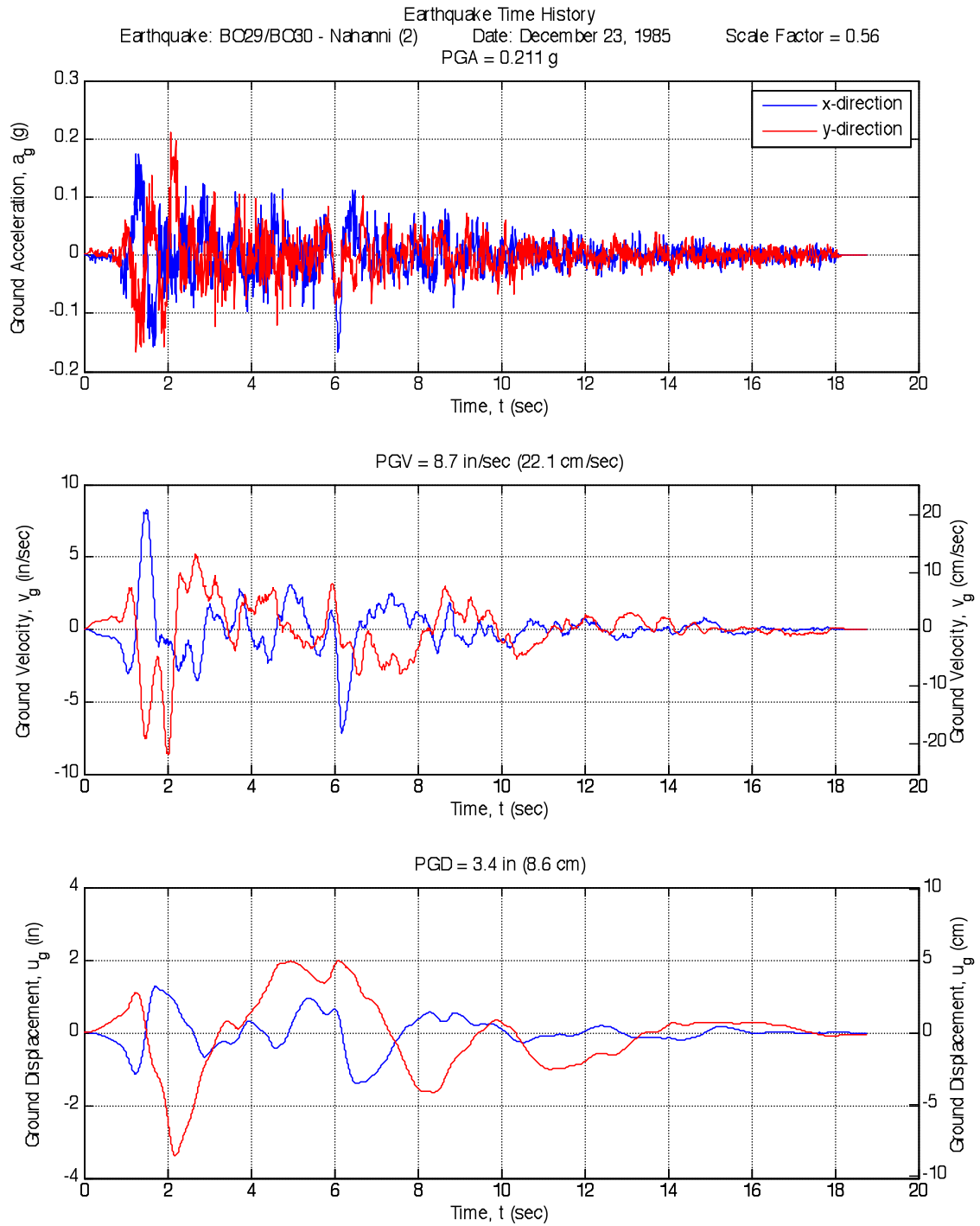


Fig. B-25. BO29/BO30 – Nahanni (Station 2) Earthquake

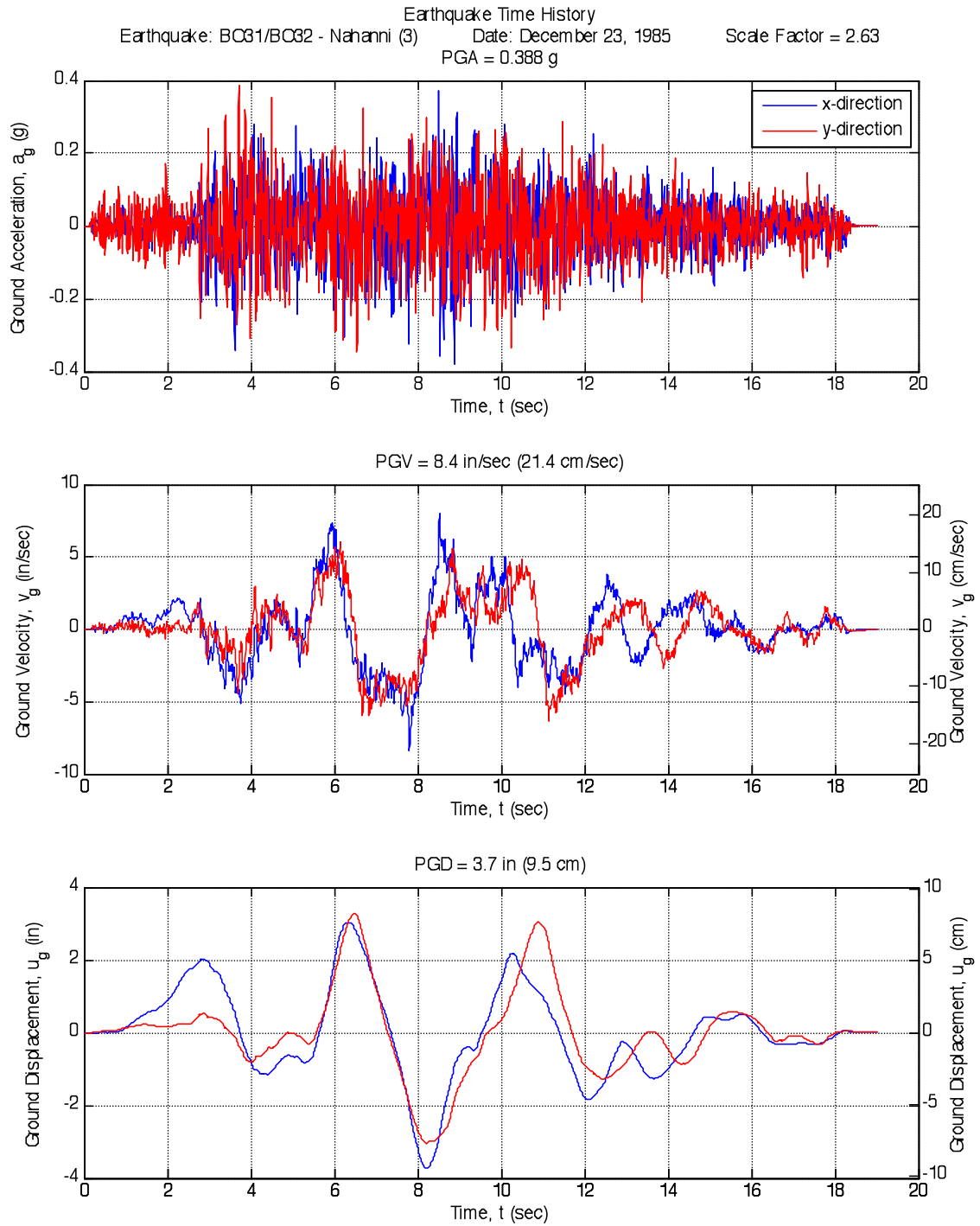


Fig. B-26. BO31/BO32 – Nahanni (Station 3) Earthquake

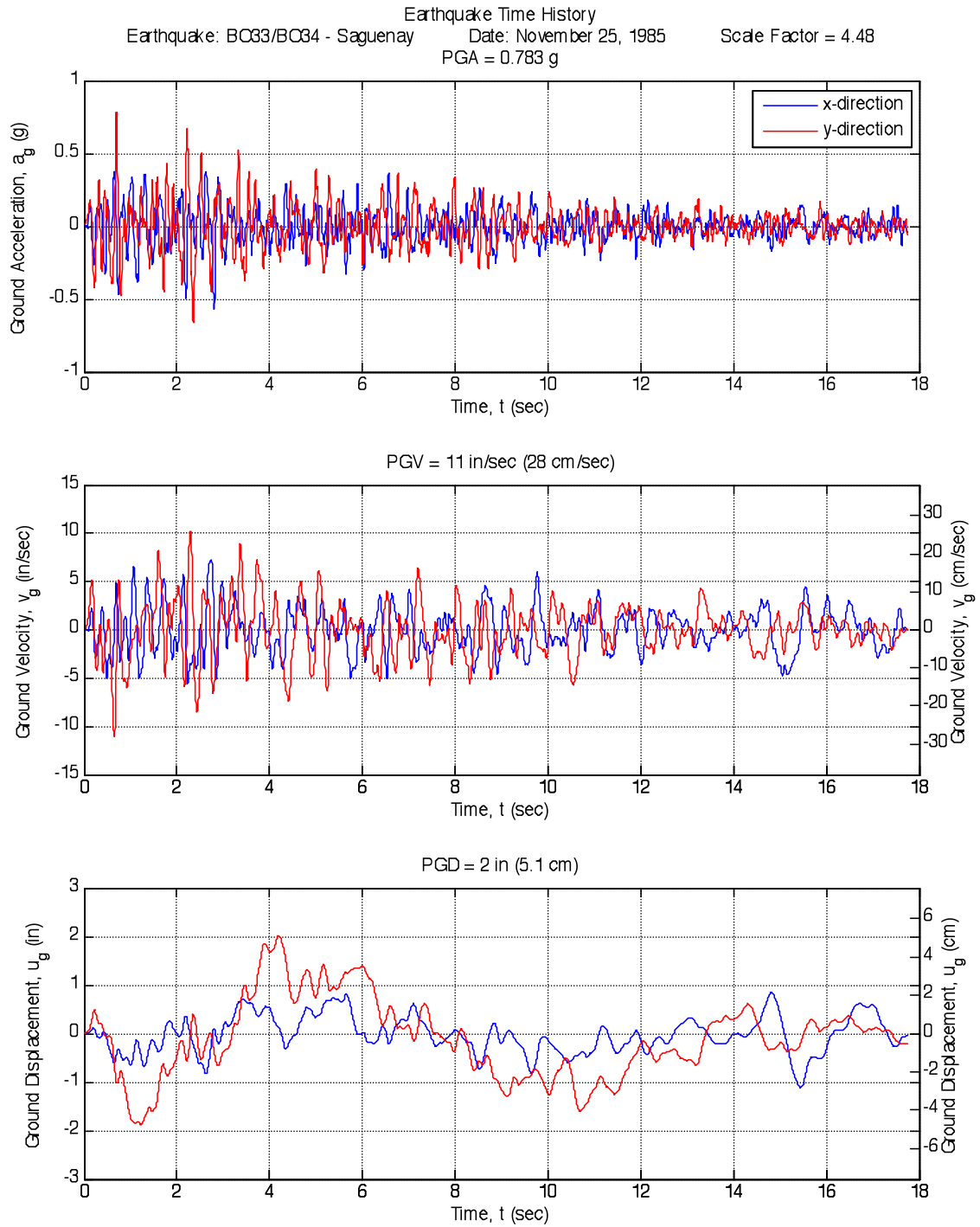


Fig. B-27. BO33/BO34 – Saguenay Earthquake

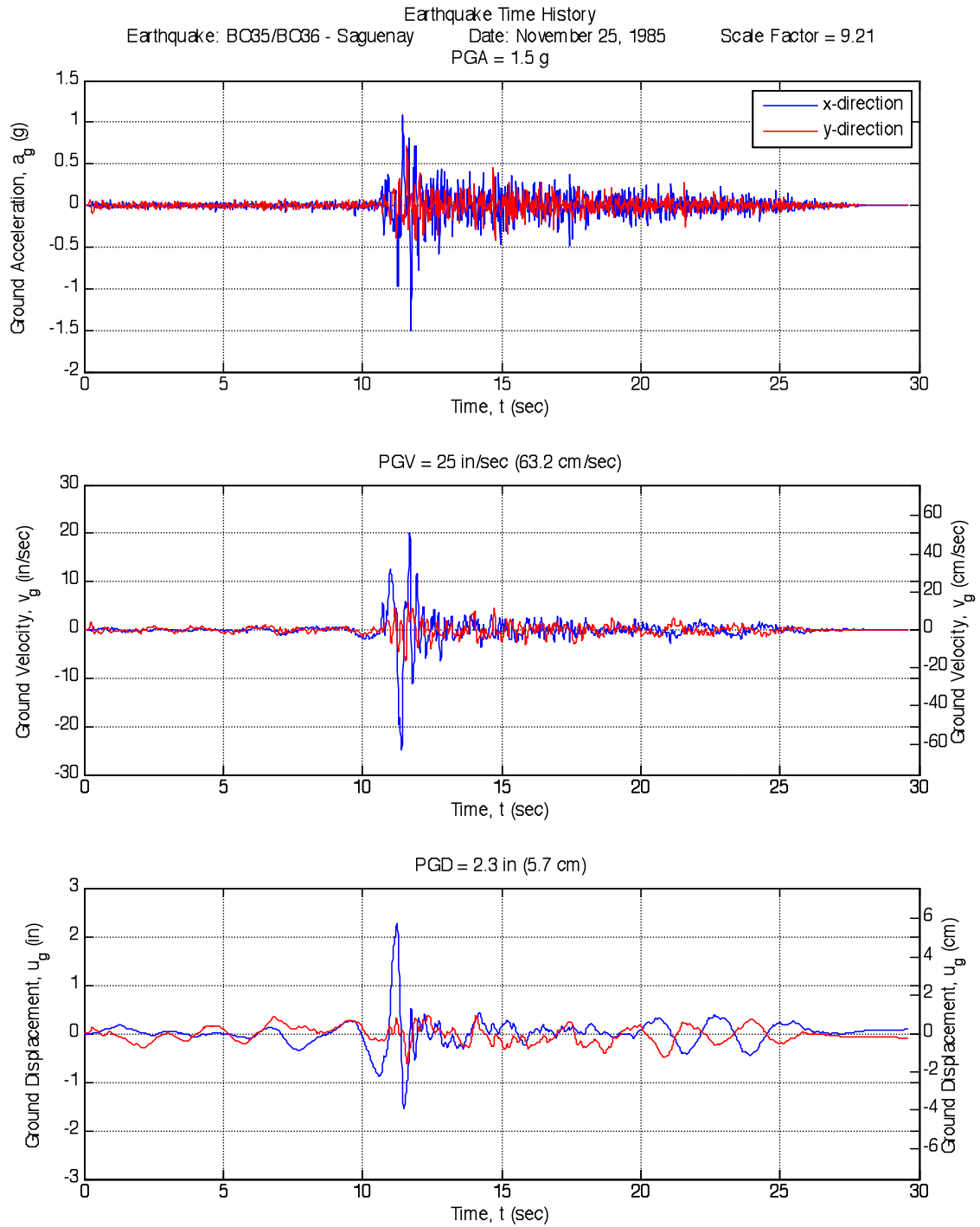


Fig. B-28. BO35/BO36 – Saguenay Earthquake

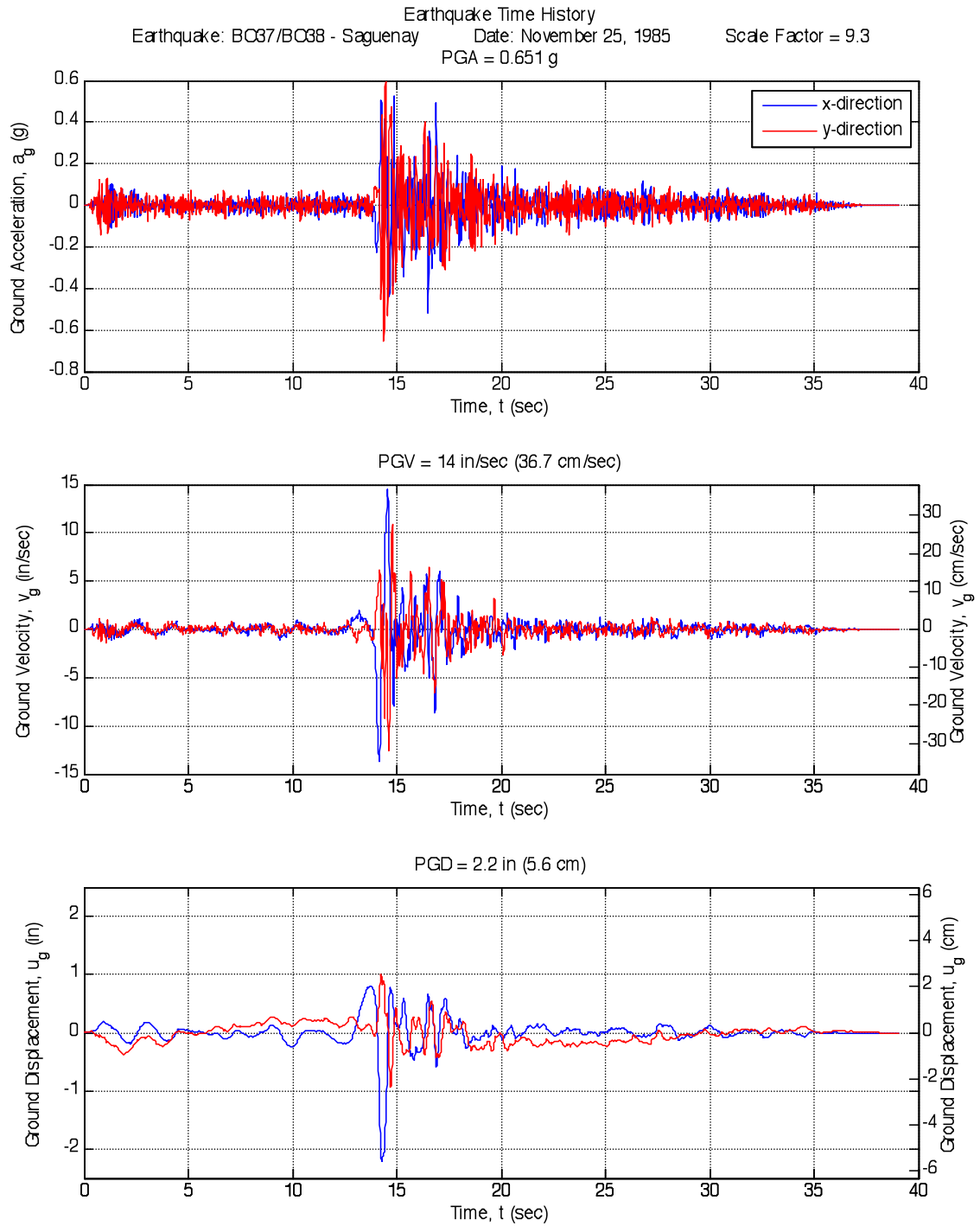


Fig. B-29. BO37/BO38 – Saguenay Earthquake

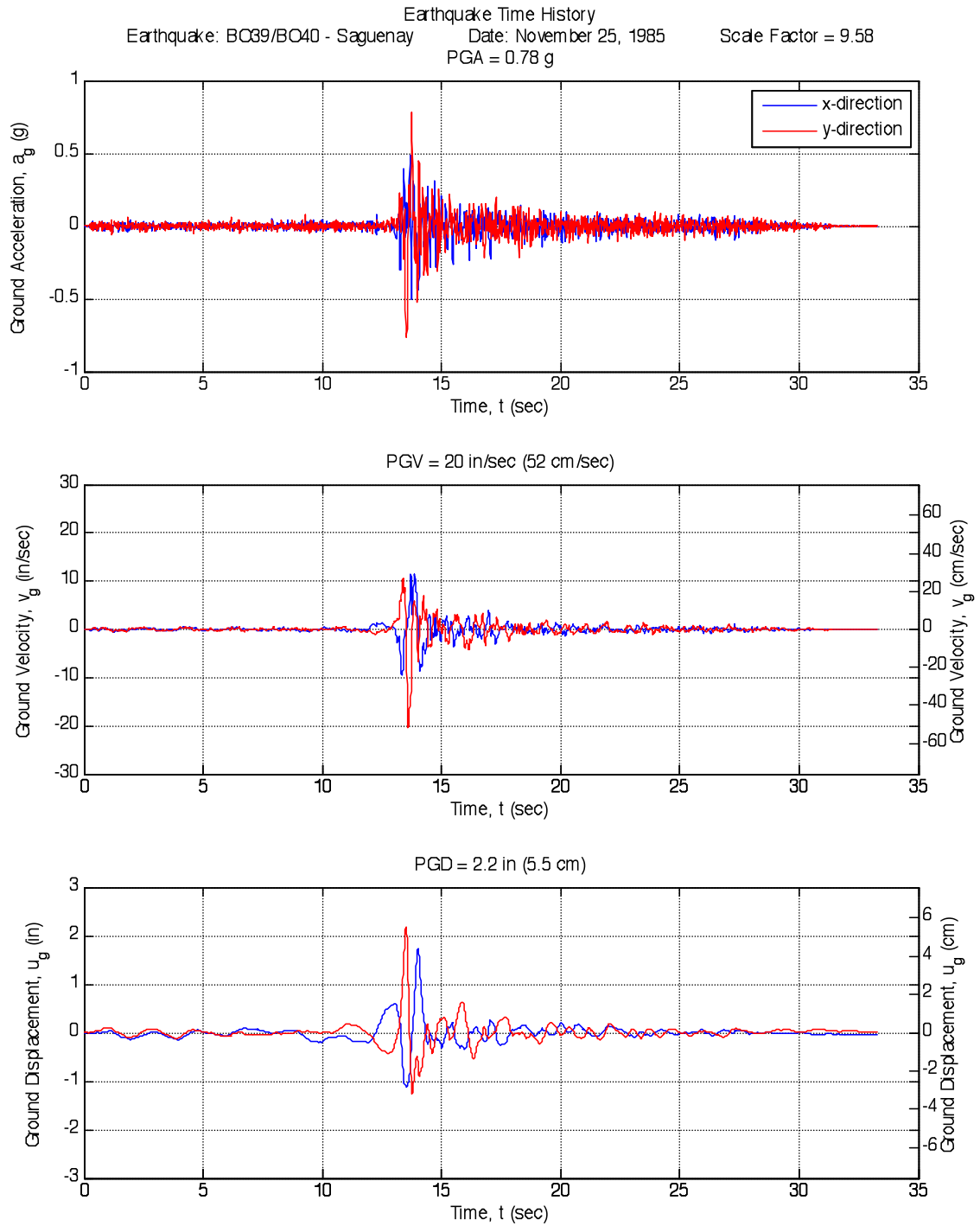


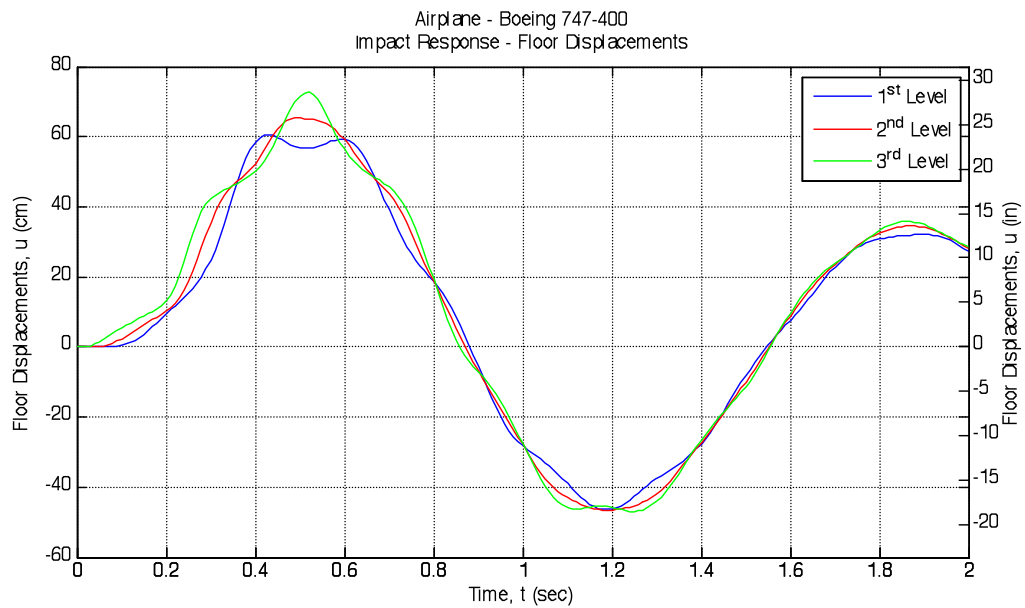
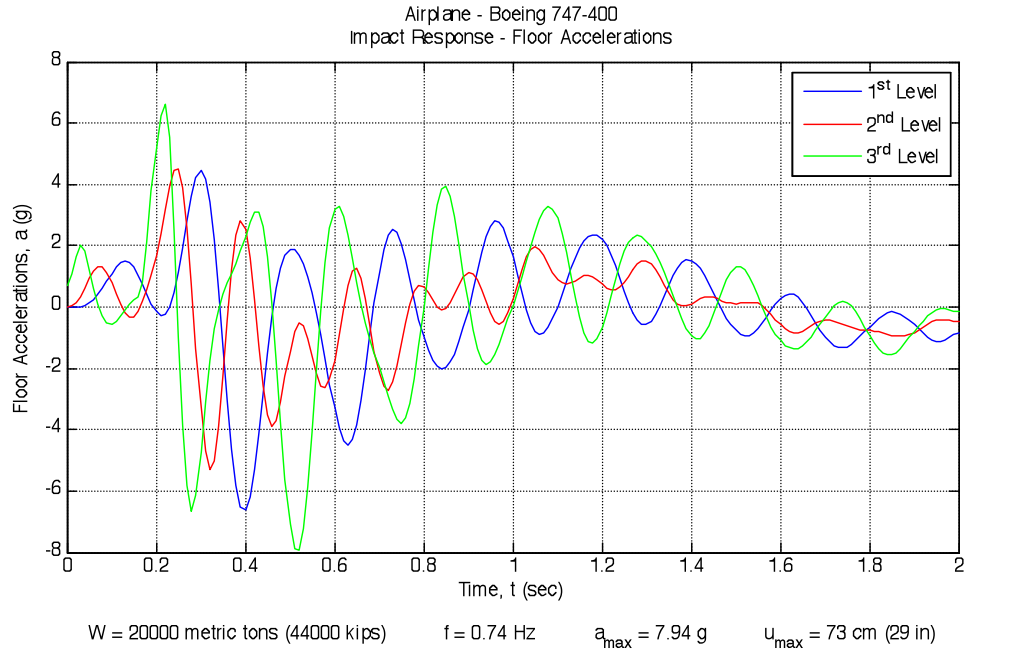
Fig. B-30. BO39/BO40 – Saguenay Earthquake

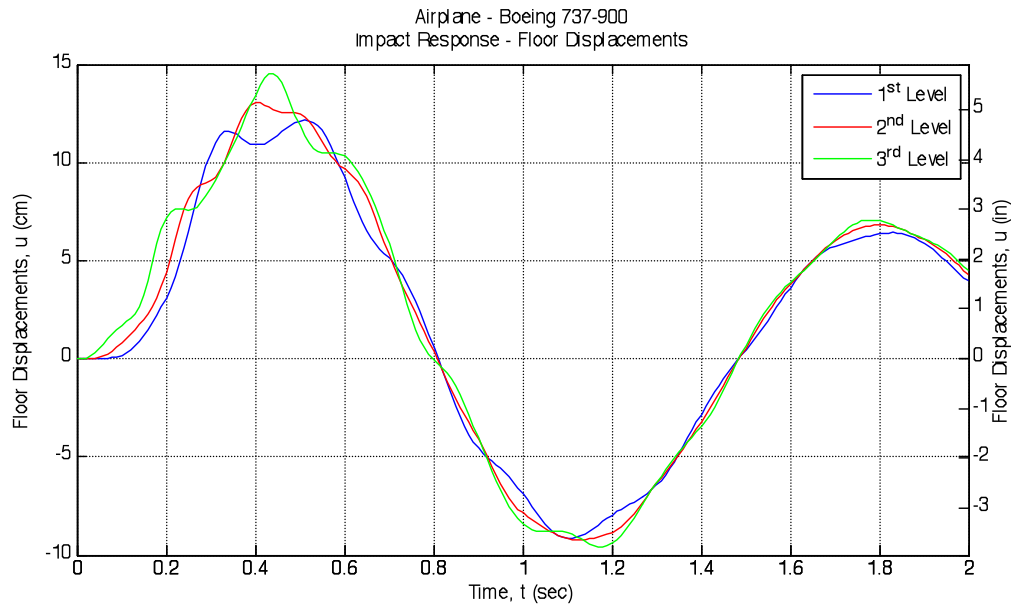
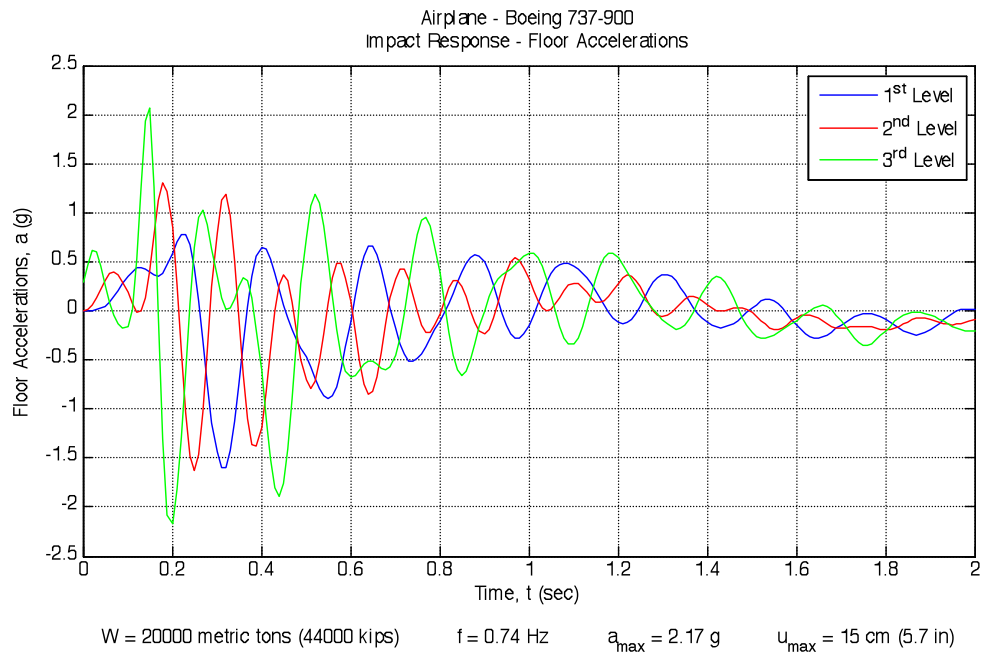
APPENDIX C: EARTHQUAKE RESPONSE RESULTS

| Model | Ground | | Non-Isolated | | 1 DOF, LE | | 1 DOF, BL | | 2 DOF, LE | | 2 DOF, BL | |
|-------|---------|----------|----------------------|-----------------------|----------------------|-----------------------|----------------------|-----------------------|----------------------|-----------------------|----------------------|-----------------------|
| | PGA (g) | PDG (in) | A _{MAX} (g) | D _{MAX} (in) |
| BO21 | 0.32 | 2.01 | 0.87 | 0.41 | 0.05 | 4.11 | 0.07 | 2.91 | 0.05 | 4.11 | 0.07 | 2.96 |
| BO22 | 0.36 | 1.40 | 1.20 | 0.57 | 0.04 | 3.55 | 0.07 | 2.18 | 0.05 | 3.55 | 0.08 | 2.22 |
| BO23 | 0.34 | 1.64 | 1.31 | 0.62 | 0.03 | 2.61 | 0.06 | 2.59 | 0.04 | 2.61 | 0.06 | 2.60 |
| BO24 | 0.24 | 1.48 | 1.24 | 0.58 | 0.03 | 2.64 | 0.06 | 3.16 | 0.03 | 2.65 | 0.06 | 3.19 |
| BO25 | 0.29 | 2.17 | 0.95 | 0.45 | 0.03 | 2.31 | 0.05 | 2.93 | 0.03 | 2.31 | 0.05 | 2.96 |
| BO26 | 0.31 | 1.60 | 0.62 | 0.29 | 0.03 | 2.48 | 0.08 | 2.66 | 0.03 | 2.48 | 0.08 | 2.68 |
| BO27 | 0.25 | 1.81 | 0.65 | 0.31 | 0.03 | 2.79 | 0.04 | 1.01 | 0.03 | 2.80 | 0.04 | 1.02 |
| BO28 | 0.24 | 3.14 | 0.55 | 0.26 | 0.06 | 4.77 | 0.05 | 1.89 | 0.06 | 4.81 | 0.05 | 1.90 |
| BO29 | 0.17 | 1.39 | 0.20 | 0.10 | 0.03 | 2.93 | 0.05 | 2.52 | 0.03 | 2.94 | 0.05 | 2.55 |
| BO30 | 0.21 | 3.38 | 0.25 | 0.12 | 0.05 | 4.11 | 0.06 | 3.01 | 0.05 | 4.12 | 0.06 | 3.04 |
| BO31 | 0.38 | 3.73 | 0.56 | 0.27 | 0.08 | 6.60 | 0.06 | 2.98 | 0.08 | 6.64 | 0.06 | 3.00 |
| BO32 | 0.39 | 3.28 | 0.44 | 0.21 | 0.06 | 5.14 | 0.06 | 3.09 | 0.06 | 5.17 | 0.06 | 3.13 |
| BO33 | 0.57 | 1.12 | 1.82 | 0.86 | 0.02 | 1.43 | 0.05 | 1.32 | 0.02 | 1.43 | 0.05 | 1.32 |
| BO34 | 0.78 | 2.02 | 4.11 | 1.95 | 0.03 | 2.22 | 0.05 | 1.58 | 0.03 | 2.23 | 0.05 | 1.58 |
| BO35 | 1.50 | 2.26 | 4.67 | 2.22 | 0.04 | 3.08 | 0.12 | 3.82 | 0.04 | 3.08 | 0.13 | 3.88 |
| BO36 | 0.71 | 0.63 | 2.03 | 0.96 | 0.01 | 0.79 | 0.05 | 1.11 | 0.01 | 0.79 | 0.05 | 1.13 |
| BO37 | 0.52 | 2.21 | 1.14 | 0.54 | 0.04 | 3.05 | 0.08 | 3.05 | 0.04 | 3.05 | 0.08 | 3.20 |
| BO38 | 0.65 | 1.00 | 2.19 | 1.03 | 0.02 | 1.34 | 0.05 | 1.37 | 0.03 | 1.34 | 0.05 | 1.41 |
| BO39 | 0.51 | 1.74 | 1.96 | 0.92 | 0.03 | 1.83 | 0.08 | 2.93 | 0.03 | 1.84 | 0.08 | 3.02 |
| BO40 | 0.78 | 2.18 | 1.45 | 0.69 | 0.03 | 2.54 | 0.11 | 3.44 | 0.04 | 2.55 | 0.12 | 3.66 |
| SE21 | 0.76 | 27.68 | 0.95 | 0.45 | 0.32 | 27.68 | 0.41 | 31.18 | 0.31 | 27.75 | 0.41 | 31.32 |
| SE22 | 0.49 | 6.24 | 1.01 | 0.47 | 0.11 | 9.58 | 0.21 | 11.24 | 0.11 | 9.57 | 0.21 | 11.29 |
| SE23 | 0.61 | 20.15 | 1.85 | 0.88 | 0.27 | 22.99 | 0.31 | 26.23 | 0.27 | 23.07 | 0.31 | 26.31 |
| SE24 | 0.54 | 11.44 | 1.10 | 0.52 | 0.29 | 25.19 | 0.30 | 25.99 | 0.29 | 25.25 | 0.30 | 26.08 |
| SE25 | 0.90 | 9.55 | 2.35 | 1.12 | 0.28 | 23.83 | 0.31 | 24.48 | 0.28 | 23.90 | 0.31 | 24.59 |
| SE26 | 0.82 | 9.90 | 3.82 | 1.81 | 0.31 | 26.12 | 0.36 | 27.56 | 0.30 | 26.26 | 0.37 | 27.77 |
| SE27 | 1.76 | 9.54 | 5.04 | 2.40 | 0.26 | 20.97 | 0.38 | 22.18 | 0.26 | 21.00 | 0.38 | 22.21 |
| SE28 | 1.39 | 10.73 | 4.32 | 2.06 | 0.14 | 10.99 | 0.27 | 12.40 | 0.14 | 10.99 | 0.27 | 12.41 |
| SE29 | 1.64 | 10.40 | 9.14 | 4.37 | 0.19 | 15.17 | 0.33 | 14.77 | 0.20 | 15.22 | 0.33 | 14.83 |
| SE30 | 1.57 | 11.23 | 6.25 | 2.96 | 0.18 | 15.12 | 0.33 | 14.52 | 0.19 | 15.19 | 0.33 | 14.59 |
| SE31 | 1.27 | 8.68 | 4.58 | 2.17 | 0.19 | 15.11 | 0.31 | 14.10 | 0.19 | 15.19 | 0.32 | 14.11 |
| SE32 | 0.90 | 9.46 | 3.28 | 1.54 | 0.10 | 7.55 | 0.22 | 8.40 | 0.10 | 7.59 | 0.22 | 8.40 |
| SE33 | 0.80 | 9.42 | 1.92 | 0.92 | 0.15 | 12.58 | 0.22 | 13.48 | 0.15 | 12.61 | 0.22 | 13.52 |
| SE34 | 0.65 | 5.47 | 4.29 | 2.04 | 0.09 | 7.50 | 0.15 | 6.79 | 0.09 | 7.52 | 0.15 | 6.80 |
| SE35 | 0.61 | 8.45 | 1.21 | 0.57 | 0.09 | 7.21 | 0.17 | 9.34 | 0.09 | 7.22 | 0.17 | 9.36 |

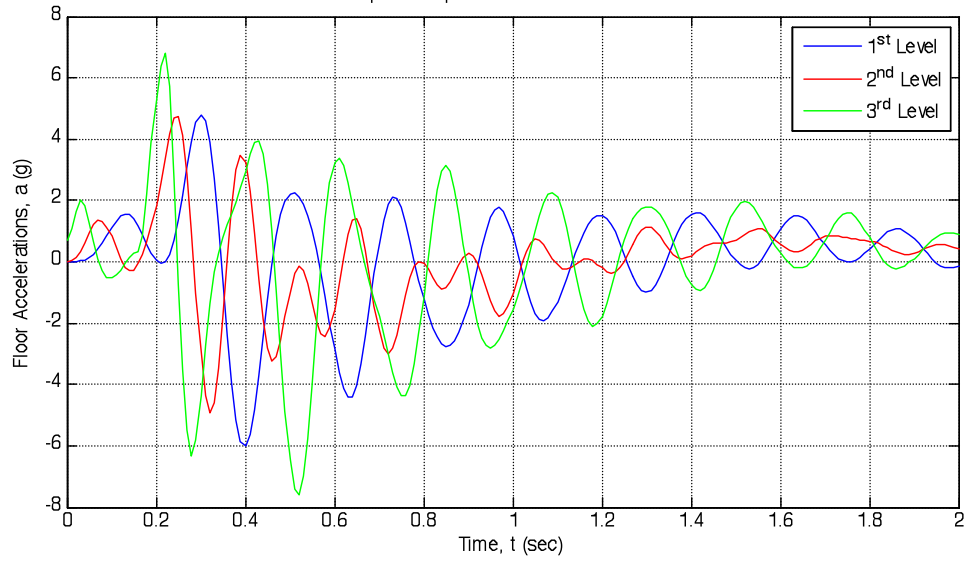
| | | | | | | | | | | | | |
|------|------|-------|------|------|------|-------|------|-------|------|-------|------|-------|
| SE36 | 0.78 | 10.74 | 1.45 | 0.69 | 0.24 | 20.05 | 0.29 | 20.62 | 0.24 | 20.12 | 0.29 | 20.70 |
| SE37 | 0.56 | 7.06 | 1.73 | 0.82 | 0.13 | 10.66 | 0.15 | 10.11 | 0.13 | 10.66 | 0.15 | 10.12 |
| SE38 | 0.53 | 8.53 | 2.30 | 1.10 | 0.18 | 15.60 | 0.24 | 16.12 | 0.19 | 15.67 | 0.24 | 16.16 |
| SE39 | 0.58 | 6.98 | 1.65 | 0.77 | 0.12 | 10.42 | 0.16 | 8.69 | 0.12 | 10.44 | 0.16 | 8.72 |
| SE40 | 0.75 | 9.76 | 2.80 | 1.33 | 0.13 | 11.20 | 0.17 | 11.44 | 0.13 | 11.19 | 0.18 | 11.46 |
| LA21 | 1.28 | 14.89 | 1.91 | 0.91 | 0.31 | 26.43 | 0.43 | 28.86 | 0.32 | 26.48 | 0.44 | 28.94 |
| LA22 | 0.92 | 13.48 | 1.49 | 0.70 | 0.31 | 26.45 | 0.39 | 26.62 | 0.31 | 26.53 | 0.39 | 26.74 |
| LA23 | 0.42 | 9.11 | 0.67 | 0.32 | 0.21 | 17.71 | 0.27 | 21.65 | 0.21 | 17.75 | 0.27 | 21.73 |
| LA24 | 0.47 | 23.14 | 0.83 | 0.39 | 0.56 | 48.20 | 0.69 | 57.28 | 0.57 | 48.48 | 0.69 | 57.67 |
| LA25 | 0.87 | 11.44 | 1.65 | 0.78 | 0.26 | 21.28 | 0.27 | 21.48 | 0.26 | 21.36 | 0.28 | 21.61 |
| LA26 | 0.94 | 17.06 | 1.75 | 0.83 | 0.22 | 18.54 | 0.25 | 19.79 | 0.22 | 18.53 | 0.25 | 16.80 |
| LA27 | 0.93 | 11.11 | 1.59 | 0.76 | 0.45 | 37.84 | 0.60 | 43.19 | 0.45 | 37.95 | 0.61 | 43.38 |
| LA28 | 1.33 | 17.23 | 2.44 | 1.16 | 0.37 | 30.94 | 0.56 | 39.63 | 0.37 | 31.01 | 0.56 | 39.75 |
| LA29 | 0.81 | 13.94 | 3.52 | 1.65 | 0.24 | 20.30 | 0.26 | 20.03 | 0.24 | 20.40 | 0.26 | 20.18 |
| LA30 | 0.99 | 37.26 | 3.87 | 1.84 | 0.35 | 30.14 | 0.41 | 32.90 | 0.35 | 30.27 | 0.41 | 33.09 |
| LA31 | 1.30 | 14.14 | 2.83 | 1.34 | 0.23 | 19.25 | 0.25 | 18.88 | 0.23 | 19.32 | 0.25 | 18.97 |
| LA32 | 1.19 | 17.93 | 3.34 | 1.58 | 0.23 | 18.81 | 0.27 | 19.29 | 0.23 | 18.86 | 0.28 | 19.35 |
| LA33 | 0.78 | 19.84 | 2.59 | 1.22 | 0.44 | 37.58 | 0.48 | 40.38 | 0.44 | 37.68 | 0.49 | 40.53 |
| LA34 | 0.68 | 19.67 | 2.43 | 1.15 | 0.43 | 37.08 | 0.50 | 39.63 | 0.44 | 37.19 | 0.50 | 39.78 |
| LA35 | 0.99 | 35.26 | 2.97 | 1.40 | 0.75 | 64.55 | 0.88 | 75.37 | 0.75 | 64.72 | 0.89 | 75.61 |
| LA36 | 1.10 | 32.52 | 2.30 | 1.09 | 0.80 | 68.39 | 0.96 | 79.32 | 0.80 | 68.60 | 0.96 | 79.61 |
| LA37 | 0.71 | 30.43 | 1.71 | 0.81 | 0.45 | 39.10 | 0.67 | 54.58 | 0.45 | 39.27 | 0.67 | 54.70 |
| LA38 | 0.78 | 36.40 | 1.17 | 0.55 | 0.59 | 50.50 | 0.78 | 64.32 | 0.59 | 50.65 | 0.78 | 64.48 |
| LA39 | 0.50 | 8.91 | 0.91 | 0.43 | 0.19 | 16.22 | 0.28 | 18.14 | 0.19 | 16.28 | 0.28 | 18.18 |
| LA40 | 0.63 | 26.72 | 0.91 | 0.43 | 0.53 | 45.20 | 0.57 | 49.78 | 0.53 | 45.32 | 0.57 | 49.95 |

APPENDIX D: IMPACT RESPONSE TIME HISTORIES



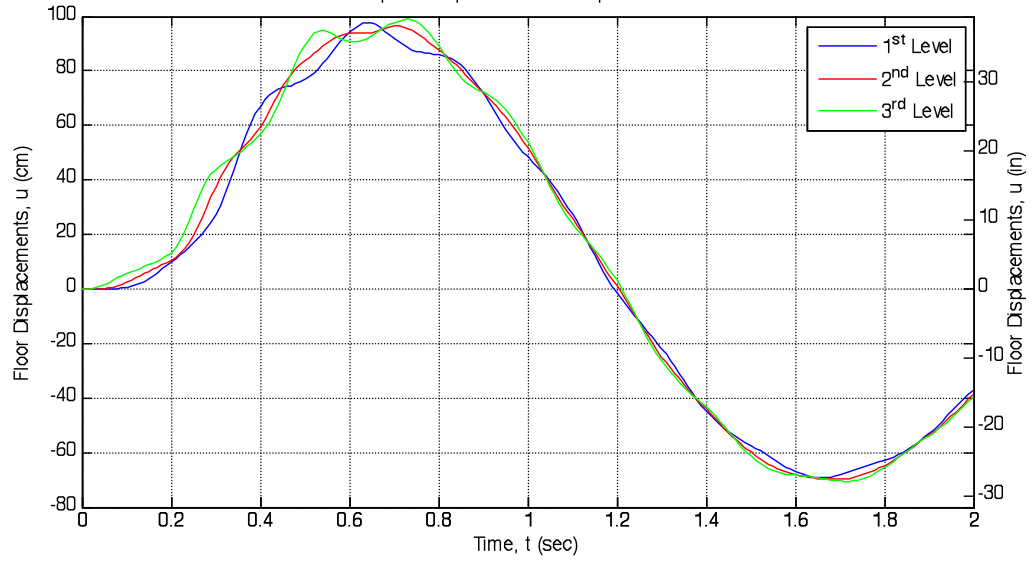


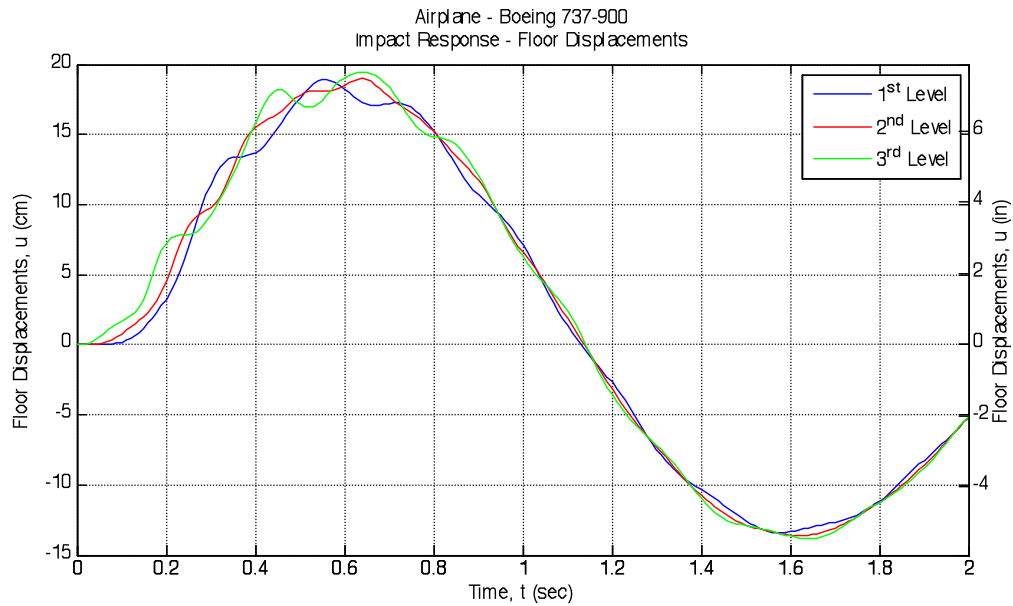
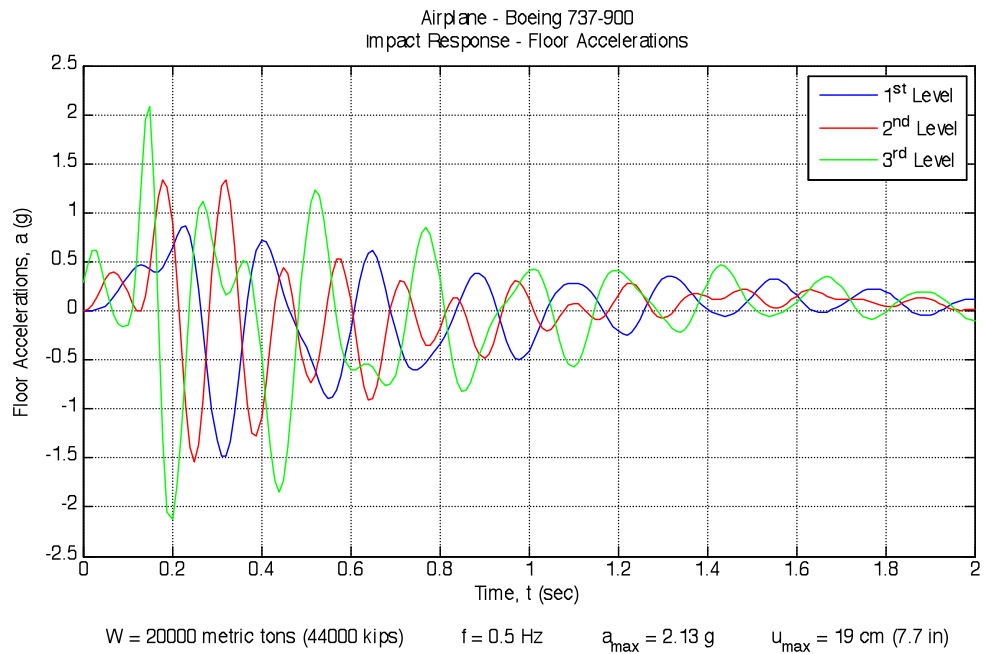
Airplane - Boeing 747-400
Impact Response - Floor Accelerations



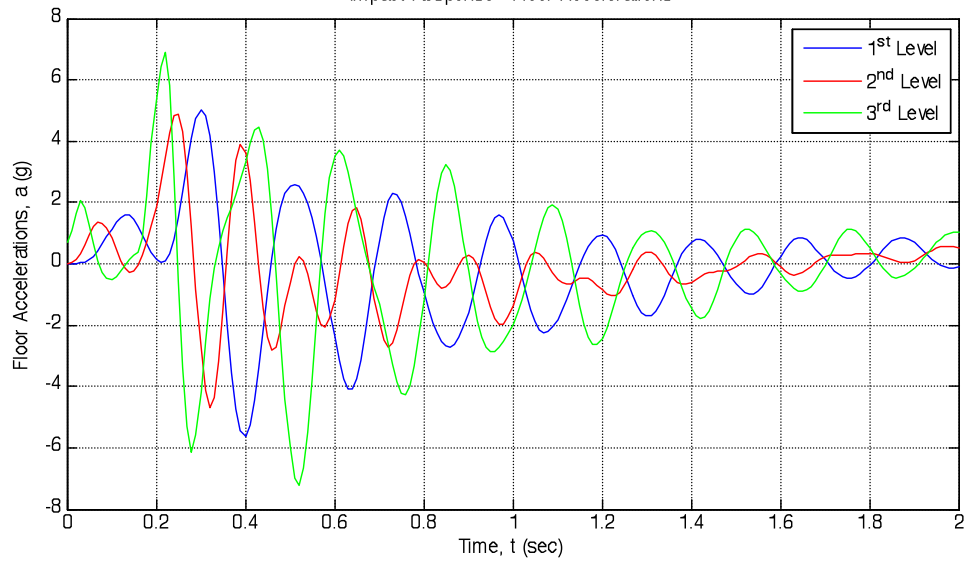
W = 20000 metric tons (44000 kips) f = 0.5 Hz $a_{max} = 7.59$ g $u_{max} = 99$ cm (39 in)

Airplane - Boeing 747-400
Impact Response - Floor Displacements



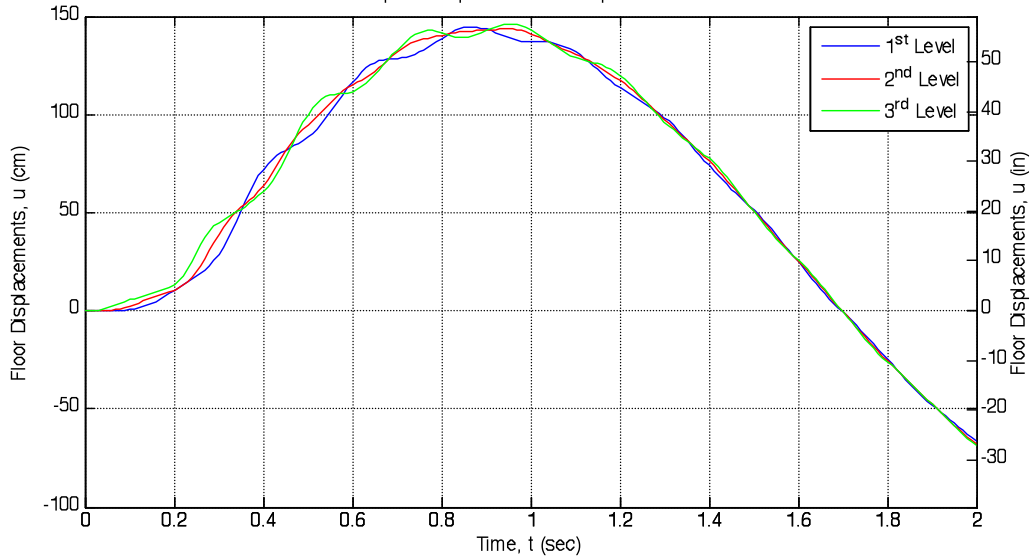


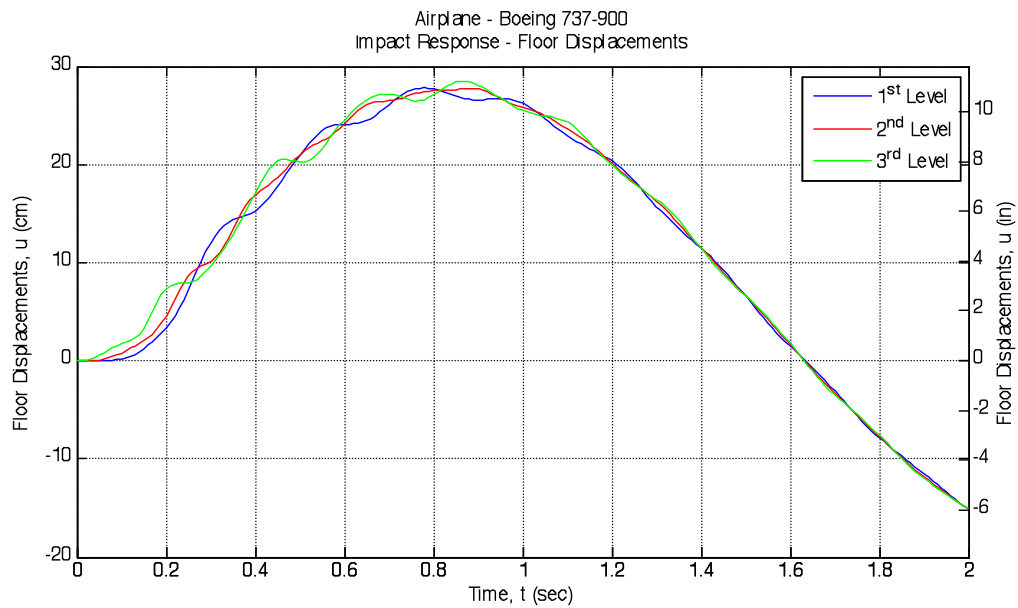
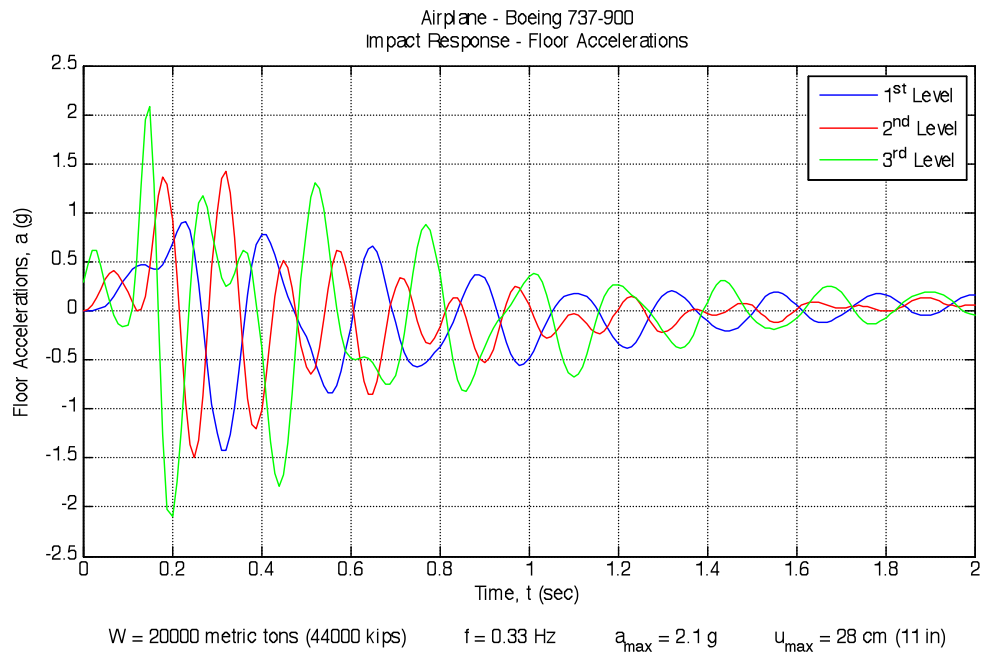
Airplane - Boeing 747-400
Impact Response - Floor Accelerations



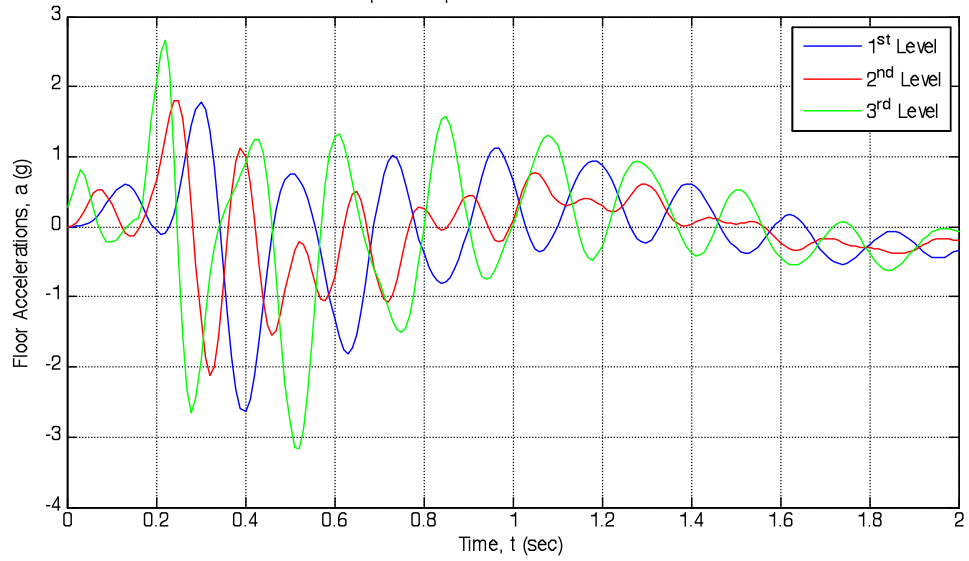
W = 20000 metric tons (44000 kips) f = 0.33 Hz $a_{max} = 7.22 \text{ g}$ $u_{max} = 1.5e+002 \text{ cm (58 in)}$

Airplane - Boeing 747-400
Impact Response - Floor Displacements



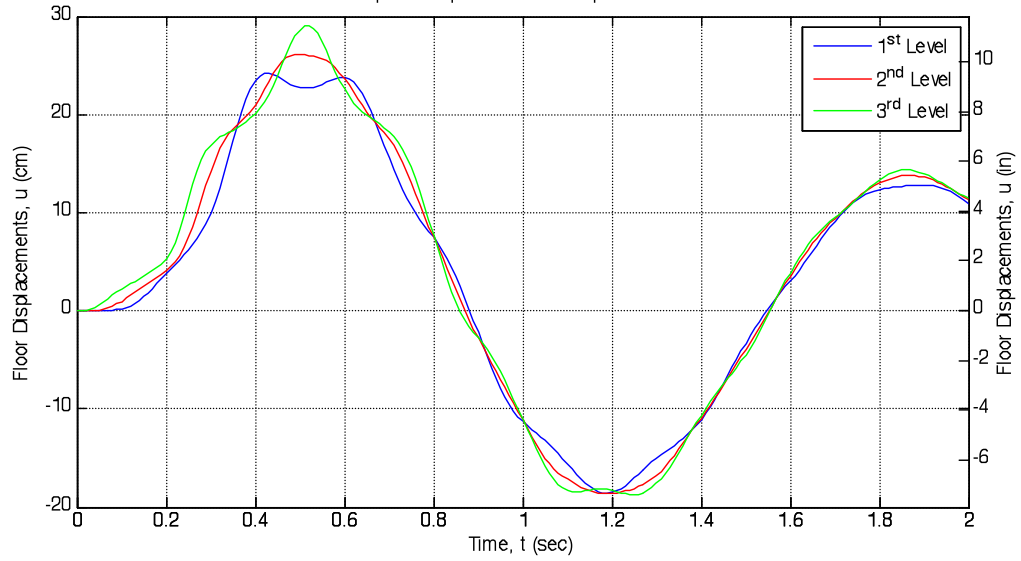


Airplane - Boeing 747-400
Impact Response - Floor Accelerations

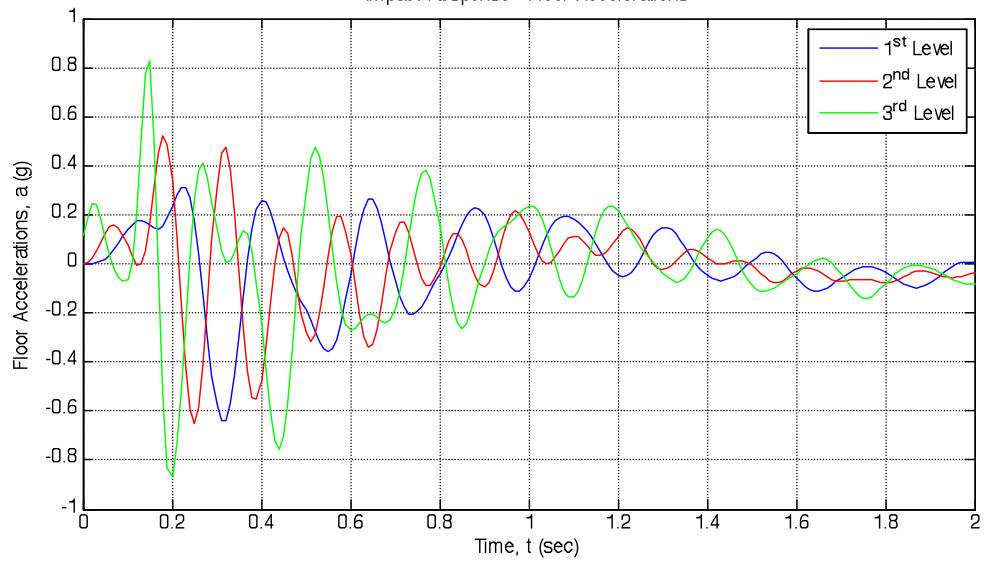


$W = 50000$ metric tons (110000 kips) $f = 0.74$ Hz $a_{\max} = 3.18$ g $u_{\max} = 29$ cm (11 in)

Airplane - Boeing 747-400
Impact Response - Floor Displacements

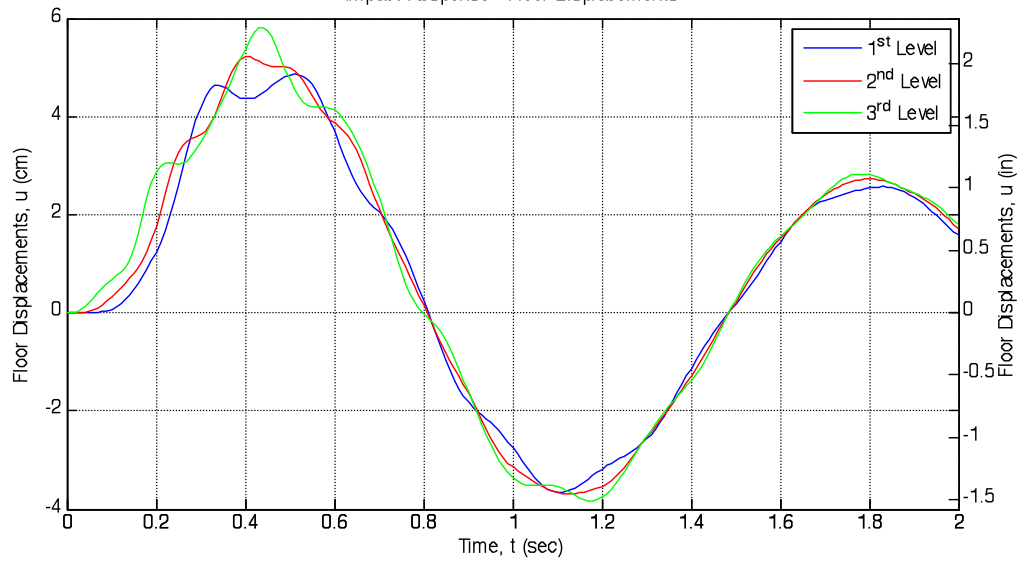


Airplane - Boeing 737-900
Impact Response - Floor Accelerations

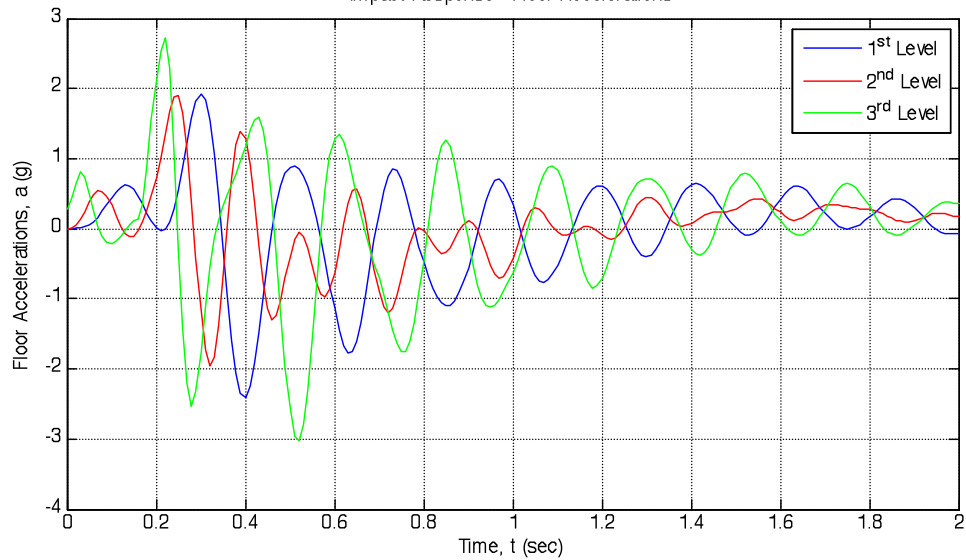


$W = 50000$ metric tons (110000 kips) $f = 0.74$ Hz $a_{\max} = 0.866$ g $u_{\max} = 5.8$ cm (2.3 in)

Airplane - Boeing 737-900
Impact Response - Floor Displacements

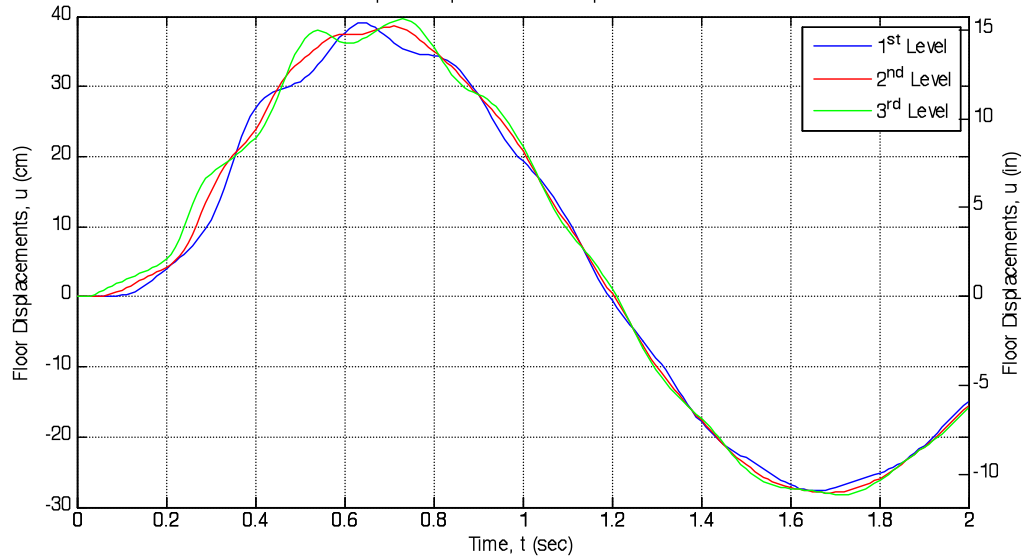


Airplane - Boeing 747-400
Impact Response - Floor Accelerations

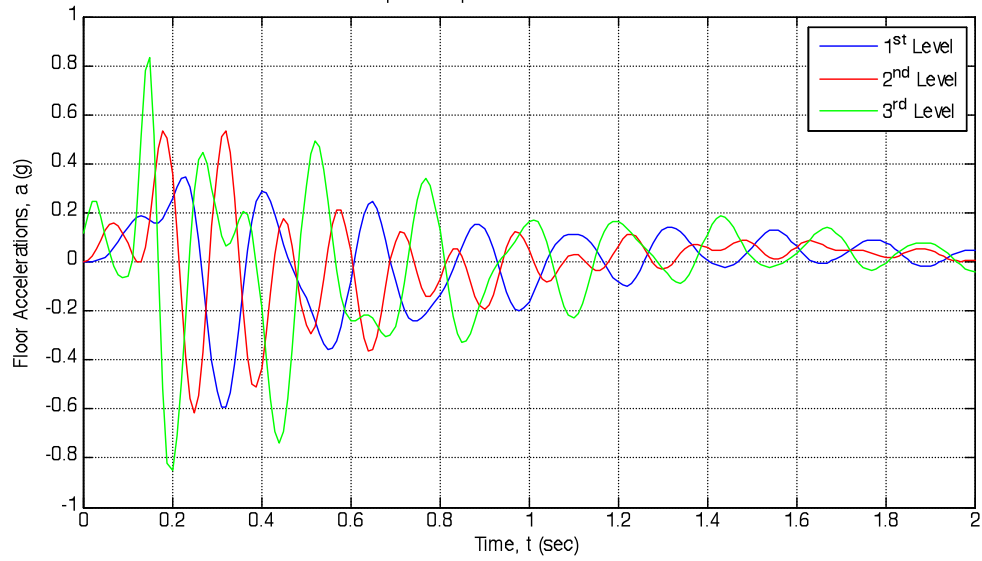


W = 50000 metric tons (110000 kips) f = 0.5 Hz a_{max} = 3.03 g u_{max} = 40 cm (16 in)

Airplane - Boeing 747-400
Impact Response - Floor Displacements

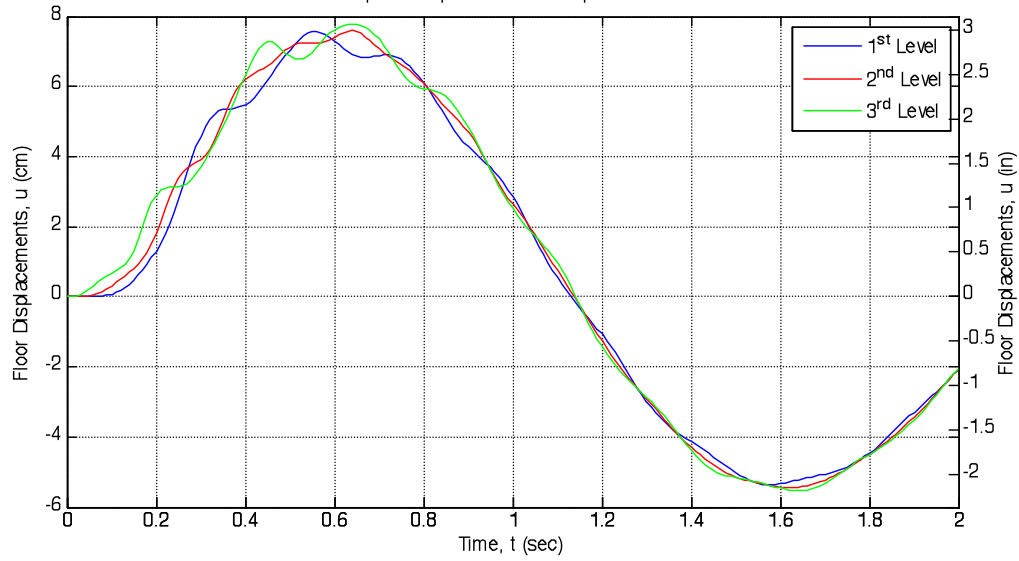


Airplane - Boeing 737-900
Impact Response - Floor Accelerations

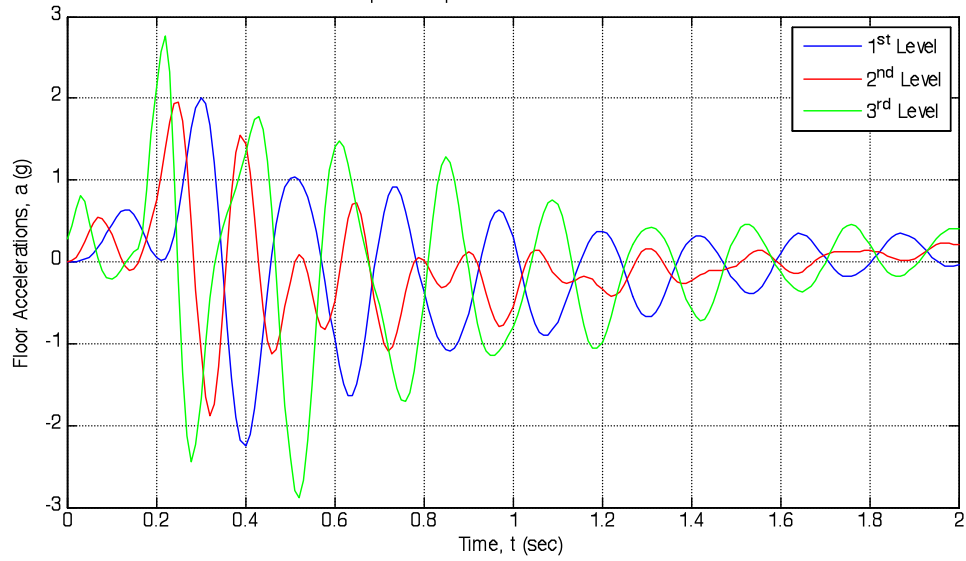


$W = 50000$ metric tons (110000 kips) $f = 0.5$ Hz $a_{\max} = 0.851$ g $u_{\max} = 7.8$ cm (3.1 in)

Airplane - Boeing 737-900
Impact Response - Floor Displacements

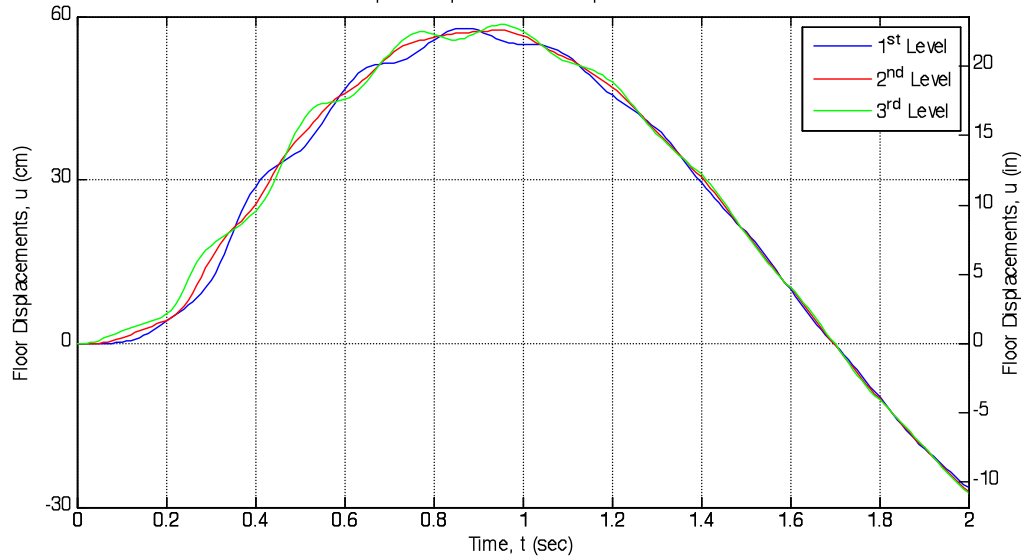


Airplane - Boeing 747-400
Impact Response - Floor Accelerations

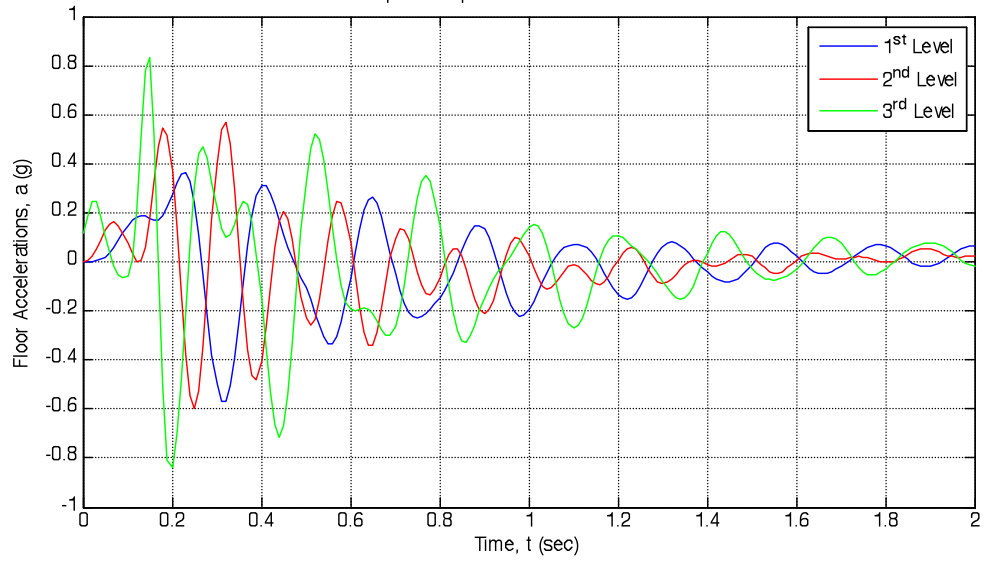


$W = 50000$ metric tons (110000 kips) $f = 0.33$ Hz $a_{\max} = 2.89$ g $u_{\max} = 58$ cm (23 in)

Airplane - Boeing 747-400
Impact Response - Floor Displacements

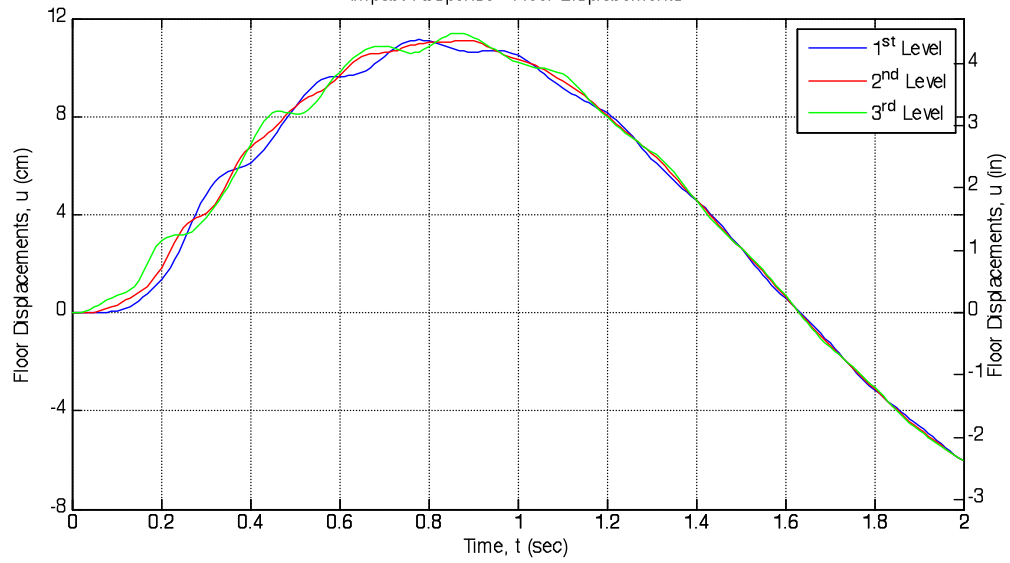


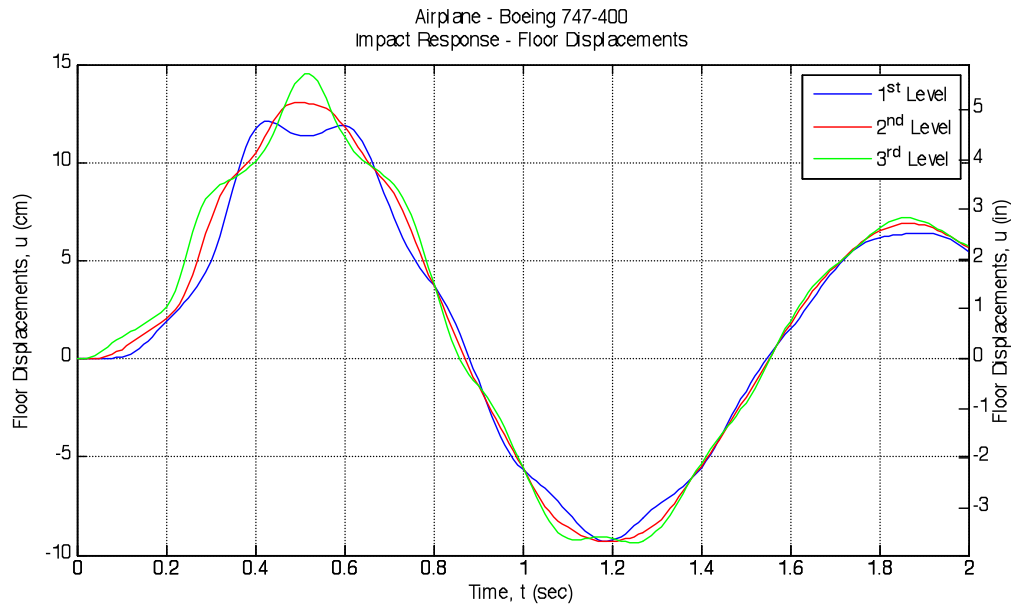
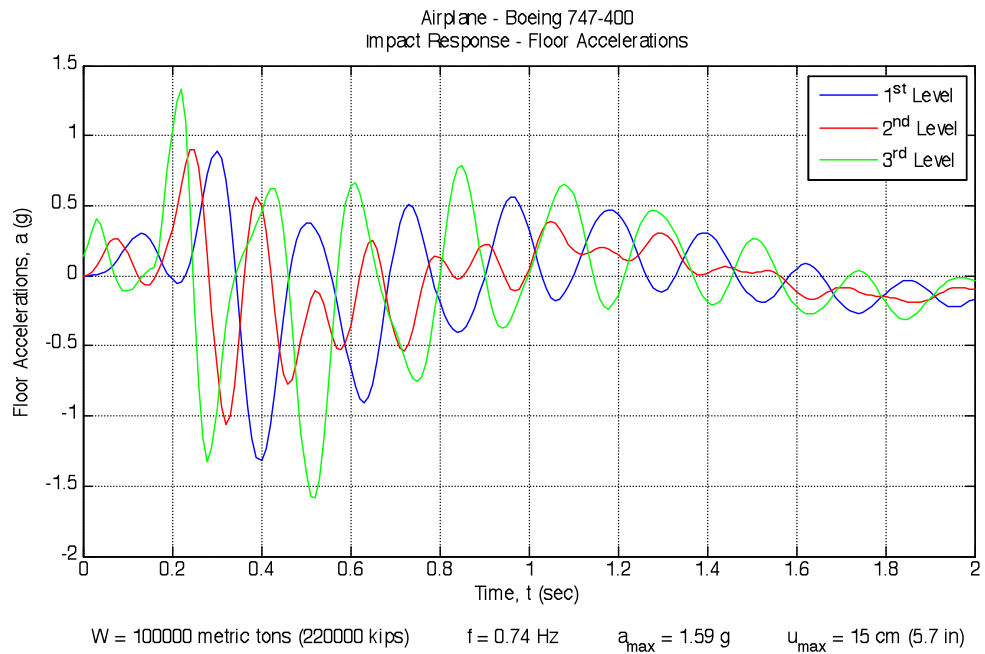
Airplane - Boeing 737-900
Impact Response - Floor Accelerations



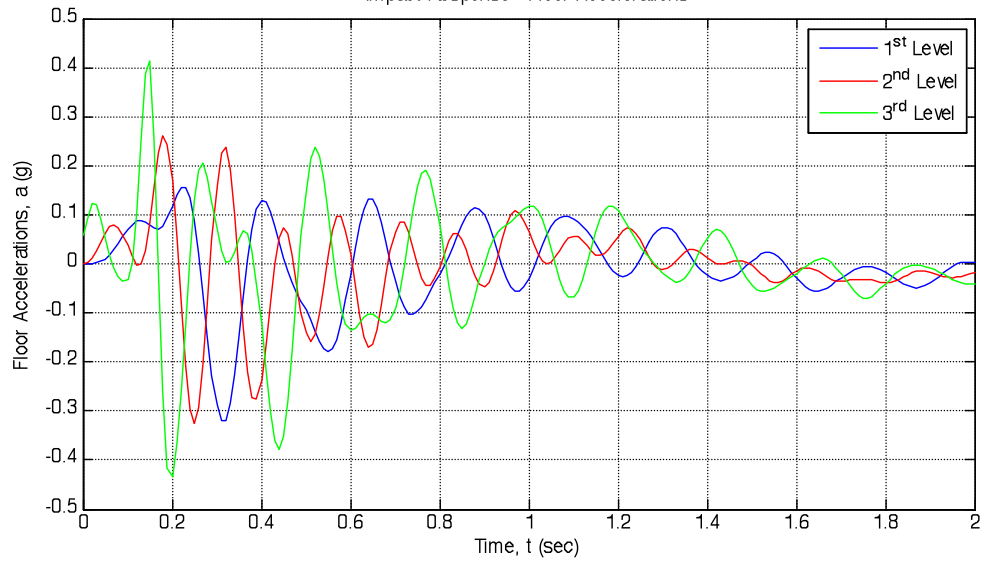
$W = 50000$ metric tons (110000 kips) $f = 0.33$ Hz $a_{\max} = 0.842$ g $u_{\max} = 11$ cm (4.5 in)

Airplane - Boeing 737-900
Impact Response - Floor Displacements



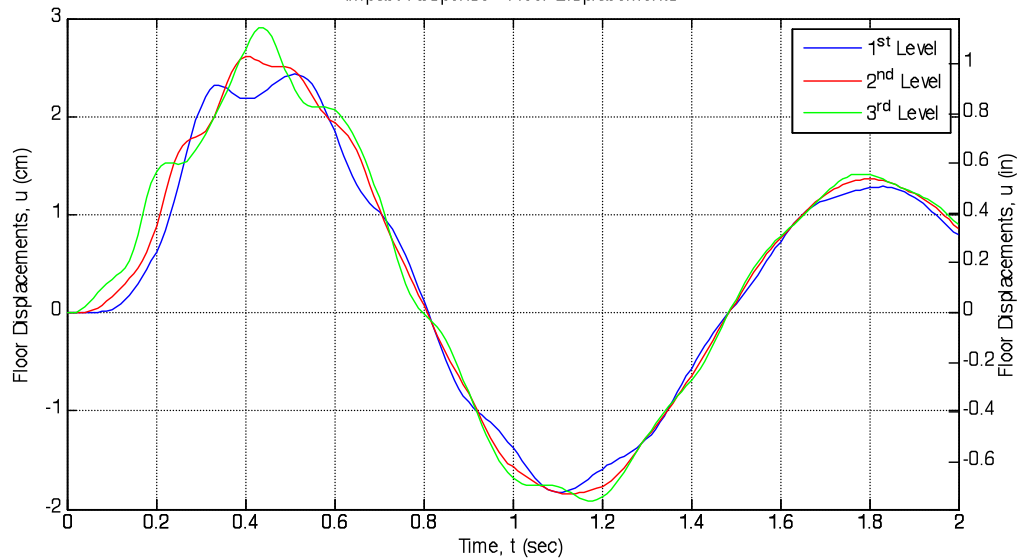


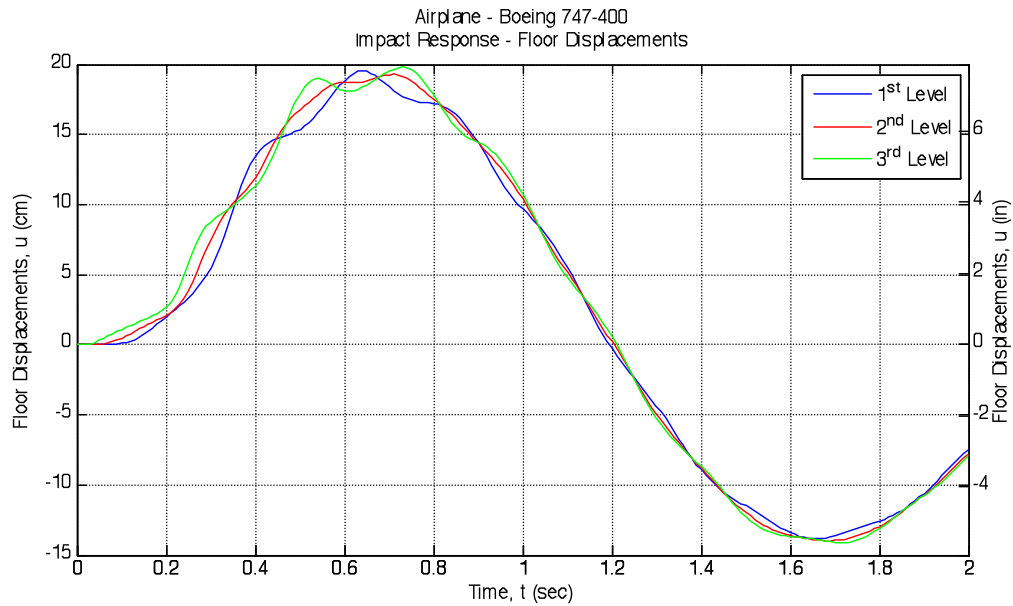
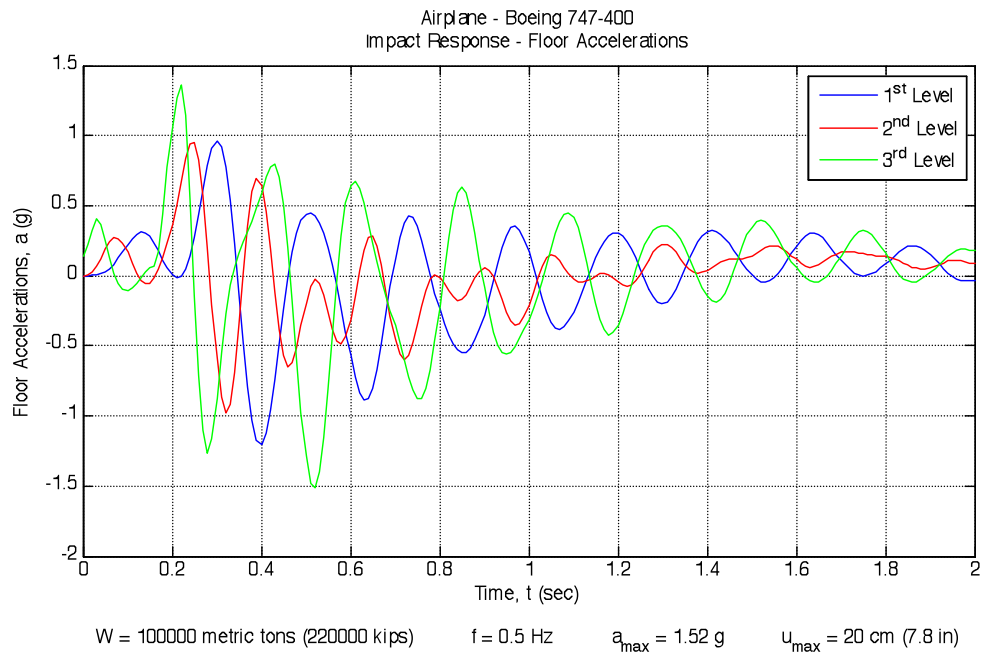
Airplane - Boeing 737-900
Impact Response - Floor Accelerations



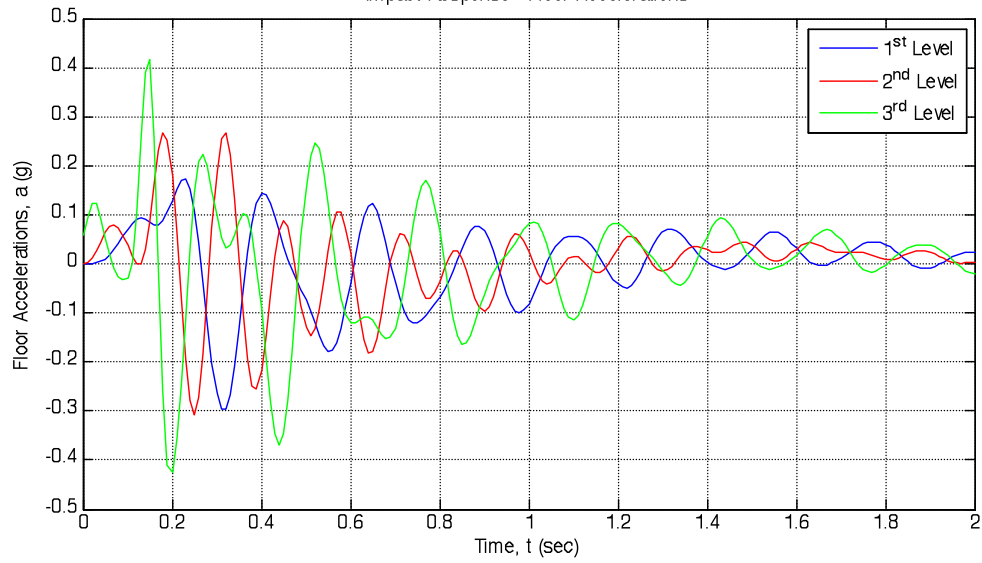
$W = 100000$ metric tons (220000 kips) $f = 0.74$ Hz $a_{\max} = 0.433$ g $u_{\max} = 2.9$ cm (1.1 in)

Airplane - Boeing 737-900
Impact Response - Floor Displacements



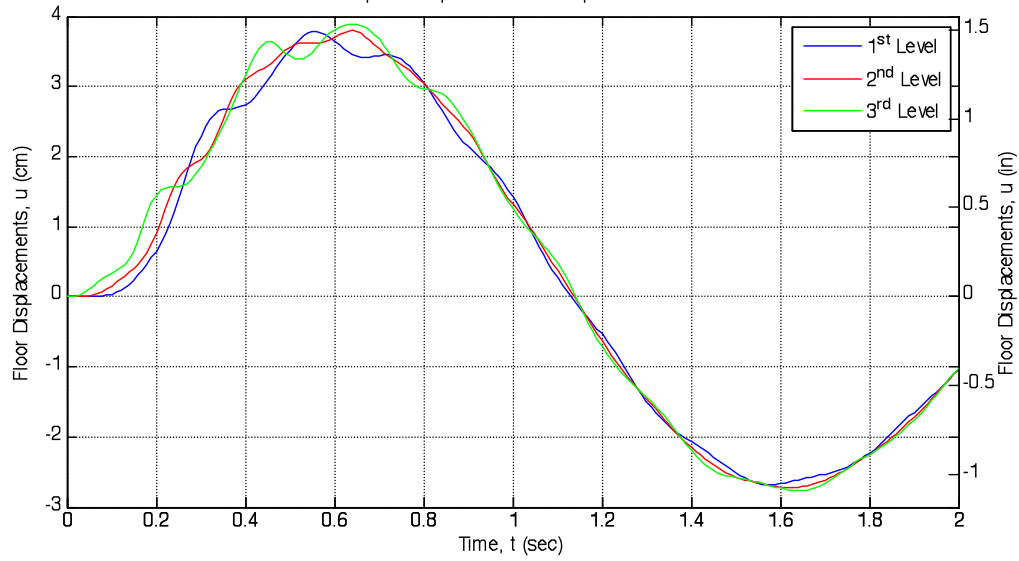


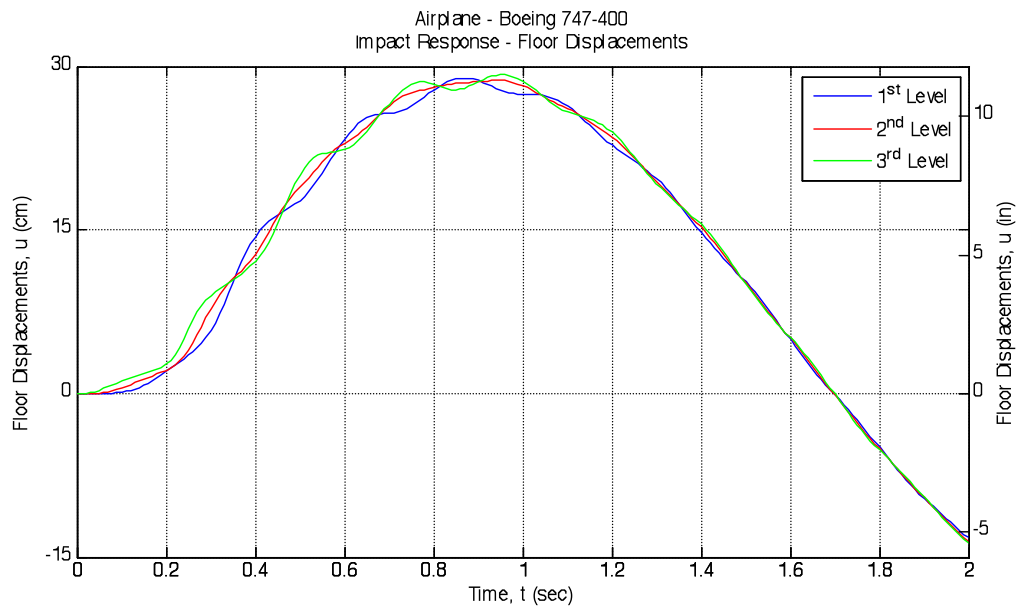
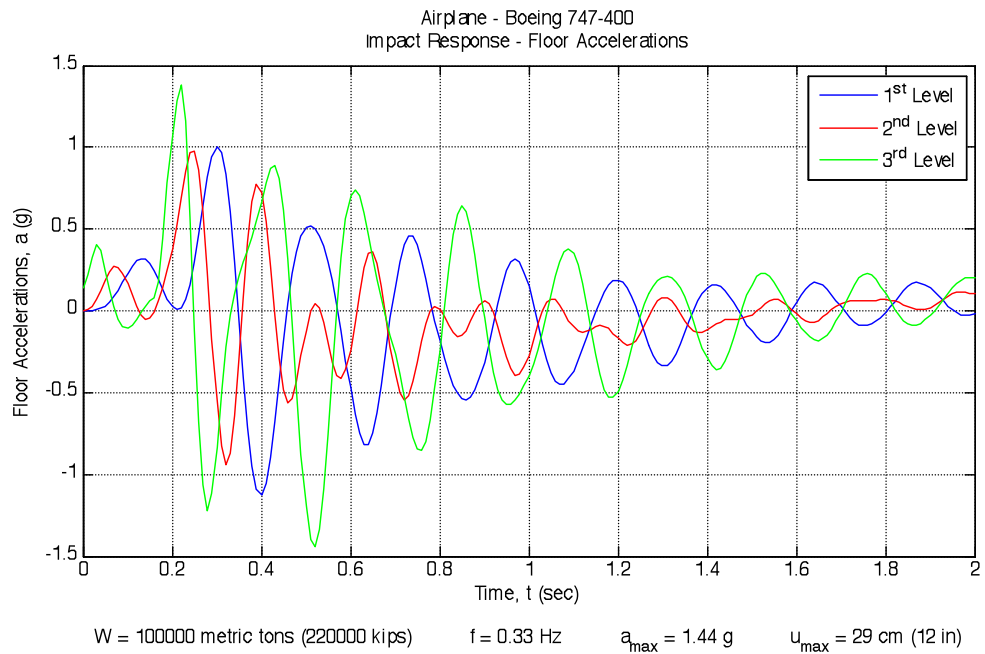
Airplane - Boeing 737-900
Impact Response - Floor Accelerations



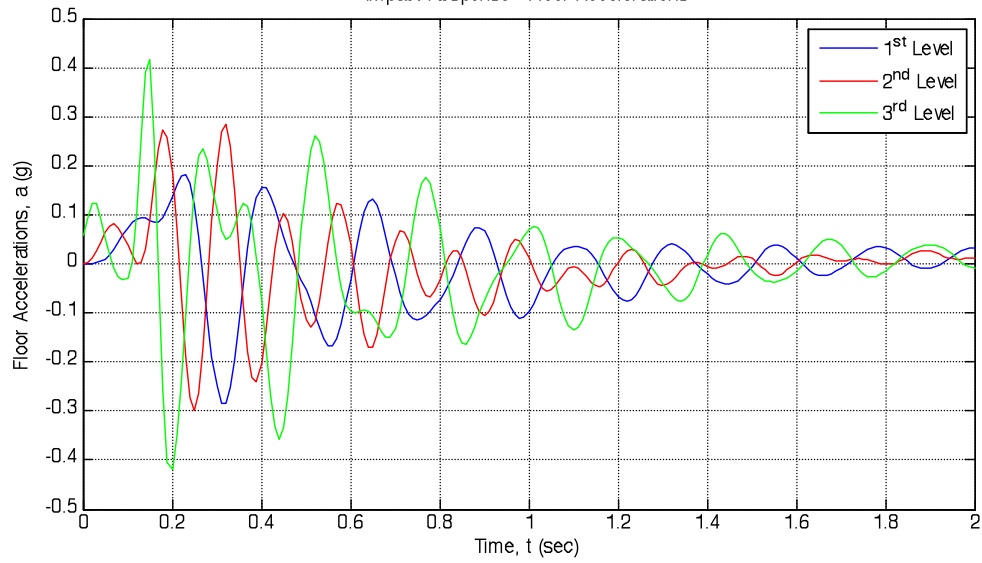
$W = 100000$ metric tons (220000 kips) $f = 0.5$ Hz $a_{\max} = 0.425$ g $u_{\max} = 3.9$ cm (1.5 in)

Airplane - Boeing 737-900
Impact Response - Floor Displacements





Airplane - Boeing 737-900
Impact Response - Floor Accelerations



$W = 100000$ metric tons (220000 kips) $f = 0.33$ Hz $a_{\max} = 0.421$ g $u_{\max} = 5.7$ cm (2.2 in)

Airplane - Boeing 737-900
Impact Response - Floor Displacements

